The effects of methanol fuel on combustion in premixed dual fuel engine

BYUNGJOO LEE

4414241

Faculty of Mechanical, Maritime and Materials Engineering

MSc. Thesis Report

Delft University of Technology, Faculty 3mE

Mechanical engineering

TU delft Report Nr: 2808

IHC MTI B.V Report Nr: AO 149

The effects of methanol fuel on combustion in premixed dual fuel engine

by

Byungjoo Lee

in partial fulfillment of the requirements for the degree of

Master of Science

in Mechanical Engineering

at the Delft University of Technology,
Process & Energy Faculty 3mE,
Sustainable Process and Energy Technology
December, 2016

The committee members

Ir. K. Visser (chairman)	TU Delft 3mE, Department M&TT, section Ship Design, Production and Operations
Prof.dr.ir. B.J. Boersma	TU Delft 3mE, Department Process & Energy
Dr.ir. Rene Pecnik	TU Delft 3mE, Department Process & Energy
Ir. H. Sapra	TU delft 3mE, Department M & TT
Ir. B.T.W. Mestemaker	Royal IHC, IHC MTI B.V.

Abstract

The environmental pollution and depleting fossil fuels have been considered as a critical issue all over the world. Many efforts have been devoted to investigating alternative fuels to tackle these problems. Alcohol fuels are potential candidates to alternative energy as it can mitigate pollutant emission. In addition, alcohol fuels can be applied to current diesel engines with technical modifications. This thesis mainly focuses on the effects of methanol fuel on in-cylinder process in premixed dual fuel engine. Different fuel ratios were tested to investigate the effects of methanol fuel. Existing diesel engine models, which have been developed by TU delft, were used to conduct computer simulations. To describe dual fuel combustion, separated vibe functions were adopted in the existing models. The simulation results indicated that the cooling effect caused by high heat of evaporation of methanol affected in-cylinder processes. With increase of methanol injection, start of ignition delayed due to the cooling effect. The longer ignition delay improved premixing of pilot fuel and it led to higher heat release rates. In case of maximum temperature, it was affected by both the cooling effects and diesel injection timing. With advanced diesel injection timing (-5.5 TDC), maximum temperature of dual fuel mode was higher than only diesel mode due to strong premixed combustion. Due to the lower LHV of methanol fuel, brake specific fuel consumption became higher with increase of methanol injection. Brake thermal efficiency decreased with increase of methanol injection due to lower combustion efficiency. The current models are not able to differentiate different combustion durations for diesel and methanol fuels. Further developments of the models are recommended to increase simulation accuracy. Furthermore, simulation on different diesel injection timing is recommended to better understand methanol combustion.

Acknowledgements

This report represents the work performed for my master thesis. The main objective of the thesis is to understand the effects of methanol fuel on combustion.

First of all, I would like to thank to Ir. Klaas Visser, who is the chairman of the graduation committee, for giving me the great opportunity to study this interesting topic. Another special thanks to Mr. Benny Mestemaker, who is the supervisor at IHC MTI. B.V. He shared his abundant and technical knowledge with me and it helped me to keep on track.

On a personal note, I am grateful to B. Jung, E. Oh, J. Yu and many SPET friends who were always there for me whenever I had personal issues. With their presence and support, I was able to overcome many difficulties.

Last but not least, I would like to say many thanks to Ir. Harsh Sapra, who is not only my supervisor but also is willing to be a good friend of mine for the whole thesis work. His insightful knowledge and encouragement increased my motivation. I do highly appreciate his rigorousness, patience and support.

Delft, University of Technology
December, 2016

Byungjoo Lee

Nomenclature

Abbreviation

CRR	Combustion Reaction Rate
IC	Inlet valve Closed
EO	Exhaust valve Open
SOC	Start of combustion
EOC	End of combustion
TDC	Top Dead Centre
BDC	Bottom Dead Centre
RCO	Reaction coordinates
NAHRR	Net Apparent Heat Release Rate
GAHRR	Gross Apparent Heat Release Rate
RMD	Methanol/Diesel mass ratio
SECA	Sulphur Emission Control Area
SI	Spark Ignition
CI	Compression Ignition
DF	Dual fuel
MCR	Maximum Continuous Rating
BSFC	Brake Specific Fuel Consumption
BTE	Brake Thermal Efficiency
HRR	Heat Release Rate

DIT	Diesel Injection Timing
CA	Crank Angle
HFO	Heavy Fuel Oil
MGO	Marine Gas Oil
UHC	Unburned Hydro Carbon

Symbol

A_b	Bore Area	[m^2]
D_b	Bore Diameter	[m]
$\dot{E}_f$	Energy of Fuel	[W]
L_s	Stroke Length	[m]
$\dot{Q}_{comb}$	Combustion heat	[W]
$\dot{Q}_{loss}$	Heat loss	[W]
T	Temperature	[K]
V	Volume	[m^3]
V_s	Stroke Volume	[m^3]
X	Normalized reaction rate	[--]
Z	Normalized rate of combustion	[--]
a	Vibe parameter linked to combustion efficiency	[--]
a_k	coefficients for the polynomial	[J/Kg/K]
b	Weight Factors in multiple Vibe Function	[--]

c_m	Mean piston speed	[m/s]
c_p	Specific heat at constant pressure	[J/Kg/K]
c_v	Specific heat at constant volume	[J/Kg/K]
h	Specific enthalpy	[J/Kg]
k	Reaction rate constant	[--]
m	Shape parameter in Vibe function	[--]
m	mass	[Kg]
n_{comp}	Compression exponent	[--]
p	Pressure	[pa]
r_c	Effective compression volume ratio	[--]
t	Time	[s]
u	Specific internal energy	[J/Kg]
Xg	Energy fraction of Methanol	[--]
α	crank angle	[Degree]
α_{g-w}	heat loss to the walls coefficient	[W/m^2/K]
η_{comb}	Combustion efficiency	[--]
ε	Geometric compression ratio	[--]
ξ	Fuel burn rate (or Combustion reaction rate)	[Kg/s]
λ	Air excess ratio	[--]
λ_{CR}	Radius to length ratio	[--]
σ	Stoichiometric air/fuel ratio	[--]

ρ	density	[Kg/m^3]
τ	Normalized time	[--]

Subscript

f	Fuel
max	Maximum
min	Minimum
sg	Stoichiometric gas from diesel fuel
sgg	Stoichiometric gas from methanol fuel
ref	Reference
comb	Combustion
norm	Normalized
D	Diesel
M	Methanol

Table of contents

1. Introduction

1.1 Background information and Motivation

The gravity of environmental pollution due to fossil fuel has been a critical issue all over the world for many years. Various industries are responsible for polluting the environment. Shipping industry cannot stay away from the responsibility as pollutant exhaust gases from ship's funnels contribute to air pollution and lead to serious environmental damages. In addition, depleting fossil fuel urged the world to find solutions. As a result, the world decided to enforce more strict environmental regulations on shipping industry to reduce its emission.

The regulation requires that sulphur content (SO_x) must limit to 0.1% within the emission control areas (SECAs) from 2015, which is shown in **Figure 1.1**. Moreover, nitrogen oxide(NO_x) emission control areas (NECAs) has been in effect from 2016 in US Caribbean area and will be introduced in Europe from 2021. Many researches have been conducted to find alternative fuels with reduced emission. MGO has been widely used as an alternative fuel in SECAs instead of HFO because HFO which contains 0.1% of sulphur does not exist. However, much higher price of MGO than HFO cannot be ignored because increase of fuel price would be a risk for shipping industry to run their business. In addition, not only SO_x and NO_x but also greenhouse gases (GHG) which is generated from fossil fuel combustion process is a severe problem of environment as it accelerates global warming. The effort to reduce CO_2 emission has been made by International Marine Organization (IMO). They introduced Energy Efficiency Design Index (EEDI) which indicates CO_2 emission of ships. [MAN Diesel & Turbo, 2014] It is inevitable to find new and more efficient combustion technologies together with new energy sources.

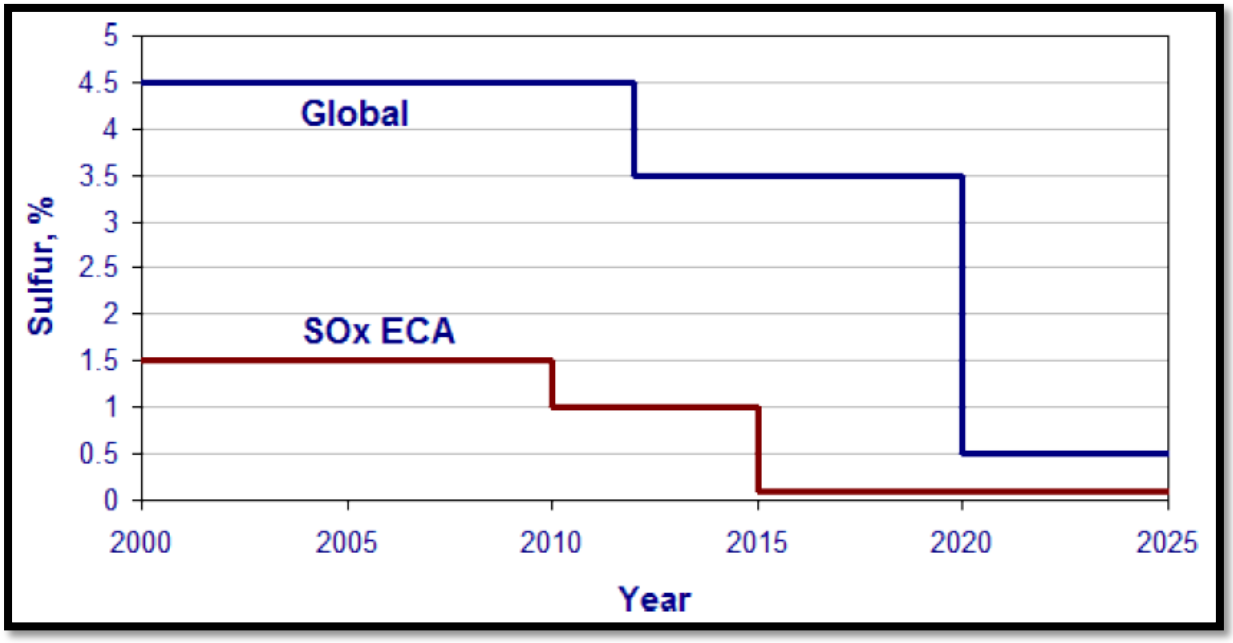

Figure 1.1 MARPOL Annex VI Fuel Sulfur Limits [IMO, 2016]

It is known that alcohol fuels (Methanol and Ethanol) are potential candidates to alternative green energy in order to reduce CO_2 emissions. If alcohol fuels are produced by biomass, it can generate less CO_2 compared to conventional fuels [Maurya et al., 2011] Especially, in case of methanol, it has been proved as a promising alternative marine fuel by the project, "Efficient Shipping with Low Emissions" (Effship) supported by Stena line, the third largest ferry company in the world [Fagerlund et al., 2014]. Stena Germanica, which is a ferry ship, has adopted modified 4-stroke engines to burn methanol as main fuel. Methanol engine for 2 stroke engine was also made by MAN B & W. Although alcohol fuel engines are in use on board, further researches and studies on alcohol fuel engines are required to better understand engine performance with alcohol fuels.

1.2 Thesis objective

This thesis studies on modeling and combustion performance of methanol dual fuel engine. One major challenge of methanol combustion is to overcome its poor auto-ignition caused by low cetane number. Introduction of pilot fuel can be the solution as the high reactivity pilot fuel can induce combustion of methanol fuel. An advantage of premixed dual fuel combustion engines is that the cost of engine modification is relatively lower than of direct injection type. In addition, premixed combustion concept is able to achieve relatively lean combustion than compression ignition because primary fuels are homogeneously premixed with air before ignition. It can lead to lesser NO_x emission than direct injection type. [Haraldson, 2015]. In this regard, premixed dual fuel methanol engine is expected as a possible solution to fulfill NOx Tier III regulations without Selective Catalytic Reduction (SCR) and Exhaust Gas Recirculation (EGR) [Haraldson, 2015]. For these reasons, many studies and researches on premixed dual fuel engine are being carried out. An attempt has been made to simulate direct injection engine type as well, but it turned out to be difficult due to lack of information such as detail engine data and test conditions.

The main objective of the thesis is to investigate the performance of methanol dual fuel engine. More specifically, the thesis focuses on influence of methanol fuel on in-cylinder process. Furthermore, the effects of different methanol/diesel fuel ratios on in-cylinder process are discussed.

TU delft has developed diesel engine models based in MATLAB/Simulink environment. Modification of the existing engine models is also an additional objective of this thesis to perform premixed dual fuel combustion with methanol fuel. The analysis of in-cylinder process will be carried out by studying the simulation results.

1.3 Thesis outline

The background information and motivation are introduced in Chapter 1. Overall thesis objectives can be found in chapter 1 as well.

Chapter 2 starts with literature review of alcohol fuels. General information of alcohol fuels is presented. Both background information of emissions and characteristics of methanol emission are included in the literature review. The last part of literature review covers characteristics of dual fuel engine and introduction of current applications.

Hypothesis can be found in chapter 3 and in chapter 4, the fundamental features of the model C, which consists of heat release calculation model and in-cylinder process model, is explained. As both models are built based on single-zone model, characteristics of single-zone model are briefly introduced.

Chapter 5 starts with overall methodology and assumptions for model modifications. The model modifications for both heat release model and in-cylinder model are explained in this chapter. Vibe functions in the in-cylinder model and heat of combustion in the heat release model need to be separated to describe diesel and methanol combustion independently.

Chapter 6 covers the simulation results of dual fuel combustion. First of all, the results from the heat release model and the in-cylinder model will be compared. Then analysis of in-cylinder process carry out through pressure, temperature, heat release rate, brake specific fuel consumption and brake thermal efficiency.

Finally, chapter 7 contains the overall conclusions and recommendation for further work.

2. Literature review

2.1 General information of Methanol

Methanol is known as one of the prospective future fuel candidates for internal combustion engines. It is viable to apply in current engines with technical modifications. From an emission point of view, methanol is a good solution to mitigate pollutant emission. Combustion of methanol produces low NO_x and particulate matters while equivalent efficiency can be expected. In addition, methanol is considered as an eco-friendly fuel because it is a miscible substance in water and easily decomposes in the environment**.** Although methanol is toxic if ingested, it has very low impact when it is released to the environment as it quickly breaks down into other compounds. In addition, a number of various bacteria consume these compounds as food [Methanol institute, 2016].

Not only shipping industries but many other industries are highly depending on conventional fossil fuels. In this situation, methanol can be an effective alternative as it can be produced from renewable feed stocks. However, in order to encourage methanol market to be stable and flourish, both economical production and constant supply are still required. For these reasons, a large quantity of methanol is produced based on fossil-based sources today. Annually, 45 million tons of methanol is produced based on fossil fuels. 80 % of methanol is produced by natural gas and 17% of methanol is produced by coal. [Broeren et al., 2013] On the other hand, only 200,000 tons of bio-methanol is produced per year. [IRENA Technology, 2013]

Technologies to produce methanol from natural gas is well matured and already highly optimized so that a large portion of methanol comes from natural gas these days. **Figure 2.1.1** illustrates methanol production procedures from natural gases. Another way to produce methanol is gasification of coal. It is a predominant method and has succeeded in producing a large scale of methanol in China [Fagerlund et al., 2014]**.**

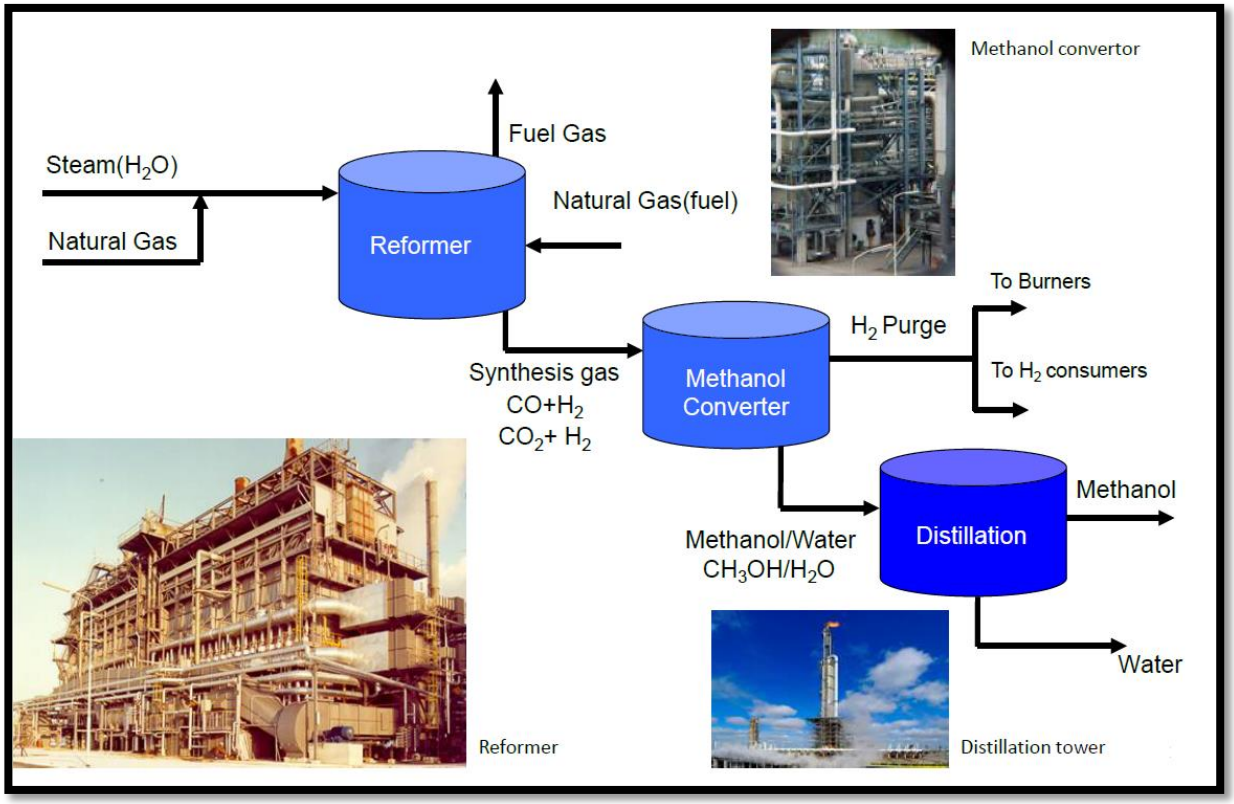

Figure 2.1.1 Conventional methanol production procedure [Stenhede, 2014]

Although natural gas is a comparatively eco-friendly substance than conventional fuels, it is still categorized as fossil-based fuel. In this respect, there must be extra efforts to promote sustainable technologies. In fact, some technologies to produce methanol from renewable sources are feasible but high investment cost and high cost of feedstock suppress the growth of sustainable technologies. Uncertainties of long term stability of renewable feedstock and regulations are also critical obstacles.

Gasification of biomass to produce methanol is one promising sustainable technology in the long term as not only NO_x and PM, but CO_2 emission is also an important concerns. Biomass could be any types of plants or animal materials and it consumes CO_2 during its cultivation. However there are some limits which need to be taken into account. The biomass supply is highly restricted by geographical location. It means that not every country or region is open to cultivate. Moreover, technical immaturity is also one of the limits. The main problems are to reduce impurities and tars which can be generated during the gasification process [Mphoswa, 2015].

The technology of recycling CO_2 to produce methanol will be a fine solution to prevent further deterioration of global warming effects. **Figure 2.12** shows the overall scheme of methanol production with recycling CO_2. High concentration of CO_2 can be captured from flue gases which are mainly emitted by power plants and various types of factories.

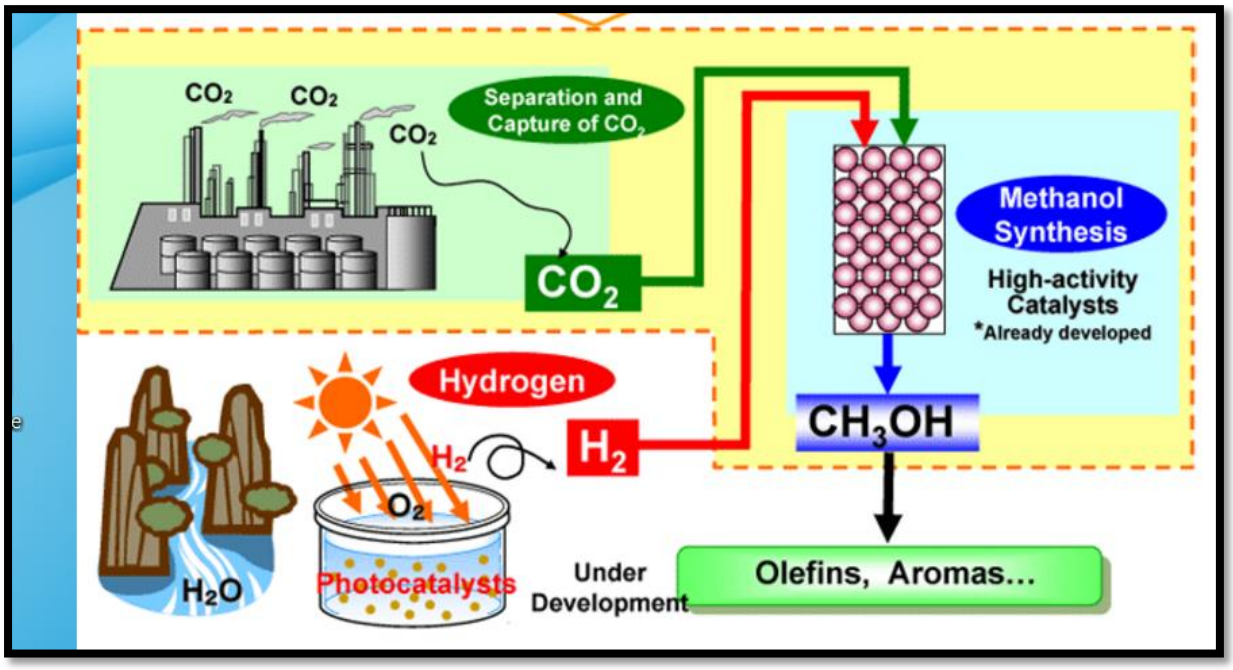

Figure 2.1.2 Methanol production with recycling CO_2 [Mitsui Chemicals, 2008]

2.2 General information of Ethanol

Ethanol is C_2H_5OH and called as either ethyl alcohol or hydroxyethane. It is one of the representative alcohol fuels along with methanol. Many researches about ethanol have been done for years to cope with significant increase of oil price and to prepare the imbalance between demand and supply in the coming decades. Although sustainable production of ethanol is more expensive than methanol, ethanol is still considered as a promising substitutive fuel for the conventional fossil fuels. Compared to methanol, the beneficial aspects of using ethanol are that ethanol is less toxic and has a higher energy density. Unlike methanol metabolism, ethanol metabolism does not produce formaldehyde and formic acid, which are known as very toxic and harmful for human body [Hovda, 2011].

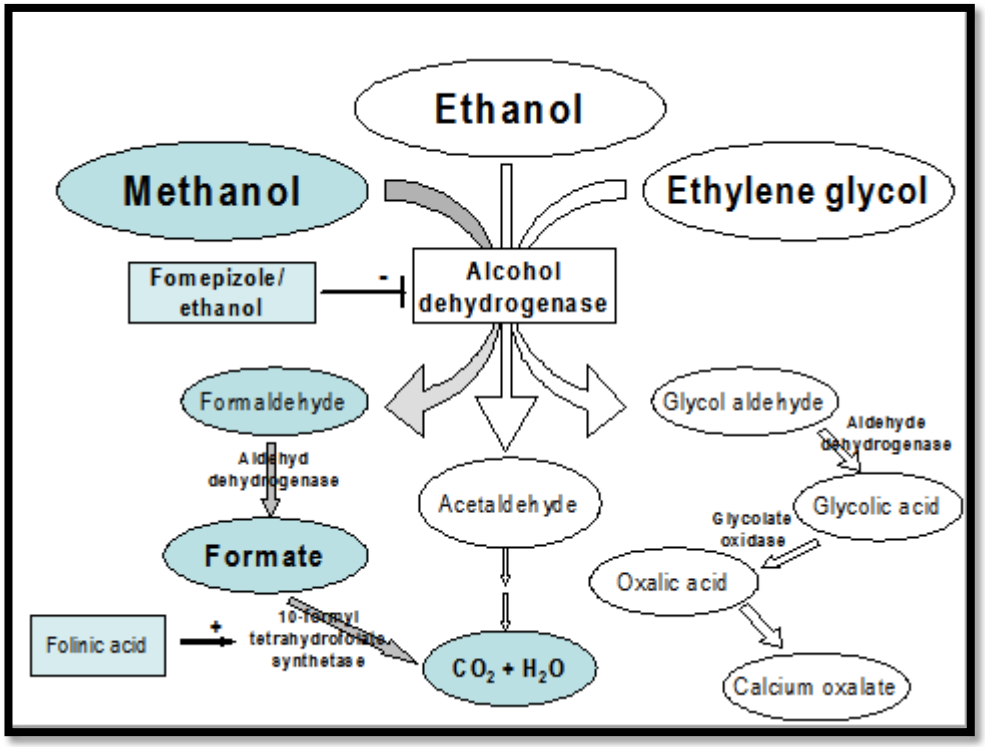

Figure 2.2.1 Metabolism of methanol and ethanol [Hovda, 2011]

Bioethanol is produced from various types of sugar containing biomass such as corn, wheat, sugarcane, switch grass, and so on. In addition, starch-rich and cellulose-rich biomass can be used as comparable feedstock to sugar-rich substance. Approximately, half of bioethanol production comes from sugar crop, specifically sugarcanes and beets. The remaining bioethanol production is from starch crop such as corn and wheat. When it comes to profitable cultivation and CO_2 mitigation, sugarcane in Brazil is the most promising feedstock to produce bioethanol because favorable weather in Brazil accelerates its growth. **Figure 2.2.2** illustrates that rapid increase of ethanol production for fuel purpose from 1975 to 2005. Increase of production stands for growing of demand for ethanol. This leads to prosperity of ethanol market and improvement of relevant technologies.

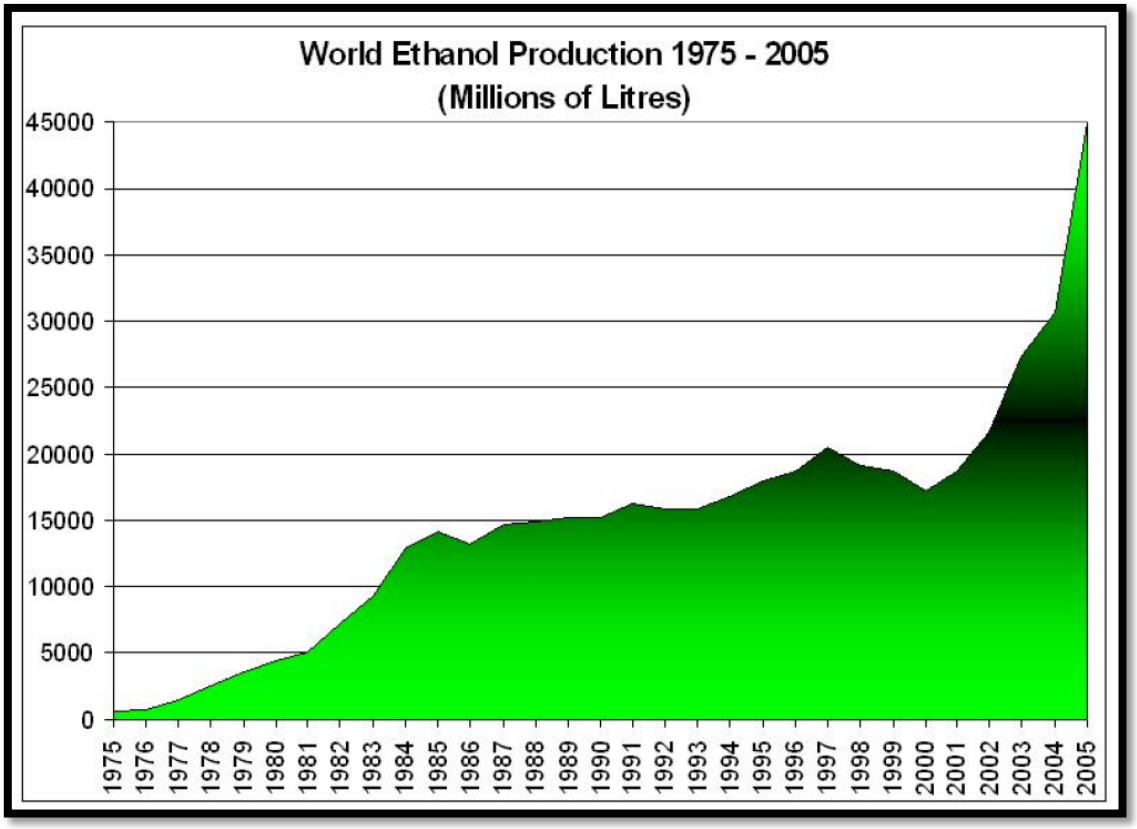

Figure 2.2.2 World ethanol production [Danielsson, 2008]

The usage of ethanol as an additive to gasoline is known as one of the most common applications nowadays. In the mixture, ethanol accounts for 5% to 10% of its total mass. There are two major reasons for using ethanol as an additive to gasoline. First of all, higher octane value of ethanol will raise the overall octane value of the fuel blend. Higher octane number of the fuel can resist premature ignition. Consequently it is able to suppress engine knocking, which may cause serious damages to the engine. Secondly, it facilitates to reduce harmful emissions such as particulates, unburned fuel and carbon monoxide because ethanol naturally contains oxygen. The effect of oxygen in the fuel is to promote more chemical reactions during combustion process.

Not only gasoline but also diesel is available to blend with ethanol, which is called as "Diesohol". It has already been introduced to engine market. One well-known blend of diesel and ethanol is "E-diesel" and it consists of 85% of diesel fuel and 15% of anhydrous ethanol. The name of another famous blend of diesel and ethanol is "O_2 Diesel". With this blend, more than 5000 buses in India are successfully able to move on the roads [Karsen et al., 2009]. The concept of the diesel

blending with ethanol originated from the effort to reduce particle emissions, which is considered as serious issue in compression combustion engines. Furthermore, with 95% of ethanol and 5% of additive is used as a fuel for compression ignition engines in Sweden, which is called as E95 and does not have any diesel fuel in it [Karsen et al., 2009].

One of the major reasons for using bioethanol is to mitigate dangerous environment impacts. However, during the cultivation of feedstock, a large amount of synthetic fertilizers are used to enhance quality of the harvest. In fact agricultural fertilizers have harmful effects on the environment. It causes groundwater contamination, ozone depletion and global warming. Therefore, technology development for sustainable agricultural production must be considered. One astonishing result is that some of the feedstock can significantly reduce GHG. **Figure 2.2.3** indicates that CO2-equivalent well-to-wheels GHG reduction per driving kilometer

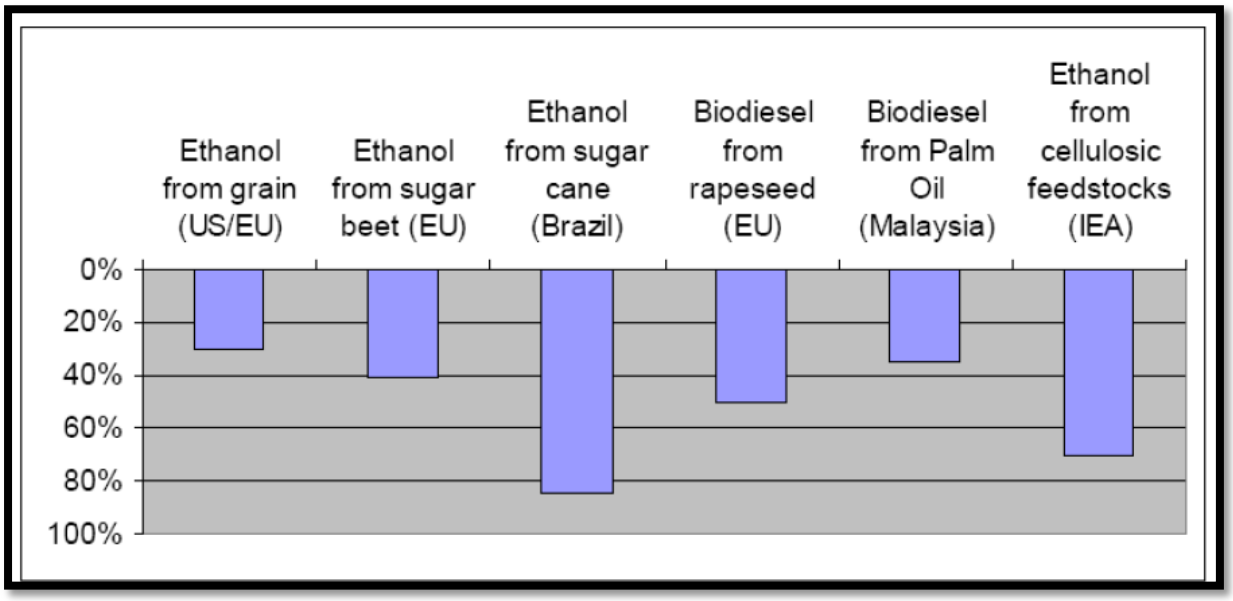

Figure 2.2.3 Well-to-wheel CO_2 Equivalent reduction [Doornbosch et al., 2007]

Cellulosic-based ethanol and sugarcane-based ethanol show significant reduction of GHG emission. It can be known that the potential for GHG mitigation highly relies on types of feedstock crop. **Figure 2.2.4** illustrates the overall flow chart for bioethanol production from sugar cranes.

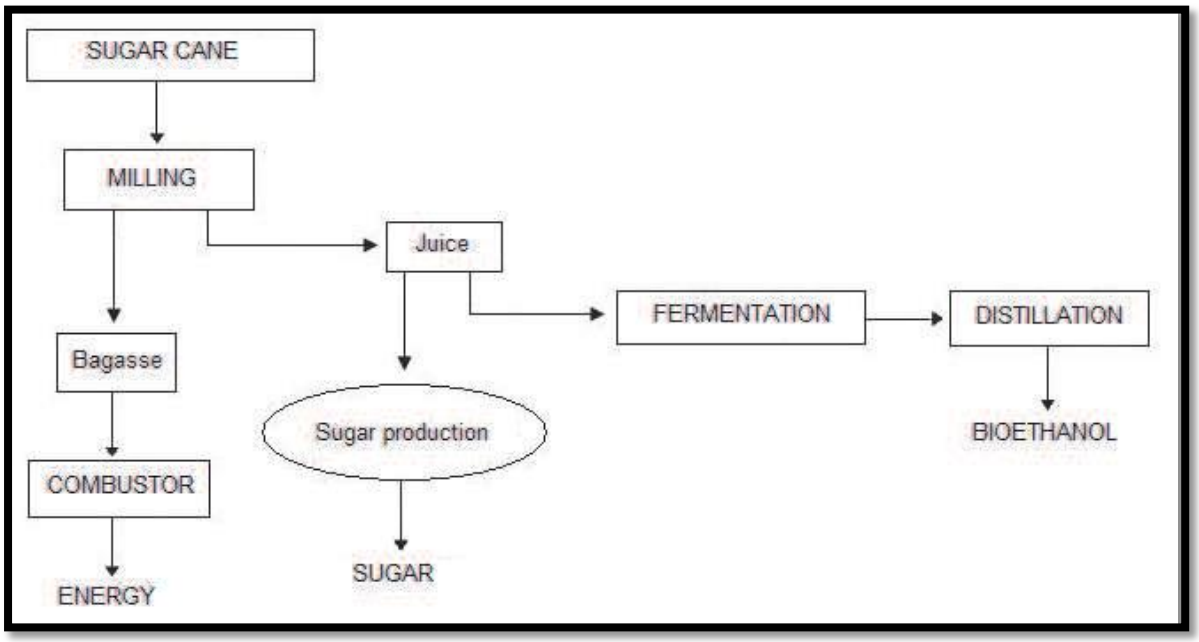

Figure 2.2.4 Flow chart for bioethanol from sugar crane [G.D Nicola et al., 2011]

2.3 Evaluation of alcohol fuels as alternative fuels

To investigate the feasibility of usage of alcohol fuels for current diesel engines, properties and characteristics of methanol and ethanol need to be evaluated. **Table 2.3.1** illustrates detailed comparison between alcohol fuels and conventional fossil fuels.

Although this thesis does not investigate Dimethyl-ether (DME), it is also considered as an attractive alternative fuel. DME is an organic compound and its chemical formula is CH_3-O-CH_3. It can be directly obtained from natural gas or through a dehydration reaction after methanol synthetic reaction. Non-toxic and colorless are the characteristics of DME. Substantial researches on DME are currently carried out to investigate combustion characteristics to determine whether it is promising alternative fuel or not. [Park, 2014]

Table 2.3.1 Properties of various types of fuel [MAN Diesel & Turbo, 2014]

Fuel properties						
Property	**DME**	**Methanol**	**Ethanol**	**Diesel**	**HFO 45**	**Gasoline**
Chemical formula	CH_3-O-CH_3	CH_3-OH	C_2H_5-OH	C8-C25	-	C4-C12
Fuel carbon (wt%)	52.2	38	52	85	-	86
Fuel hydrogen (wt%)	13	12	13	15	-	14
Fuel oxygen (wt%)	34.8	50	35	0	-	0
Molar mass (kg/kmol)	46	32	46	183	-	114
Liquid density (kg/m³)	660	798	794	840	982	740
Lower heating value (MJ/kg)	22.8	20.1	27.0	42.7	40.9	-
Boiling temperature (°C at 1 bar)	-24.9	65	78	180-360	-	27-245
Vapour pressure (bar at 20°C)	5.3	0.13	0.059	«1	-	0.25-0.45
Critical pressure (bar)	53.7	81	63	30	-	-
Critical temperature (°C)	127	239.4	241	435	-	-
Kinematic viscosity (cSt at 20°C)	0.19-0.25	0.74	1.2	2.5-3.0	-	0.6
Surface tension (N/m at 20°C)	0.012	0.023	0.022	.027	-	-
Bulk modulus (N/mm² at 20°C 2MPa)	1,549	823	902	553	-	1,300
Cetane number	55	<5	8	38-53	-	-
Octane number	Low	109	109	15-25	-	90-100
Auto ignition temperature in air (°C)	350	470	362	250-450	-	250-460
Heat of vaporisation (kJ/kg at 1 bar)	467	1,089	841	250	-	375
Minimum ignition energy (mJ at ϕ=1)	0.33	0.21	0.65	0.23	-	0.8
Stoichiometric air/fuel ratio	9	6.5	9.1	14.6	13.5	14.7
Peak flame temperature (°C at 1 bar)	1,780	1,890	1,920	2,054	-	2,030
Flamability limits (vol%)	3.4-18.28	6-36	3-19	0.5-7.5	-	1.4-7.6
Flash point (°C)	-41	12	14	52	-	-45

Chemical formula

Different from conventional fuels such as diesel and gasoline, both methanol and ethanol are considered as oxygenated fuel as they contain 50% and 35% of oxygen of its mass, respectively. It implies that more oxygen is available during combustion process when alcohol fuels are used. Consequently plenty of oxygen alleviates the emission of particular matter emission as smoke and soot are generated due to lack of the oxygen. [Turkcan et al., 2013]

C/H ratio

C/H ratio is the straightforward indication of CO_2 emission from certain fuels. C and H stand for Carbon and hydrogen contents, respectively. The higher C/H ratio is, the more CO_2 generates. However, alcohol fuels have lesser C/H ratio than diesel and gasoline. It indicates that methanol and ethanol combustion reduces CO_2 emission. Other advantage we can expect from alcohol fuels is the decrease of NO_x emission. Lower C/H ratio leads to high possibility to form H_2O. The

specific heat of water vapor is higher than other products, which are generated during combustion process. Due to high specific heat, water vapor is able to absorb large amount of heat energy. Consequently, this phenomenon reduces the adiabatic flame temperature. Less NO_x emission is expected at lower temperature,

Lower heating value (LHV)

Compared to diesel, alcohol fuels have almost half of lower heating value (MJ/Kg). To make equivalent performance as diesel fuel, larger quantities of alcohol fuels must be injected into the engine cylinders. In order to achieve that, ships need to store larger quantities of alcohol fuels and it surely requires larger volume of fuel tanks. Converting ballast tanks and existing HFO tank to alcohol fuels tanks can be one of feasible solutions to overcome the limitation of space. [Fagerlund et al., 2014] For example, the ballast tank in the Stena Germanica was converted to methanol fuel tank. [Andersson, 2015]. However, more investigation of converting ballast tank need to be studied to find out that it is applicable to other vessels.

Kinematic viscosity

It is one of the important properties for injection system in engines. In case of too low viscosity, excessive wear of the components and power loss due to pump leakage take place during engine operation**.** On the other hand, in case of too high viscosity, it affects fuel spray patterns. **Figure 2.3.1** shows effect of viscosity on spray pattern**.** In addition, it causes excessive pump resistance and filter damage. [Kegl et al,. 2013] Alcohol fuels tend to have lower kinematic viscosity. Especially methanol has much lower kinematic viscosity than diesel engine. It might exacerbate lubrication ability in injection pump but it can be overcome by applying sealing oil for lubricating in injection pump, which lubricates all running surfaces. [MAN Diesel & Turbo, 2014]

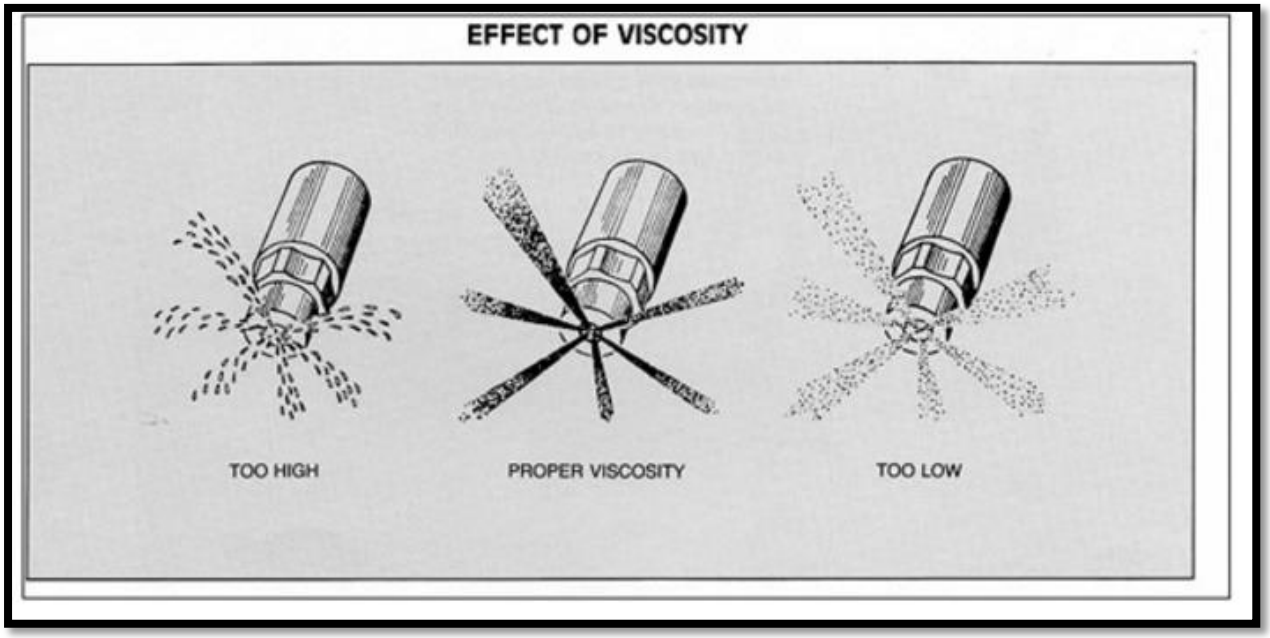

Figure 2.3.1 Effect of viscosity on spray pattern [LIBEWHIZ, 2016]

Cetane number

Cetane number indicates auto-ignition quality of the fuels and affects combustion process of compression ignition engines. Low cetance number of fuels has longer ignition delay as it is hard to achieve auto-ignition. Cetane number of alcohol fuels is much lower than that of diesel fuel. It has been pointed out as a disadvantageous aspect of alcohol fuels to be introduced into the compression ignition engines because it implies alcohol fuels have unfavorable characteristics of auto-ignition. Nevertheless, alcohol fuels still have potential to be used as an alternative maritime fuel. Auto-ignition quality is not only dependent on cetane number but also highly affected by temperature [Heywood, 1988]. With technical modification and improvement such as glow plug or pilot fuel injection system, the poor auto-ignition of alcohol fuels can be overcome. [Fagerlund et al., 2014]

Octane number

Octane number is a key parameter for premixed ignition engine. A fuel with high octane number delays self-ignition timing so that it inhibits engine knocking, which causes seriously problems to SI engines. One of positive characteristics of methanol and ethanol is that it can blend with

gasoline. This blending mixture has higher octane number than gasoline only. It makes SI engine to resist higher compression ratio and suppress knocking. As a result, SI engine with blending mixture produces higher mean indicated effective pressure (IMEP) as well as higher indicated efficiency. [Turkcan et al., 2013] There is an inverse correlation between cetane and octane number as shown in **Figure 2.3.2**. With increase of cetane number, octane number decreases.

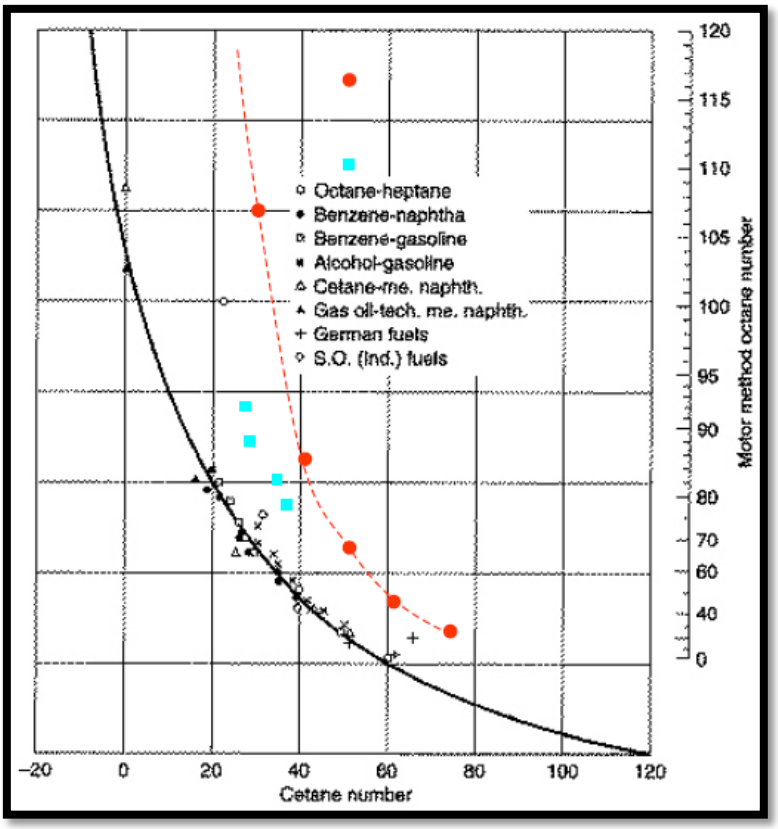

Figure 2.3.2 Inverse correlation between Cetane and Octane [saha, 2016]

Heat of vaporization and cooling effect

Heat of vaporizations (KJ/Kg) of both methanol and ethanol are roughly 4 times and 3 times higher than that of diesel fuel, respectively. Therefore significant cooling effect in the cylinders can be expected. When liquid fuel is injected into the cylinder during compression stroke, it absorbs heat energy and then it evaporates. Larger heat of vaporization means that liquid fuel needs to absorb more heat energy to vaporize. Since heat energy is used for vaporization process, in-cylinder temperature decreases. The beneficial aspect of the significant cooling effect is that it can reduce NO_x emission due to low in-cylinder temperature [Heywood, 1988].

Flammability limits

Flammability limits indicates the proportion of flammable mixtures, which mark the flammable ranges to combust. The proportion between gases and air plays a key role to produce a fire. Above the upper flammable limit (UFL) where deficient oxygen exists, the mixture is not able to burn. Below the lower flammable limit (LFL) where excessively sufficient oxygen exists, ignition does not take place. Unlike compression ignition engine, spark ignition engine requires homogenous mixtures to induce ignition. Alcohol fuels have wider range of flammability limits compared to gasoline. It allows using leaner mixtures and lean-burn engines can reduce NO_x emission.

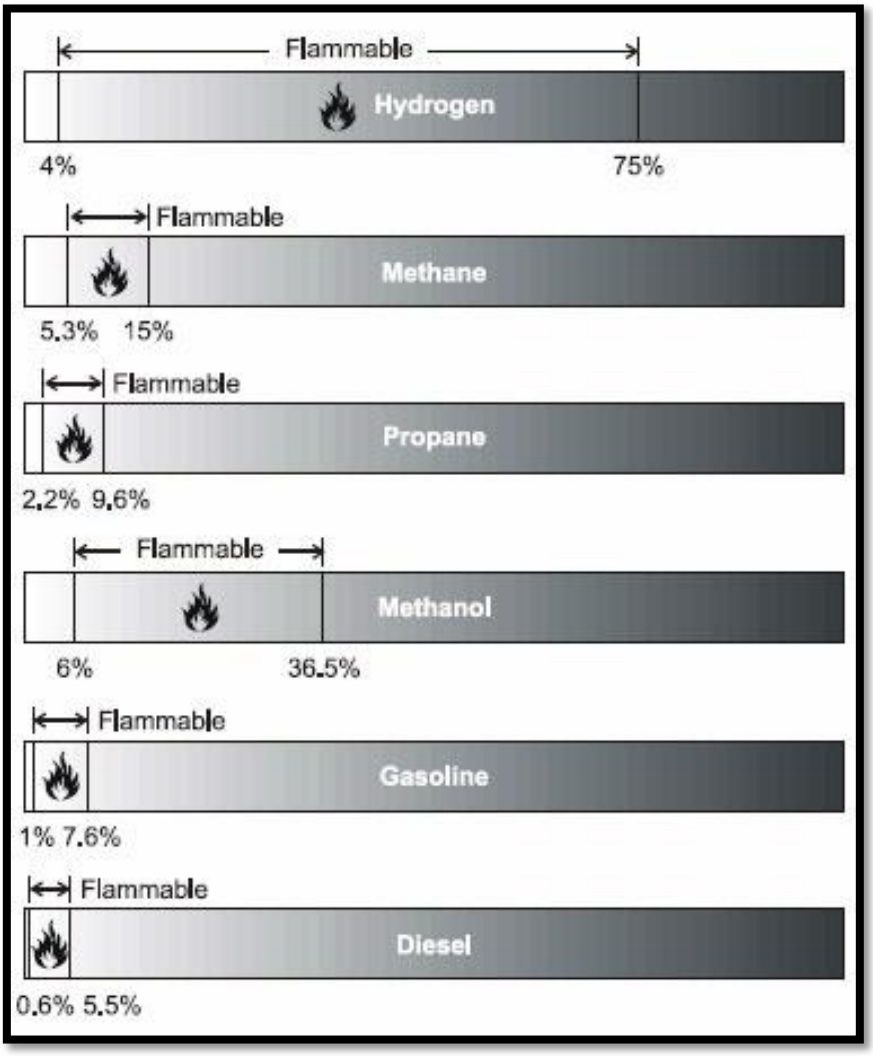

Figure 2.3.3 Flammability ranges of various fuels at atmospheric temperature [Anjeel, 2016]

Flash points

Handling and storage are essential considerations when introducing new fuel to conventional system. Flash points of 12℃ and 14℃ does not comply with the Safety Of Life At Sea (SOLAS). However, the new mandatory code for low-flash point fuels (IGF code) will enter into force on January 1, 2017. The IGF code contains all the considerations for the usage of low-flashpoint fuels and it provides mandatory criteria to minimize the risk. [T.G Osberg, 2015] Modifications on the ventilation system, insulation of electrical system, double wall design of all alcohol fuel components and additional fire detection system are necessary to enhance safety.

2.4 Emission

General information of emissions is explained in this section. The emissions of alcohol fuel combustion can be found in section **2.5**

Unburned hydrocarbons

Generally, the compression ignition engine is known for producing less unburned hydrocarbons (UHCs) compared to spark ignition engine as they have different ignition processes [Pulkrabek, 2004]. Since gasoline engine adopted premixed combustion, it has high possibility to emit a larger quantity of unburned hydrocarbons than compression ignition engine. The fundamental reason for UHCs emission is that unburned fuels are emitted from cylinders. Major causes of UHCs emission are quenching, crevice losses and oil adsorption [Königsson, 2012]. Additionally, fuel slip during scavenging process also contributes to UHCs emission.

Quenching: It occurs due to cold temperature of the cylinder wall, which is called as wall-quenching. During combustion process, the flame in the cylinder stops burning near the cold areas as flame propagation is hindered by cold temperature as shown in **Figure 2.4.1.** In result, hydrocarbon near the wall remains unburned due to incomplete combustion. [Warnatz, J et al., 1999]

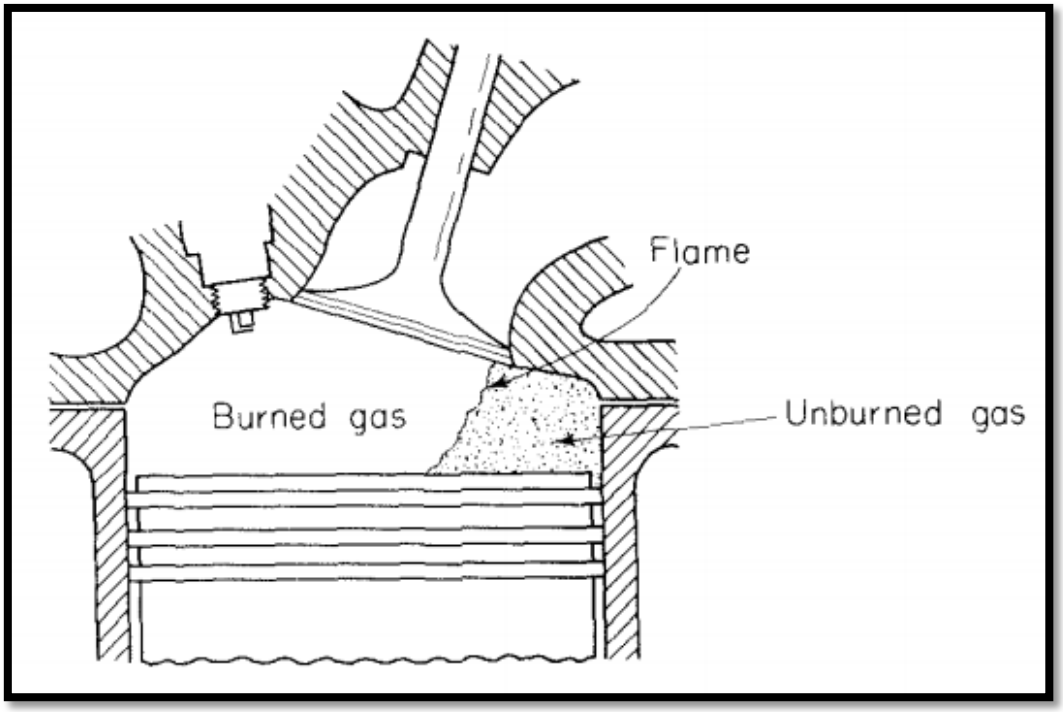

Figure 2.4.1 Flame quenching in the cylinder [Flagan et al., 1988]

Crevice losses: Crevice losses take up the largest portion of UHCs emission among the three causes. This phenomenon is noticeable in premixed combustion engines. In the cylinders, there are some gaps, which are called as crevice, such as piston ring pack, head gasket and the small volume between the piston and cylinder wall [Flagan et al., 1988]. The premixed mixtures are moved into the gaps where temperature is comparatively lower. When the flame propagates, it cannot reach to these cold regions so that HC remains unburned. During expansion process, the unburned HC is exposed to combustion gases and it escapes from the combustion chamber through exhaust valves together with exhaust gases.

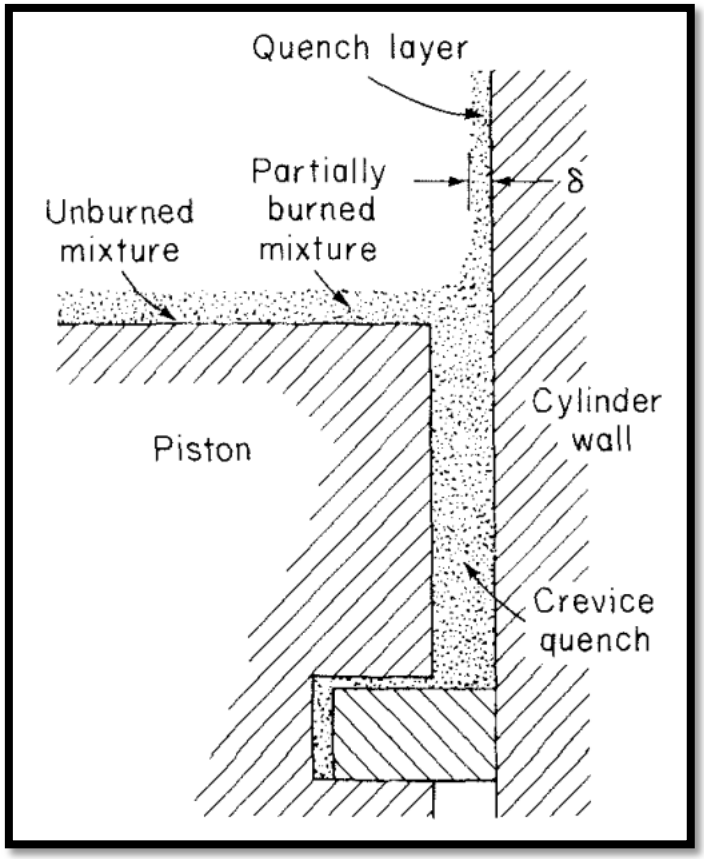

Figure 2.4.2 Schematic of quenching layer and crevice volume [Flagan et al., 1988]

Adsorption: Pressure difference between compression process and expansion process is a cause of adsorption. During the compression stroke, pressure in the cylinder goes high and it forces HC to seep into oil layer on the cylinder wall. During the expansion stroke, however, pressure in the cylinder decreases as piston goes down to BDC. The absorbed HC gets out of oil layer and is ejected together with exhaust gases.

Carbon monoxide

Carbon monoxide (CO) is one of the fatal emissions as high concentration of CO causes serious health problems to human being. It is scentless gas and is a result of incomplete combustion. Low temperature and pressure in cylinders or short of O_2 during the combustion process are the main causes of incomplete combustion. CO is generated from an intermediate step in the process of

converting to CO_2. Failure of fully oxidized to CO_2 due to lack of OH radicals causes the formation process to stop at CO.

$$\mathrm{CO} + \mathrm{OH} \Leftrightarrow \mathrm{CO}_2 + H \tag{2.1}$$

Even if engine runs in stoichiometric condition, there must be fuel rich regions because achieving perfect homogeneity is very difficult. In this result, CO emission is still substantial. On the other hand, operation of the engine in lean-burn condition contributes to reduction of CO until excessively lean mixture causes the flame to quench [Heywood, 1988]. **Figure 2.4.3** illustrates the relation between CO emission and equivalent ratio.

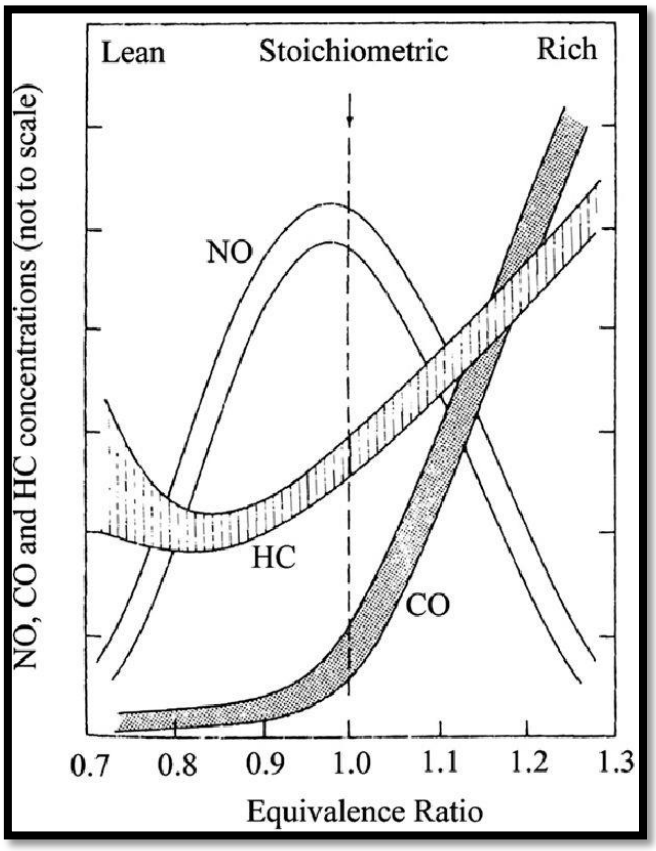

Figure 2.4.3 Relation between Air/Fuel ratio and NO, CO and HC concentration [Heywood, 1988]

One possible solution to deal with CO emission is to apply after-treatment, which is oxidation catalyst. It effectively removes CO [Dou. 2012].

Nitrogen oxides

Nitrogen oxides (NO_x) are a result of chemical reaction between nitrogen and oxygen. Nitrogen exists not only in the air but in the fuel as well. NOx causes serious environmental problems because it destroys the ozone layer. In addition, NO_x is a threat to human's body as it is the cause of respiratory diseases. NO_x mainly consists of NO, NO_2 and N_2O, although quantities of N_2O is ignorable (< 1%). NO accounts for around 90% to 95% of entire NO_x emission and NO_2 emissions make up 5% to 10%. [Staperma, 2010c] The formation of NO is called as Zeldovich-mechanism, which consists of three reversible chemical reactions [Kumar, 2010].

$$\mathrm{O} + \mathrm{N}_2 \Leftrightarrow NO + N \tag{2.2}$$

$$\mathrm{N} + \mathrm{O}_2 \Leftrightarrow NO + O \tag{2.3}$$

$$\mathrm{N} + \mathrm{OH} \Leftrightarrow \mathrm{NO} + \mathrm{H} \tag{2.4}$$

First reaction takes place in very high temperature as it has high activation energy. It can be observed that first reaction can supply nitrogen for second reaction, which also produces NO. **Figure 2.4.4** shows Nox formation with respect to temperature.

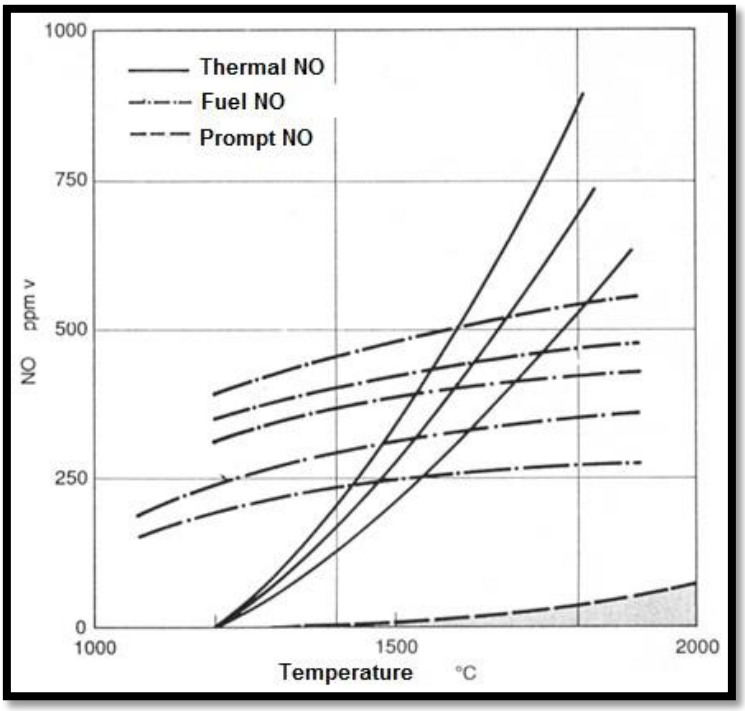

Figure 2.4.4 Relation between NO formation and temperature [Kumar, 2010].

Fuel NO is produced by the organically bound nitrogen in the fuel. Compare to nitrogen in the air, nitrogen in the fuel has weak bond so it can easily convert into NO. Thermal NO is generated by the nitrogen in the air. It is highly dependent on temperature and it starts forming over 1000℃. Prompt NO is formed in the flame front with fuel-rich condition. It is formed with relatively lower temperature than thermal NO. In typical engine combustion, only 5 to10% of NO is produced by prompt NO and 90 to 95% of NO is generated by thermal NO. [Gunter P et al., 2006]

2.5 Dual fuel engine

Fundamental principle of dual fuel engine is that high reactivity pilot fuel induces combustion of low reactivity primary fuel. Instead of spark in SI engine, dual fuel engine uses the pilot fuel. This pilot fuel automatically ignites near Top Dead Center by heat of compression. In addition, the pilot fuel contributes to both ignition and heat release during combustion. This concept has widely been adopted in natural gas engine. There are many dual fuel concepts which are widely adopted these days [Mestemaker et al,. 2016]. Among them, direct injection and port injection type will be discussed in this section.

2.5.1 In-cylinder direct injection with high pressure

In dual fuel engine, the injection of liquid pilot fuel proceeds earlier than injection of primary fuel. When primary fuel injection takes place, it should be directly injected into the engine cylinder at very high pressure. Normally this injection process occurs when the piston gets close to Top Dead Center. The main reasons for high pressure of primary fuel injection are to overcome the high in-cylinder pressure around TDC and to reduce the injection duration of primary fuel since a large amount of primary fuel needs to be injected. The high pressure accelerates the injection speed of primary fuels and this leads to stable ignition and decrease of combustion duration. In result, shorter combustion duration contributes to higher engine efficiencies because mostly heat release process takes place just after TDC where expansion process starts. In this regard, keen control of injection pressure is a critical aspect in direct injection engine. If injection pressure is in excess of its required level, the fuel jets from injection nozzle would over penetrate the combustion chamber and finally reach to the cylinder and piston surface. This causes

quenching problem, increase of heat loss to the wall and the contamination of lubrication oil in the cylinder.

Two different injection nozzle arrangements for dual fuels are mainly adopted these days. Can be used either one injector for both pilot and alcohol fuel or two separated injectors for individual fuels. The arrangement of two separated injectors is shown in **Figure 2.5.1.**

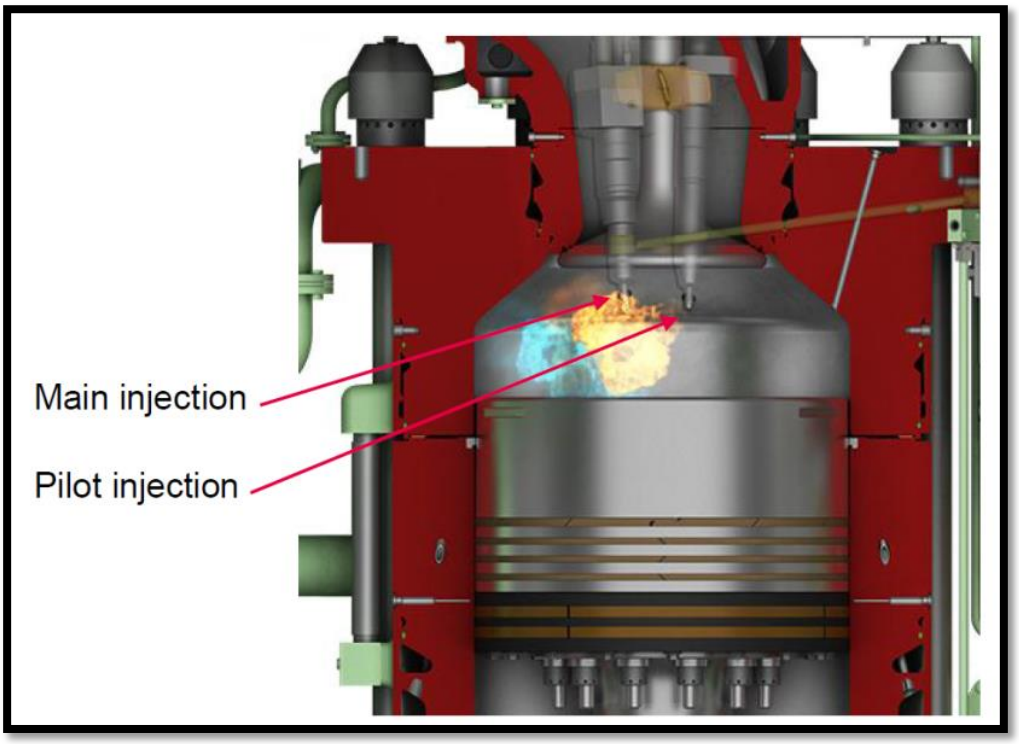

Figure 2.5.1 Two injection Nozzle for methanol dual fuel engine [Groene, 2015]

In case of using the common fuel injector as shown in **Figure 2.5.2**, it is located at the center of cylinder head and it has separated nozzle holes for diesel fuel injection and primary fuel injection. Methanol nozzle holes are circularly located around central pilot nozzle at the end of the injector body. Inside injector body, there are two separated needles and springs for pilot and primary fuel to inject the fuels independently. Detail structure of the injection nozzle is shown in **Figure 2.5.3.**

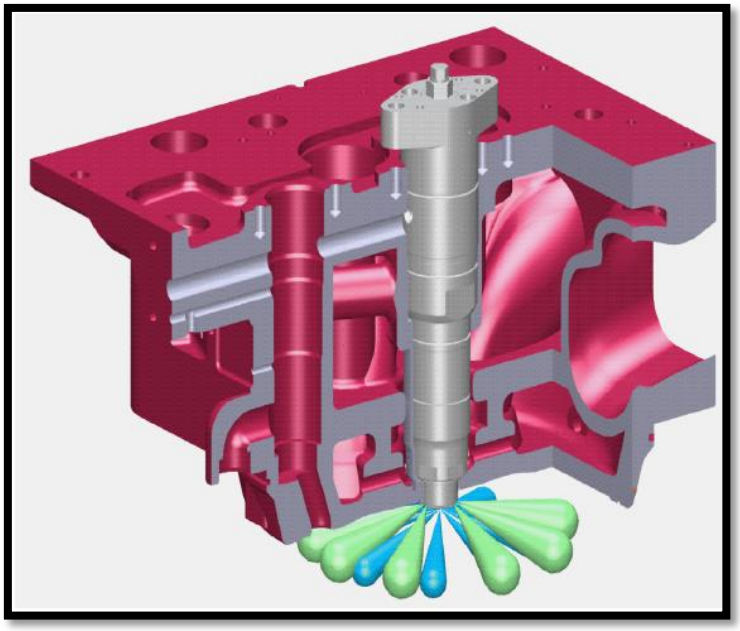

Figure 2.5.2 Single methanol-diesel injector [Haraldson, 2015]

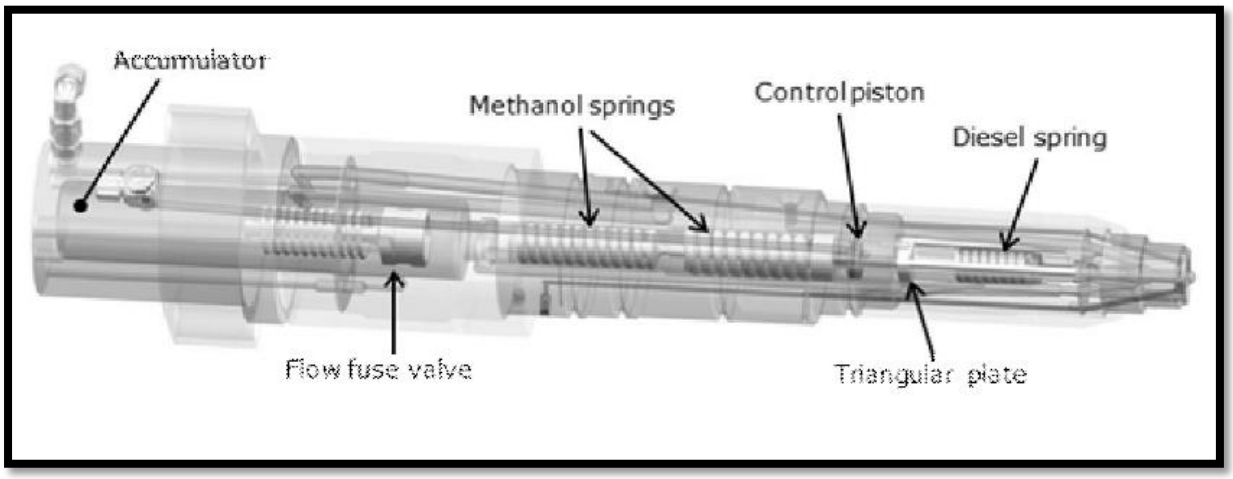

Figure 2.5.3 Overview of single methanol injector [Stojcevski et al., 2016]

The engines which employ in-cylinder direct injection concept usually inject only diesel fuel when the engines run in very low load condition or when the engines need to start. Since low cetane number is the characteristics of primary fuel, ignition ability and stable combustion are poorer than pilot fuel. For this reason, most of dual fuel engines nowadays use only diesel fuel when it starts or at very lower load condition. Later on, only diesel mode gradually switches over to dual fuel operation. In this phase, quantity of pilot fuel decreases. On the other hand, supply of

primary fuel proportionally increases. Reverse procedure takes place during engine shut down. **Figure 2.5.4** illustrates overall operation load with respect to different fuels.

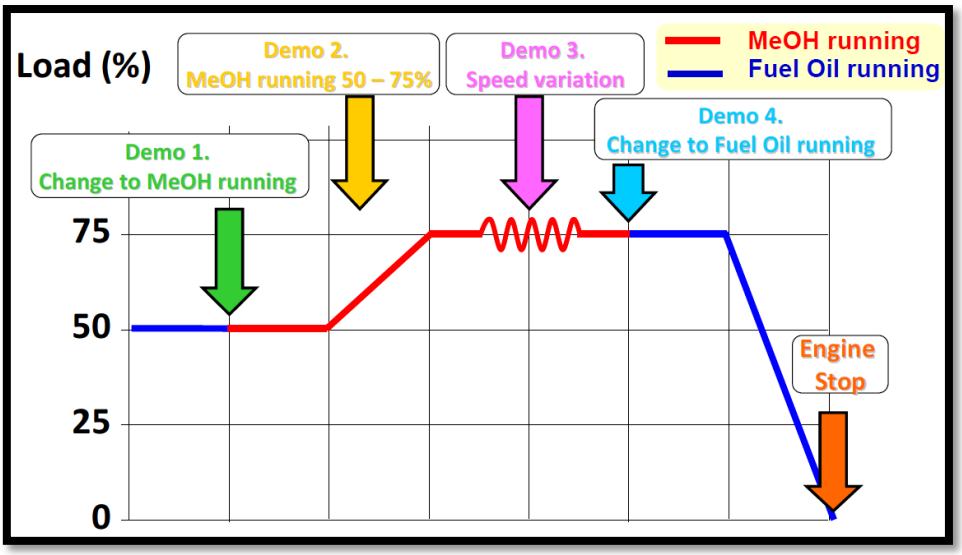

Figure 2.5.4 Operation with different fuels based on Engine load [Groene, 2015]

Combustion characteristics of in-cylinder direction injection concept

In case of in-cylinder direct injection concept, injection of liquid pilot fuel takes place first, followed soon after by the injection of primary fuel. During the atomization phase of pilot fuel, injected pilot fuel mixes with in-cylinder air, which is called as premixing process. This pre-mixture leads to rapid increase of pressure and temperature once ignition starts. However, primary fuel which is injected right after pilot fuel injection has high heat of evaporation and it prevents from prompt increase of pressure and temperature due to heat absorption. The heat from premixed combustion process expedites evaporation of primary fuel. In results, peak heat release value in premix combustion decreases and combustion duration of primary fuel can be reduced [Kang, 2002]. In addition, lower temperature during the premixed combustion phase can reduce NOx formation. **Figure 2.5.5** illustrates heat release rate of in-cylinder direct injection methanol engine.

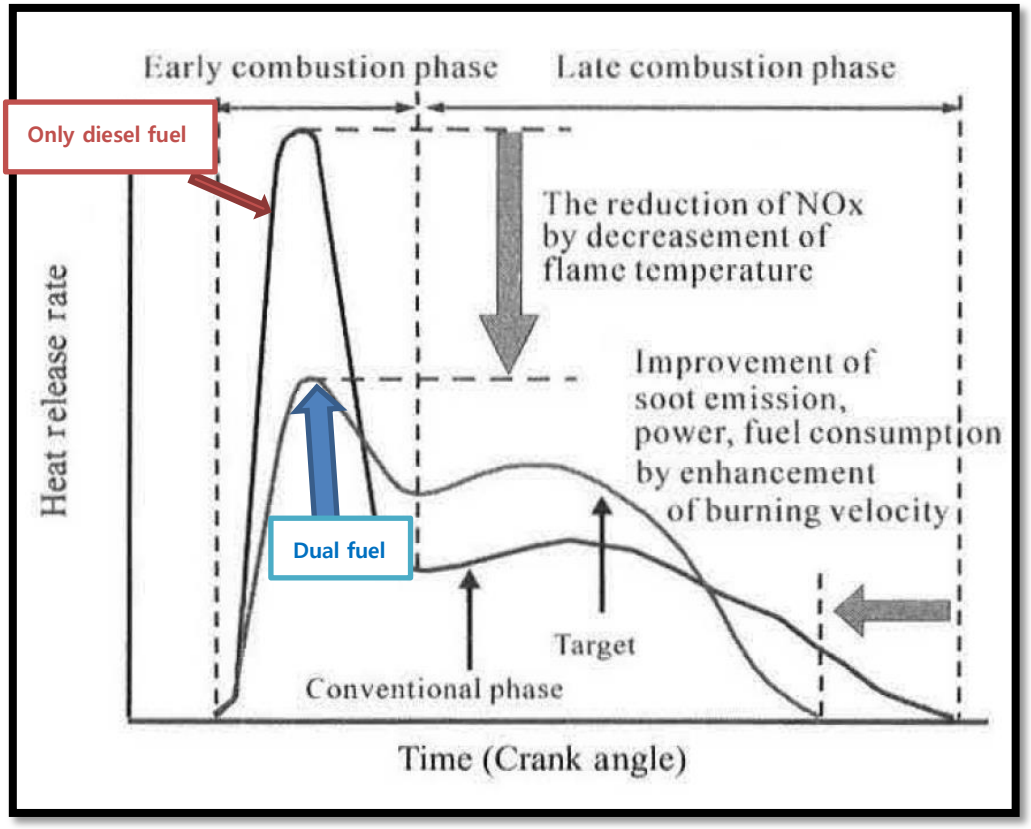

Figure 2.5.5 Heat release rate of in-cylinder direct injection methanol engine [Kang, 2002]

After pilot fuel is injected into the cylinder, initial ignition simultaneously begins at multiple points. Flames which are generated by pilot fuel start to spread outward from the center of ignition points to the immediate air-fuel mixtures. This phenomenon triggers the mixture to commence ignition. The flame from an ignition point is not able to travel far distance before it meets flames from adjacent regions. In this respect, there is less possibility to have knocking problems in spite of high compression ratio [Karim, 2015]. Once primary fuel injection takes place, primary fuel travels more distance than diesel fuel due to its poor ignition ability. While it travels, primary fuel absorbs the heat from pilot fuel combustion thereby increasing the amount of air-primary fuel mixtures. With the aid of relatively fast flame propagation of alcohol fuels, duration of diffusive combustion decreases. [Kang, 2002]

2.5.2 Premixed dual fuel engine

The concept of premixed combustion includes both SI engine and CI engine characteristics. As in

SI engines, primary fuel is existing in the form of homogeneous mixture with air in the cylinder before it starts combustion. The premix process of primary fuel begins in the inlet manifold after turbo charger as shown in **Figure 2.5.6.** With help from velocity of supply air and swirls in the cylinder, primary fuel is well mixed with air. To ignite low reactivity homogenous mixture, the pilot fuel is injected close to TDC to induce in-cylinder combustion. This pilot fuel ignites by the heat of compression like conventional compression ignition engines. Therefore major characteristics of dual fuel combustion can be defined as the combination between mixing-controlled diffusion combustion of CI engine and turbulent flame propagation of SI engines.

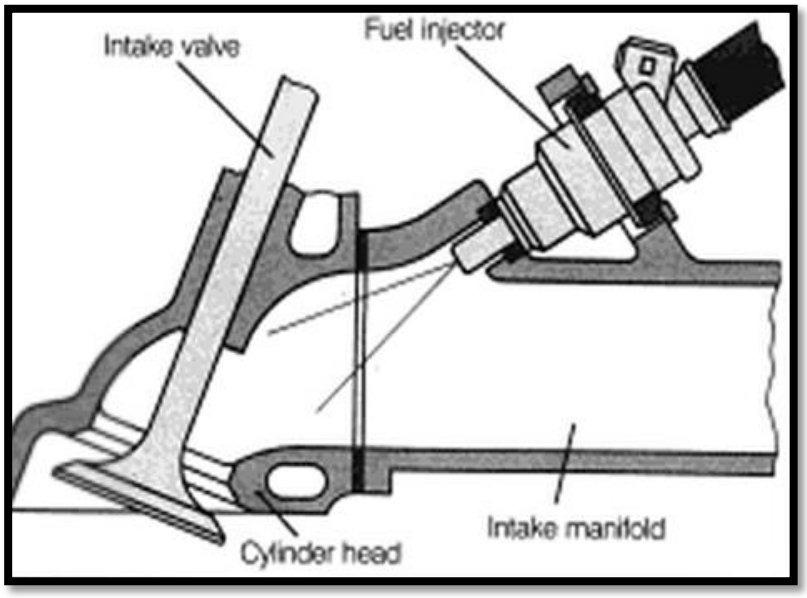

Figure 2.5.6 Port injection engine [Georgescu, 2013]

Combustion characteristics of premixed dual fuel concept

The combustion process of premixed dual fuel engine is affected by both ignition characteristics and injection spray patterns of pilot fuel. In addition, the concentration of pre-mixtures in the cylinder is also a key factor to determine combustion characteristics. [KARIM, 2015] The overall combustion process of dual fuel engine can be reflected by heat release rate. The heat release characteristics during combustion process are dependent on complex physical and chemical interactions between pilot and primary fuel. Unlike the heat release in conventional diesel engines, which mainly consists of premixed combustion and diffusive combustion, the major components of heat release rate of premixed dual fuel engine consist of three overlapping regions. Both

conventional and premixed dual fuel heat release diagrams are shown in **Figure 2.5.7 & Figure 2.5.8.**

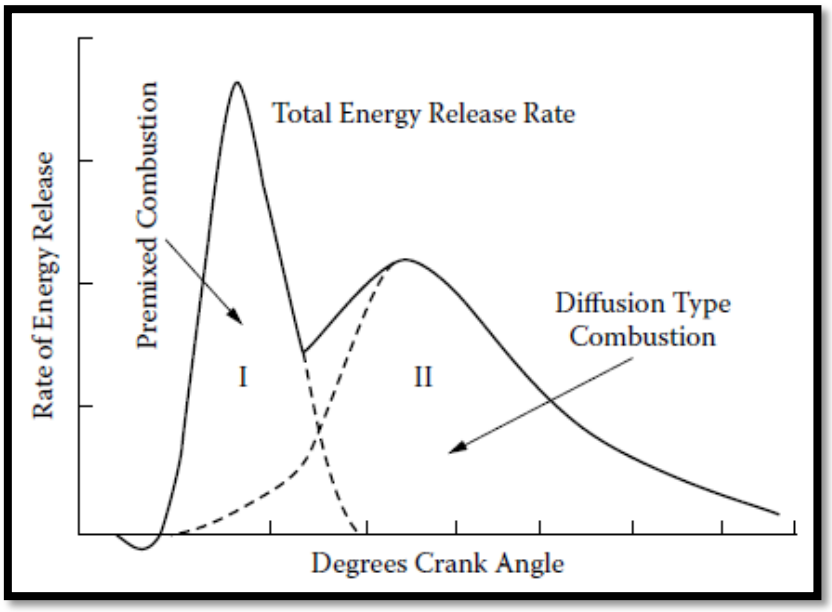

Figure 2.5.7 Heat release diagram of a conventional diesel engine [KARIM, 2015]

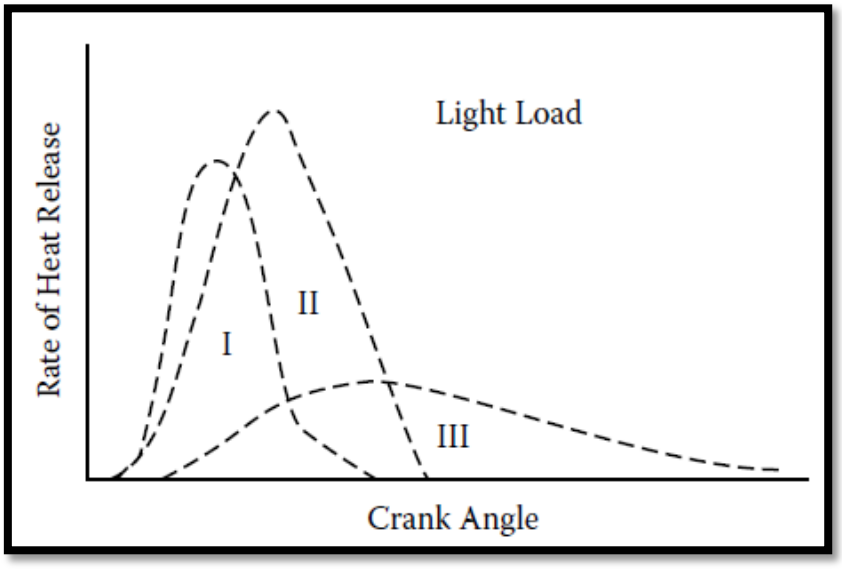

Figure 2.5.8 Heat release diagram of premixed dual fuel engine at light load [KARIM, 2015]

■ First region (I) stands for start of combustion by pilot fuel. In this region, mixtures of primary fuel-air are rarely present so that majority of heat release comes from the pilot fuel combustion. Very rapid rises in pressure and temperature caused by the pilot fuel ignition can be observed in region (I). In spite of relatively little portion of the heat release, mixtures of primary fuel-air also partly contribute to heat release in the region as small amount of the mixtures can entrain into the combusting pilot jet. In addition, the outer region of the combusting pilot jet always contacts with relatively richer fuel mixture in the cylinder.

■ Second region (II) represents the combustion which takes place in the immediate vicinity of combustion center of the pilot fuel. No continuous flame propagation can be seen in the center of pilot combustion as the very lean primary fuel mixtures are present in that zone. However with the increase of pilot injection quantity, the size of pilot combustion zone expands accordingly. Consequently, a large amount of the surrounding mixtures can have more chance to entrain into the pilot combustion region. This leads to widening of the burning regions in the vicinity of the pilot combustion zone. At this stage, partial flame propagation takes place and pre-ignition reaction activity of remaining mixtures increases due to greater heat release and temperature rise.

■ Third region (III) is formed by flame propagation through the primary fuel-air mixtures. As flame propagation spreads outward from the immediate vicinity of pilot combustion, the flame will be exposed to higher concentration of the mixtures. In the meantime, as piston goes up to TDC position, the mixtures are subjected to higher temperature and pressure. These phenomena eventually trigger off the turbulent flame propagation throughout the rest of unburned mixtures. Especially, third region (III) is highly affected by engine load as the injection amount of primary fuel varies with respect to engine load. For example, more primary fuel is injected at higher load and this leads to increase of the pre-mixture concentration in the cylinder. Figure 2.5.9 shows heavy load condition. Overlap between second region (II) and third region (III) become significant with heavy load operation.

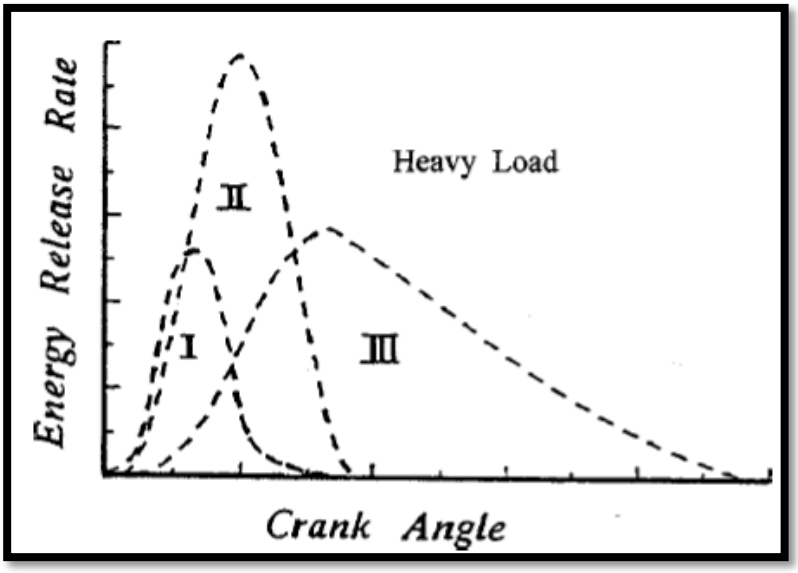

Figure 2.5.9 Heat release diagram of premixed dual fuel engine at heavy load [KARIM, 2015]

With a constant pilot injection quantity, heat release rate variations based on diverse pre-mixtures concentrations are well illustrated in **Figure 2.5.10**. As the concentration of pre-mixtures increases, it can be observed that the size of region (III) correspondingly grows.

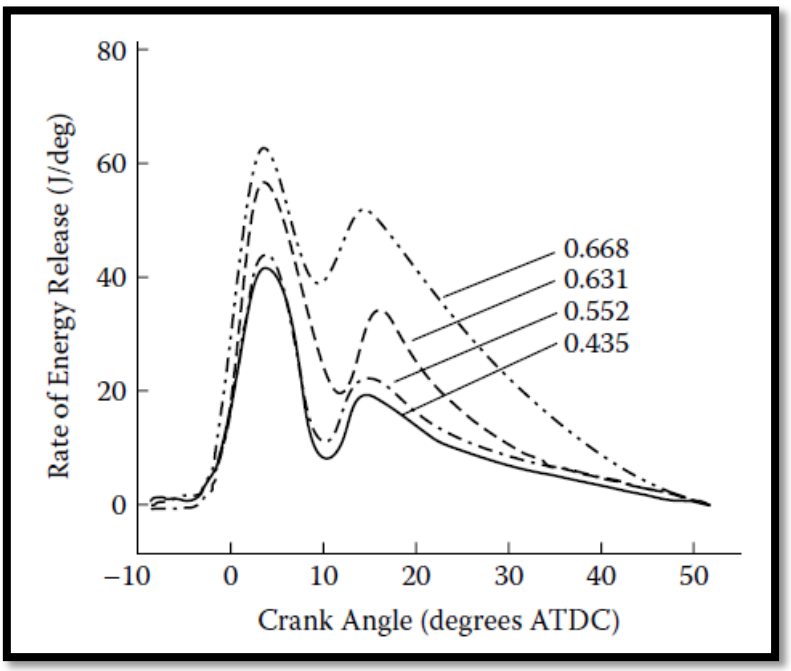

Figure 2.5.10 Heat release variation with respect to different equivalence ratio [KARIM, 2015]

2.5.3 Current application

In maritime industry, dual fuel concept is preferred technology and has dominant position on the engine market due to its unique advantage, which is fuel flexibility. The uncertainties of alcohol fuel price and availability in the future are the significant concerns for ship's owners. With dual fuel concept, the engine is able to operate in only diesel fuel mode as an alternative. It enables vessels to travel many places even though there is no supply for alcohol fuels. In addition, when price of alcohol fuel becomes higher than fossil fuel, vessels can use fossil fuel as a primary energy and it can be easily supplied from the existing fuel infrastructures. In fact, fuel price is the most important concern for ship's owners so that most of fuel selection decisions are made based on the fuel price.

Direct injection type

This concept is adopted by both Wärtsilä and MAN B & W. The major distinction between these engine makers is that Wärtsilä engines use only one fuel injector to distribute both diesel and methanol fuel. On the other hand, MAN engines have two separated fuel injectors for both fuels. Engine performance of current methanol engines will be discussed as below.

2.5.3.1 MAN B & W Methanol Engine

The engine test was carried out by 7S50ME-B9.3-LGI engine, which was the world's first 2-stroke methanol engine in the markets. The detail engine specifications are shown in **Table 2.5.1**. The proper amount of pilot fuel to guarantee the stable methanol fuel ignition is considered to be around 5 % of the diesel fuel consumption at MCR in only diesel oil mode. [Stefan Mayer et al., 2016]

Table 2.5.1 Engine specification of 7S50ME-B9.3-LGI [Stefan Mayer et al., 2016]

Engine type	Two-stroke, direct injection, crosshead, uniflow scavenging
Turbocharger	MAN: TCA55-21 with turbine bypass valve opened at high load
Fuel	Diesel and methanol
Cylinders	7
Bore	0.5 m
Connection rod	2.214 m
Stroke	2.214 m
Compression volume	16 l/cyl
Power	8,470 kW
MEP	16.9 bar
Speed	99 rpm
Max. pressure	185 bar

Heat release rate (50% load VS 100% Load)

In **Figure 2.5.11**, DI and LGI stand for Diesel Injection (Only diesel operation) and Liquid Gas Injection (Methanol operation), respectively. In LGI mode, initial heat release is produced by diesel premixed combustion. After initial combustion takes place, methanol fuel starts injecting onto ongoing combustion in liquid phase. Due to the heat of evaporation of methanol fuel, liquid methanol fuel absorbs combustion heat to vaporize. This heat of evaporation effect is observed on the graph below. There is a gradient change in heat release rate right after TDC. Additionally, this heat absorption mitigates rapid increase of heat release so that the peak point of heat release rate decreases when switching diesel fuel to methanol fuel. It can be observed that overall combustion duration becomes shorter in methanol operation.

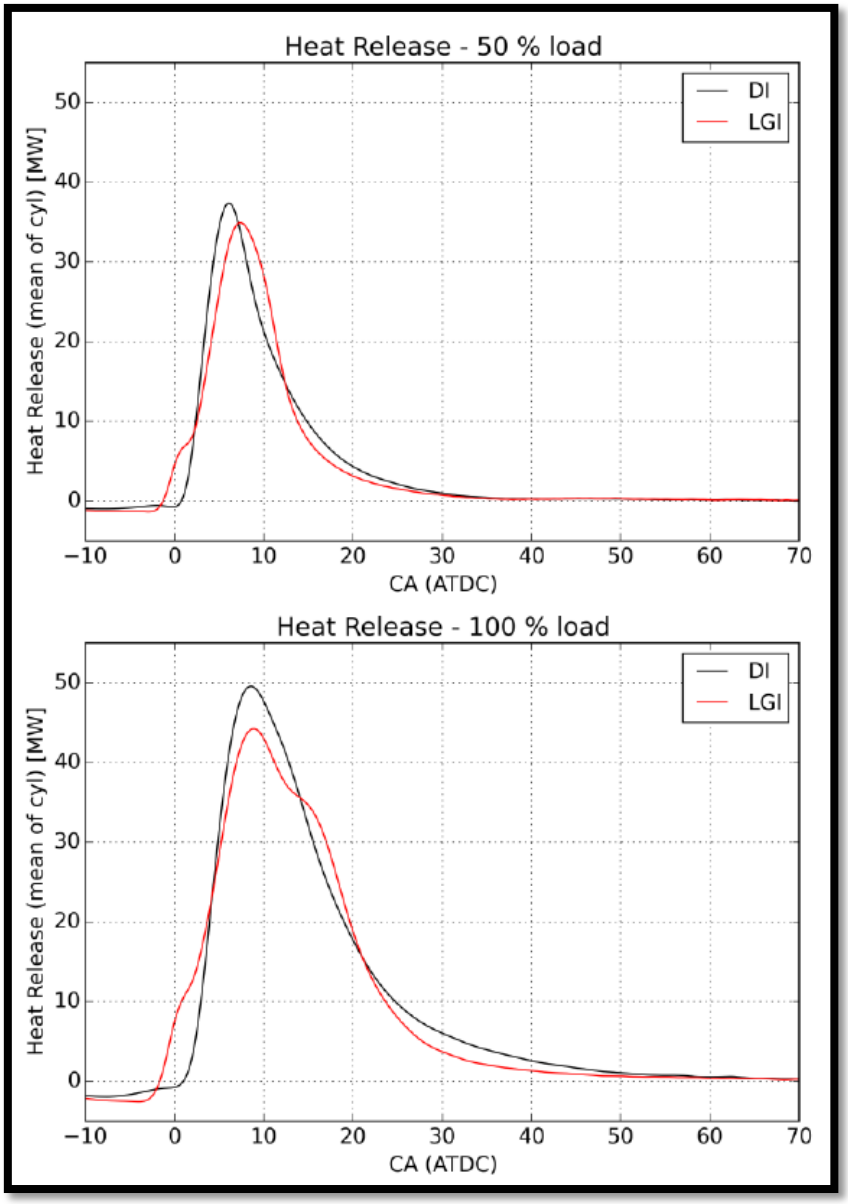

Figure 2.5.11 Heat release rate 50% and 100% [Stefan Mayer et al., 2016]

Scavenging air pressure (T/C air pressure)

Although higher mass flow went into turbo charger during methanol operation due to its lower LHV, scavenging air pressure was lower than diesel operation, which can be seen in **Figure 2.5.12**. The decrease of combustion duration is the key to understand this phenomenon. It is proved by the heat release graph that combustion duration become shorter when methanol was used as a primary fuel. Consequently shorter combustion duration improved engine efficiency. It means that

more energy was consumed during in-cylinder process to improve the efficiency. As a result, less energy allowed going into turbo charger in the end. This effect is large enough to compensate the effect of increased methanol fuel mass. [Stefan Mayer et al., 2016]

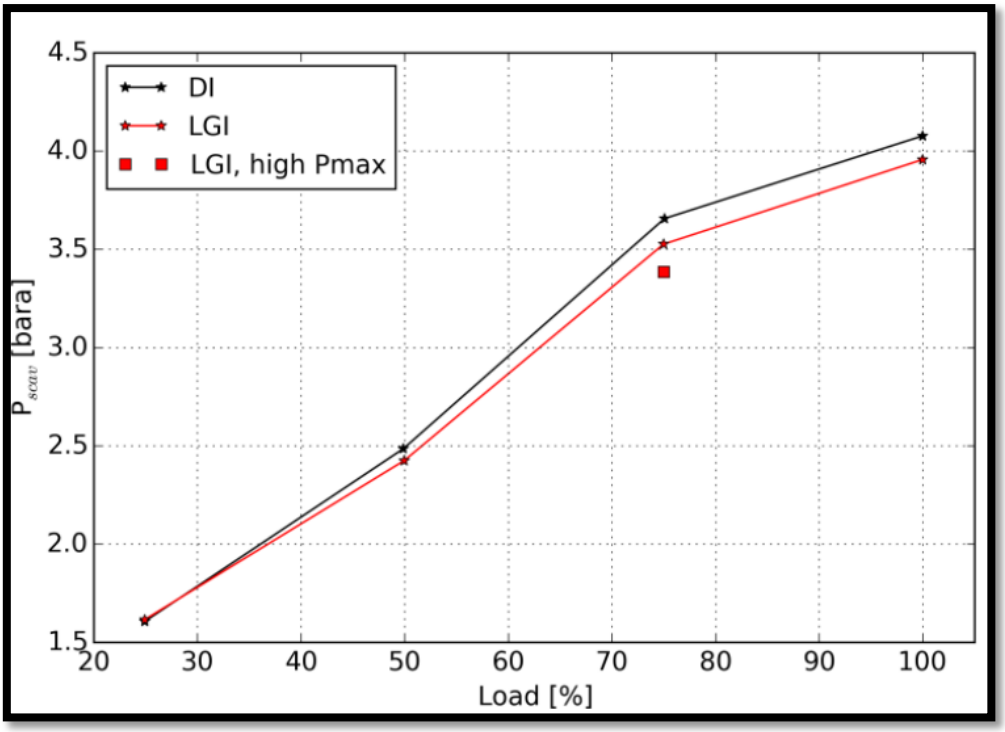

Figure 2.5.12 Scavenge air pressure [Stefan Mayer et al., 2016]

NOx Emission

Figure 2.5.13 illustrated the NOx emission test result**.** NOx emission of methanol combustion reduced by 30% compared to diesel combustion. This is mainly due to the higher heat of evaporation for methanol. It helps to decrease maximum in-cylinder temperature. [Kang, 2002]

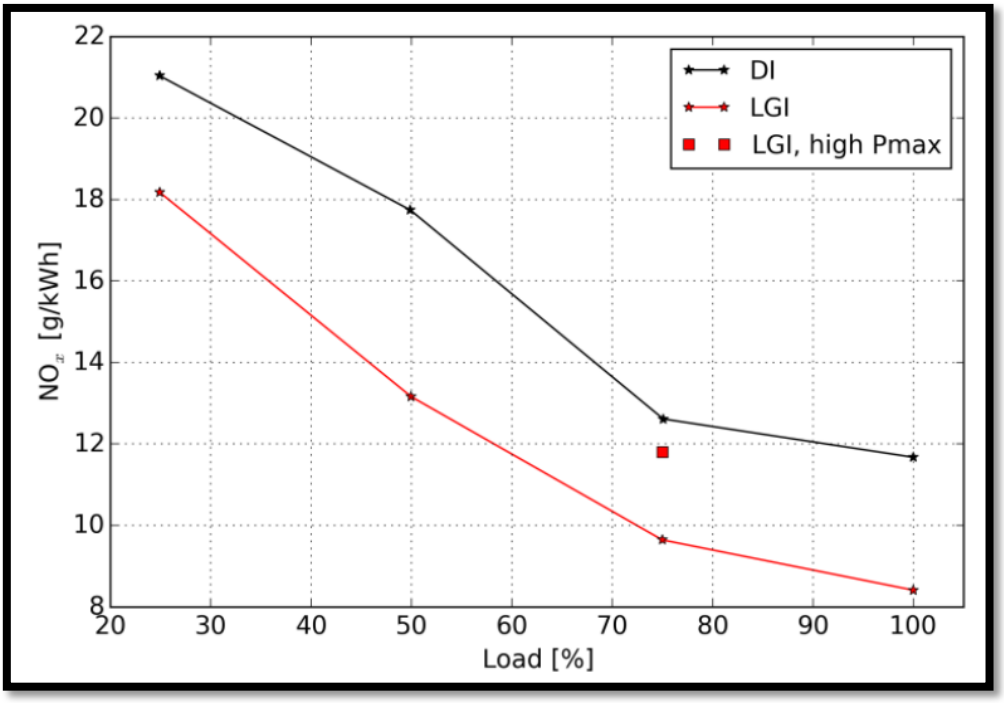

Figure 2.5.13 NOx Emission comparison (Diesel VS Methanol) [Stefan Mayer et al., 2016]

CO Emission

One reason for lower CO emission during methanol combustion is that the methanol fuel jet facilitates the effective air-fuel mixing. It helps to achieve complete combustion. In addition, the chemical structure of methanol proves that it contains oxygen. Consequently, during combustion process, more oxygen is available for combustion. It helps to reduce CO emission because one of reasons for CO emission is shortage of O_2

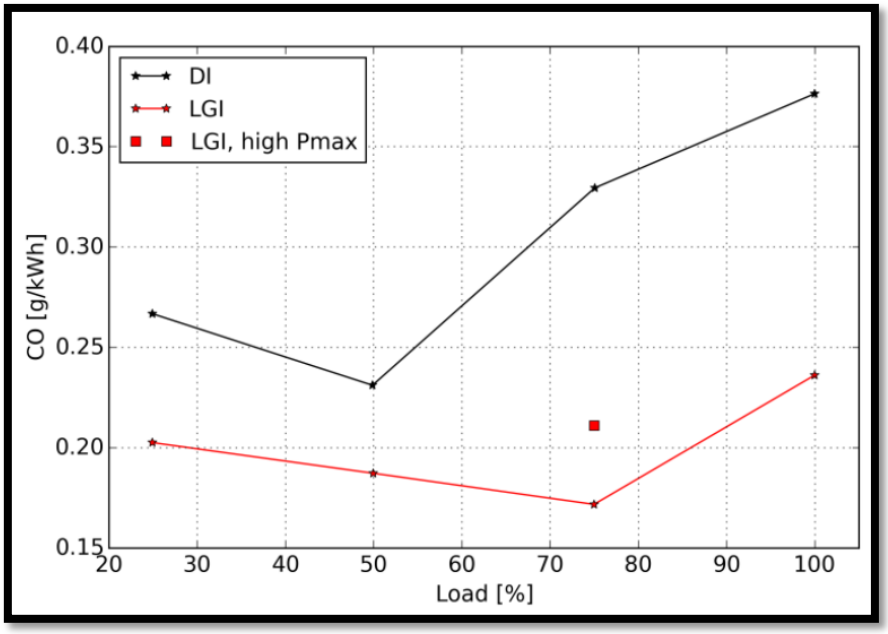

Figure 2.5.14 Specific CO emissions [Stefan Mayer et al., 2016]

HC Emission

Throughout the entire operating load range, HC emissions of methanol combustion were always higher than that of diesel combustion. This was caused by strong flame quenching effect near the combustion chamber wall due to its high heat of evaporation. In addition, fuel slip also contributed to HC emission.

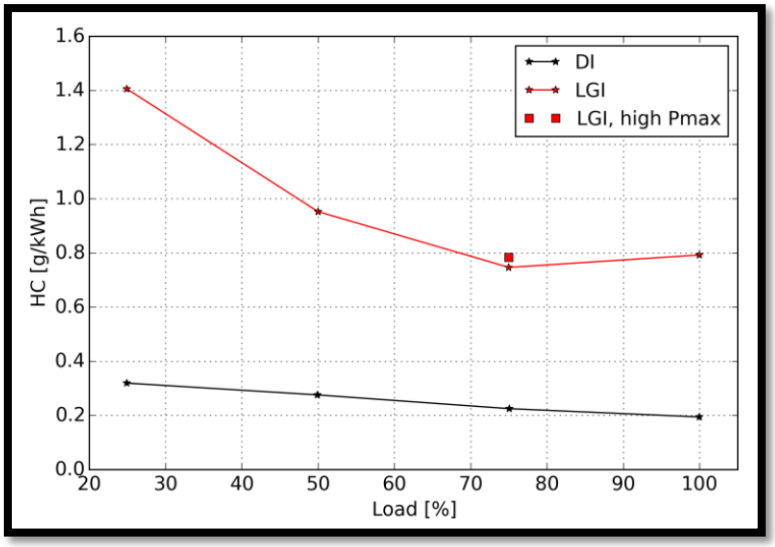

Figure 2.5.15 HC emissions [Stefan Mayer et al., 2016]

2.5.3.2 Wärtsilä Methanol Engine

Unlike MAN methanol engine, Wärtsilä adopted 4 strokes type instead of 2 strokes to convert conventional engines into methanol dual fuel engines. Overall test results are similar with MAN engine results. Wärtsilä 4L32LNGD engine was chosen to carry out the engine performance test when methanol was used as a primary fuel. The minimum operation load in methanol running mode was about 25% load. The specification of test engine can be found in **Table 2.5.2**.

Table 2.5.2 Test Engine specification, 4L 32LNGD [Haraldson, 2015]

Engine type	4L 32LNGD
Engine Maker	Wärtsilä
Stroke	4 Stroke
RPM	750
Compression ratio	13.8:1
Output	410 KW/cylinder
Inlet valve open	52 CA (BTDC)
Inlet valve close	28 CA (ABDC)
Exhaust valve open	56 CA (BBDC)
Exhaust valve close	44 CA (ATDC)

Heat release rate

The heat release rates were measured with different energy share ratios between methanol and diesel fuel. With the increase of methanol energy fraction, the peak value of heat release decreased and peak point crank angle retarded. **Figure 2.5.16** illustrates the test results of heat release rate. During the late combustion process, the downstream gradient of higher methanol fraction case (Red) is steeper than lower methanol fraction case (Green), showing faster combustion with higher methanol fraction.

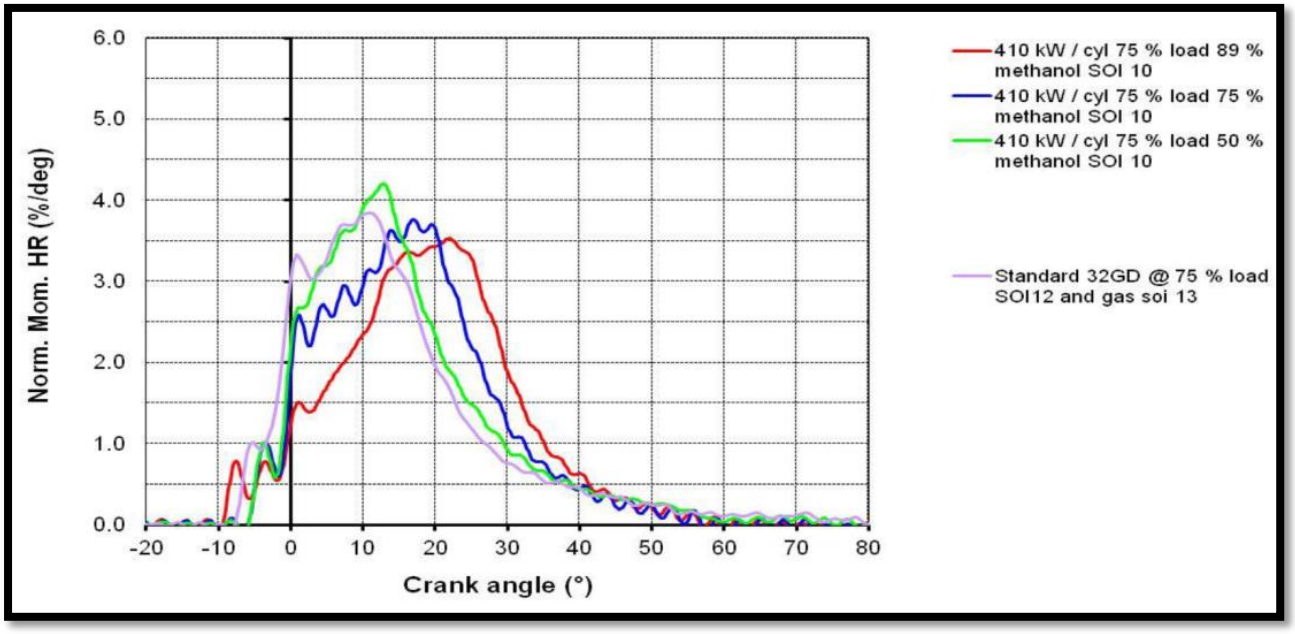

Figure 2.5.16 Heat release rate, 4L 32LNGD engine [Haraldson, 2015]

NO_x Emission

Pure light fuel oil operation at 75% load was given as reference (Red) to compare with methanol operations. **Figure2.5.17** illustrates the laboratory results and it tells that methanol operation significantly reduced NOx emissions. Methanol operations show that NOx emissions of all cases are below 6 g/KWh. It complies with Tier II NOx emission limits, which is shown in **Figure 2.5.18.**

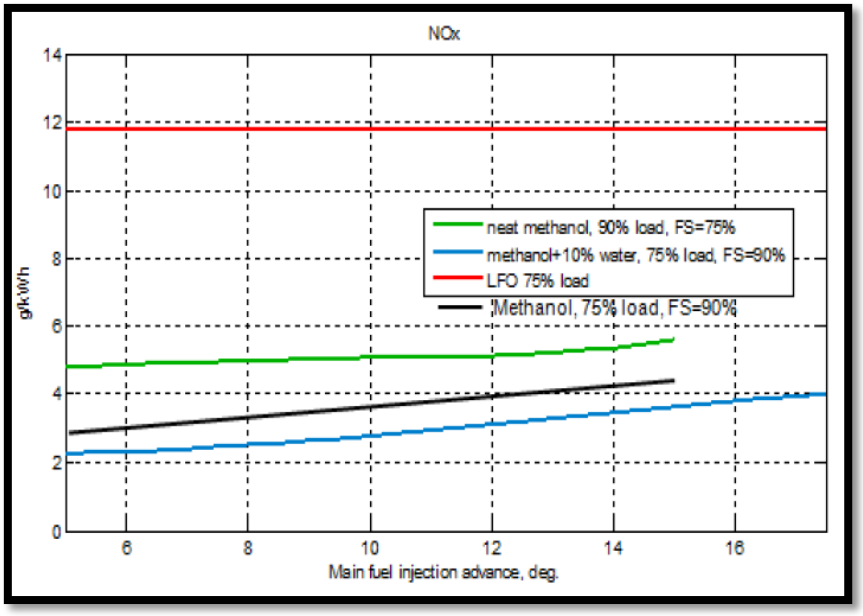

Figure 2.5.17 NOx emissions, 4L 32LNGD engine [Haraldson, 2015]

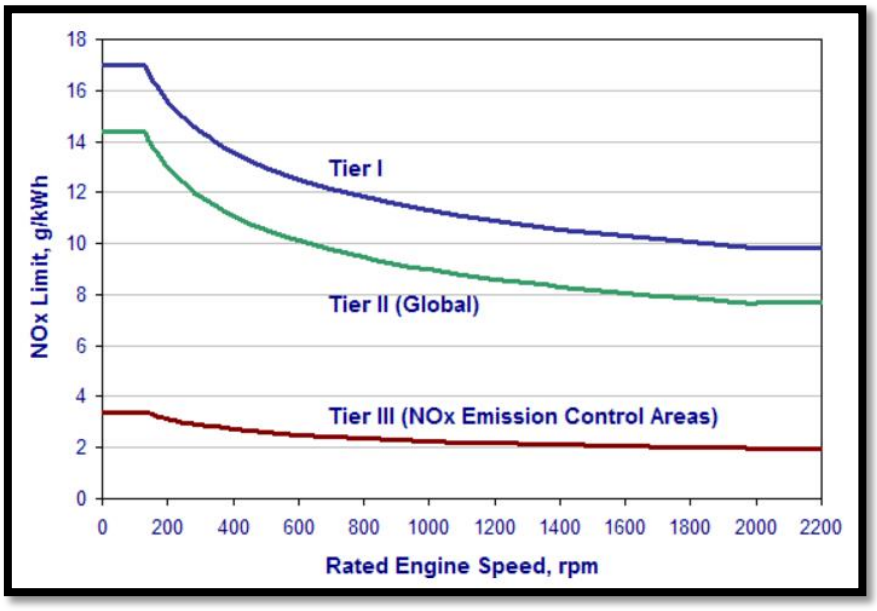

Figure 2.5.18 MARPOL Annex VI NOx Emission Limits [IMO, 2016]

3. Hypothesis

■Effects of heat of evaporation on in-cylinder temperature in dual fuel premixed engine.

Methanol fuel has distinctive characteristics in its properties compared to diesel oil. One significant difference from diesel fuel is that methanol fuel has almost 4 times higher heat of vaporization [KJ/KG]. In other words, methanol fuel requires larger quantity of heat energy to evaporate fuel droplets. Therefore in-cylinder temperature decreases due to heat absorption during vaporization process. This low temperature suppresses excessive combustion rate thereby the maximum in-cylinder temperature is lower than of diesel oil operation.

■Effect of fuel ratio between pilot and primary fuels on ignition delay and heat release rate

In dual fuel engine, fuel ratio between pilot fuel (Diesel fuel) and primary fuel (Methanol fuel) highly affects combustion process as it leads to change of ignition delay. Increase of methanol fuel injection prolongs ignition delay due to its high heat of evaporation value. The larger portion of methanol fuel enhances the effect of heat absorption and the lower temperature reduces chemical reaction speed. In this respect, the larger portion of methanol fuel leads to retarded start of combustion. In addition, with increase of methanol fuel, amount of heat release in premixed combustion phase increases as more pilot fuel is premixed due to longer ignition delay.

■Specific fuel consumption and brake thermal efficiency

Fuel economy is represented by brake specific fuel consumption (BSFC, g/KWh). Lower heating value (LHV) has the significant influence on the determination of BSFC. Since LHV of methanol fuel has roughly half of diesel oil's LHV, methanol dual fuel combustion has higher BSFC value than diesel combustion.

Brake thermal efficiency can be referred to as the fuel conversion efficiency. It can be described by the ratio of the engine output to the amount of fuel input. Since LHV of methanol is lower than that of diesel, more fuel needs to be injected to produce the same output. As a result, thermal efficiency will decrease with increase of methanol injection. In addition, with increase of

methanol fuel, higher cooling effect can be expected. The cooling effect decreases the temperature of in-cylinder charges and it leads to increase of flame quenching. As a result, less fuel can be converted into engine output.

4. Base models

To investigate in-cylinder process, Model C is used in this thesis, which was developed by Ding-Yu. [Ding, 2011]Model C is suitable for simulating in-cylinder process and it consists of Heat release rate model and in-cylinder process model. In the chapter, fundamental features of Model C are introduced. In addition, Model C has been built based on single-zone model. Differences between single zone and multi-zone are discussed in section **4.2** to better understand the concept of the zone.

4.1 Introduction of Model C

4.1.1 Heat release calculation model

Heat release rate is the one of the most essential information to analyze in-cylinder combustion process. Definition of Heat Release Rate (HRR) is that the chemical energy of the fuel is released by the combustion process. There are three most common definitions to describe heat release rate.

(a) Net Apparent Heat Release Rate (*NAHRR*):

$$NAHRR = \dot{\mathrm{Q}}_{\mathrm{comb}} - \dot{Q}_{loss} + \dot{E}_f = m * C_v * \frac{dT}{dt} + p * \frac{dV}{dt} \ [\mathrm{J/S}] \tag{4.1}$$

(b) Gross Apparent Heat Release Rate (*GAHRR*):

$$GAHRR = \dot{\mathrm{Q}}_{\mathrm{comb}} + \dot{E}_f = m * C_v * \frac{dT}{dt} + p * \frac{dV}{dt} + \dot{Q}_{loss} \ [J/S] \tag{4.2}$$

(c) Combustion Reaction Rate (*CRR*):

$$\mathrm{CRR} = \xi = \frac{m*C_v*\frac{dT}{dt}+p*\frac{dV}{dt}+\dot{Q}_{loss}}{u_{comb}+e_f} \ [Kg/s] \tag{4.3}$$

NAHRR is the net heat released by the fuel burning during combustion. Both in-cylinder pressure and temperature are the key factors to calculate NAHRR. However, it does not include the heat loss to the walls. On the other hand, GAHRR includes heat loss to the walls. With the definition of GAHRR, all the heat produced by combustion process can be calculated. However, it is difficult to get accurate heat loss value from the measurement. Therefore, a proper estimation of heat loss is required to increase the accuracy of GAHRR. From a physical point of view, CRR means the rate at which fuel burn. It can be calculated when GAHRR is divided by the sum of the effective combustion value (u_{comb}) and specific energy of fuel (e_f). Each term in the equations above (4.3) have physical meanings. $m * C_v * \frac{dT}{dt}$ indicates the change in internal energy due to temperature variation. $p * \frac{dV}{dt}$ presents the work done by the piston motion. $\dot{Q}_{loss}$ means heat loss to the cylinder head, piston crown and cylinder wall. The first denominator term of CRR (u_{comb}) can be defined as below,

$$\mathrm{u_{comb}} = u_{comb}^{ref} - \Delta\, u_{comb}^{ref} \tag{4.4}$$

The first term above (4.4) stands for the reference internal energy of closed system and second term indicates the change of internal energy caused by the temperature difference from the reference condition.

Based on the three definitions, Heat Release Rate can be calculated in Heat release rate model. The primary inputs of the model are in-cylinder pressure as well as crank angle. In-cylinder temperature is calculated based on ideal gas law. The final output is the Combustion Reaction Rate (CRR). With the CRR, Reaction coordinates (RCO) can be obtained after integration of CRR. The RCO is a suitable parameter for curve fitting and vibe parameters can be determined based on the RCO.

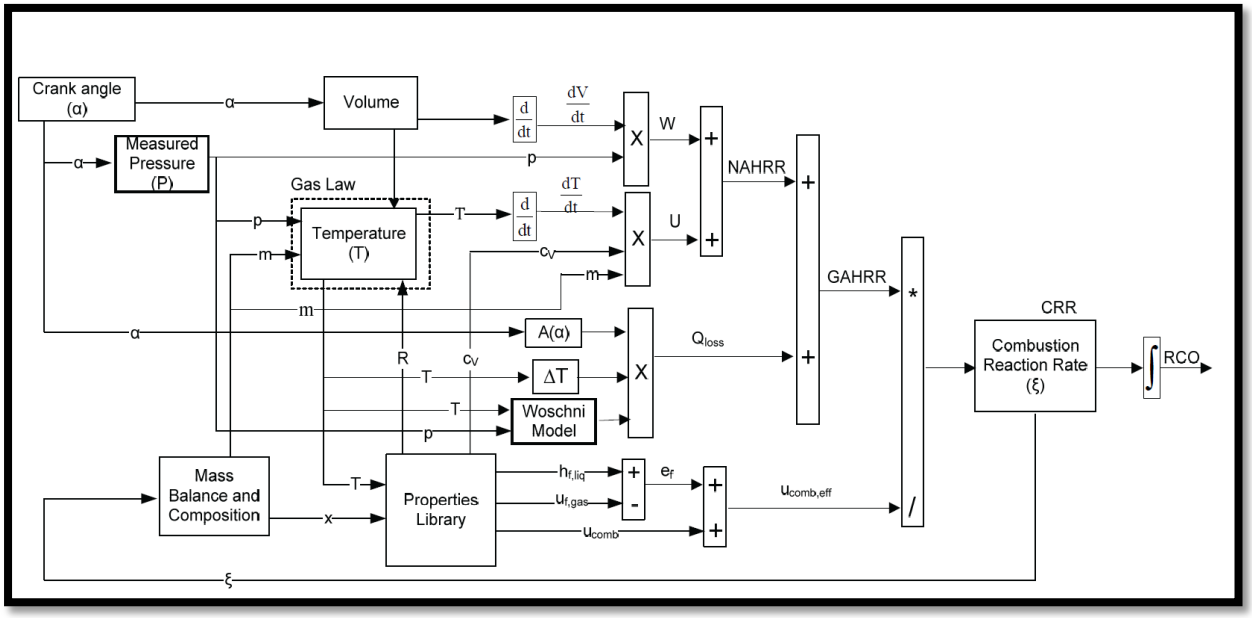

Figure 4.1 Heat release rate calculation model [Ding, 2011]

4.1.2 In-cylinder process model

To investigate and analyze in-cylinder process, understanding of fundamental features of Model C is necessary because the main purpose of the model C is to simulate in-cylinder process from inlet valve close (IC) to exhaust valve open (EO). Integration of the first law of thermodynamics (4.5) is required to calculate in-cylinder temperature, which is considered as the final output of this model.

$$\frac{\mathrm{dT}}{\mathrm{dt}} = \dot{Q_{comb}} - \dot{Q_{loss}} - p * \left(\frac{dV}{dt}\right) + \dot{E_f}\,, \tag{4.5}$$

Combustion reaction rate (ξ) is an important parameter because the heat release model is built up based on fuel burn rate, which stands for mass of fuel burnt per unit time. This parameter acts as heat source ($\dot{Q_{comb}}$) in the above equation (4.5) when it is multiplied with heat of combustion ($\mathrm{u_{comb}}$), which is a function of temperature. Moreover, reaction rate (ξ) is provided as an input value for mass balance and composition block in the form of a multiple vibe function. It helps to keep track of both the mass balance and composition in the cylinder. Output composition

becomes an input of properties library to calculate properties of the in-cylinder mixtures. In-cylinder volume is also an important parameter and is calculated by cylinder geometry, dimensions and crank angle (α). Under the assumption that engine speed is constant, the crank angle is calculated by the equation (4.6) below.

$$\mathrm{V}(\alpha) = \mathrm{A_b} * L_s * \left[\frac{1}{\varepsilon - 1} + \frac{1}{2} * \left\{\left(1 + \cos(\alpha) + \frac{1}{\lambda_{CR}} * \left(1 - \sqrt{1 - \lambda_{CR}^2 * \sin^2 \alpha}\right)\right)\right\}\right], \qquad (4.6)$$

where λ_{CR} and ε are crank radius to rod length ratio and geometric compression ratio, respectively. To calculate in-cylinder pressure, the gas law is applied and several values are necessary such as gas constant(R), mass (m), cylinder volume (V) and feedback of in-cylinder temperature (T). To calculate work (W), differential of volume ($\frac{\mathrm{dV}}{\mathrm{dt}}$) needs to be preceded and this can be performed in a simulation environment. To estimate heat loss, reliable heat transfer coefficient is calculated by using Woschni's model. The energy of fuel (E_f) stands for the energy carried by the fuel into cylinder upon entry.

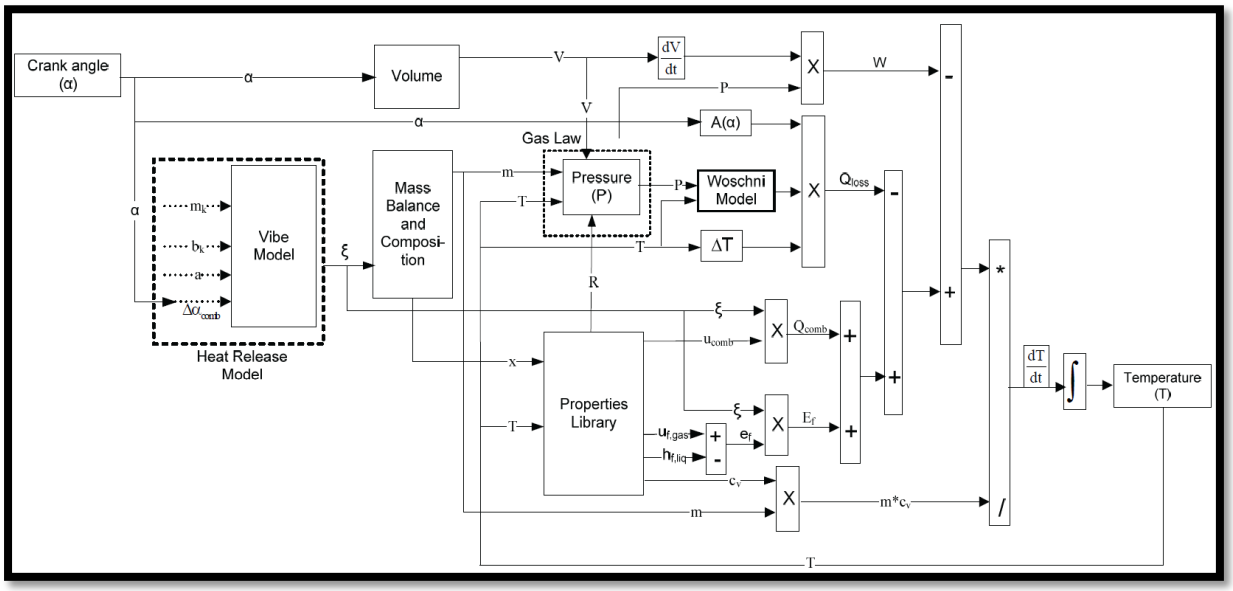

Figure 4.2 General block diagram of in-cylinder process model [Ding, 2011]

4.2 Single zone model VS Multi-zone model

4.2.1 Single zone model

Figure 4.3 describes singe-zone model. In the single-zone model, the thermodynamic properties in the cylinder are expressed in average values. There is no specific distinction between burned gas zone and un-burned gas zone. The in-cylinder contents are considered as uniform and homogeneous and spatially non-uniform thermodynamic properties are not considered in the single zone model. The advantage of single-zone is that it is easy and simple to find out the effects of in-cylinder process. In practice, during the real combustion process, burned gases form at different times and locations in the cylinder. Therefore there must be temperature gradients in the burned gases. However, due to no distinction between un-burned and burned zone, there is no temperature gradient in the cylinder with single zone concept. Since it does not consider the temperature gradient in burned gases zone or mixing gases zones between burned and un-burned gases, it is difficult to predict the accurate in-cylinder gas temperature.

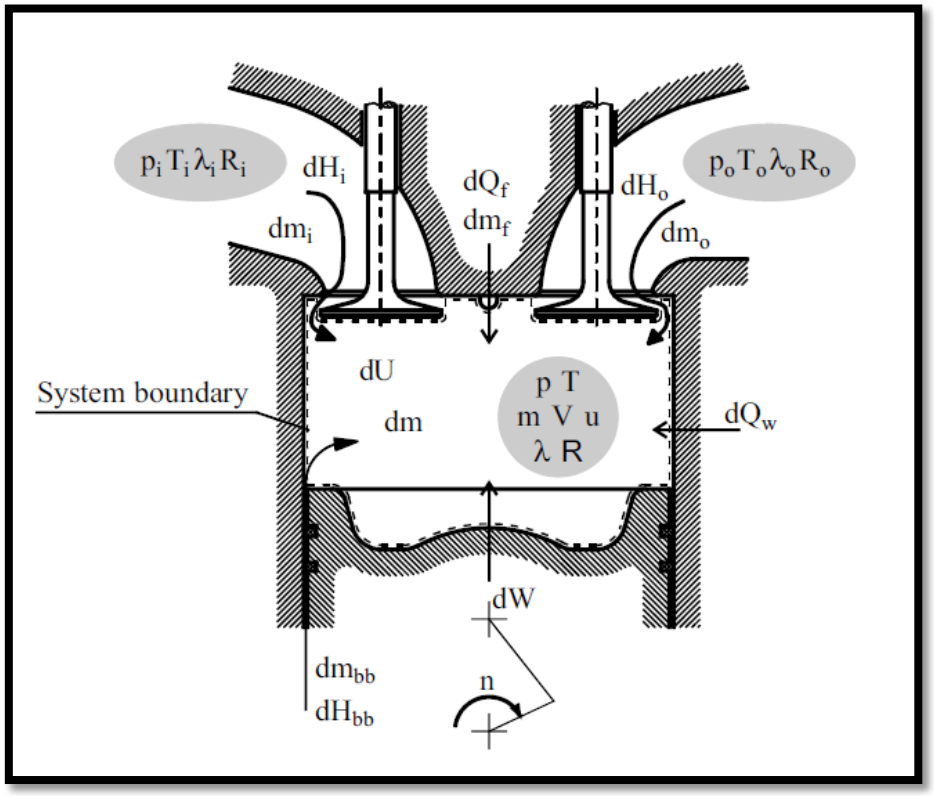

Figure 4.3 Single-zone cylinder model [Gunter P et al., 2006]

To comply with the single-zone principle, in-cylinder gas is treated as a single-zone in the control volume. Fuel droplets evaporate as soon as they are injected into the control volume. As the fuel injection rate and the evaporation rate are considered to be the same, dwelling time of the fuel droplet becomes zero. In addition, it is assumed that injected fuel droplets burn as soon as they are evaporated, which means that evaporation rate and combustion rate are identical.

4.2.2 Multi-zone model

To predict more accurate thermodynamic properties during in-cylinder process, multi-zones can be introduced. Each zone is treated as an independent thermodynamic system. Also each zone is considered to have its own uniform and homogeneous properties. **Figure 4.4** shows that two-zone model and it consists of zone 1 and zone 2. Zone division is made based on the flame front. Unburned mixtures such as fresh air, injected fuel and residual combustion products from the previous cycle are the main contents of zone 1. This zone 1 has its own thermodynamic properties. (P, V_1, T_1, λ_1). Zone 2 stands for burned mixture zone and it has different thermodynamic properties from Zone 1 (P, V_2, T_2, λ_2), except the in-cylinder pressure. However the implementation of a multi-zone concept is more difficult and complicated than single zone model.

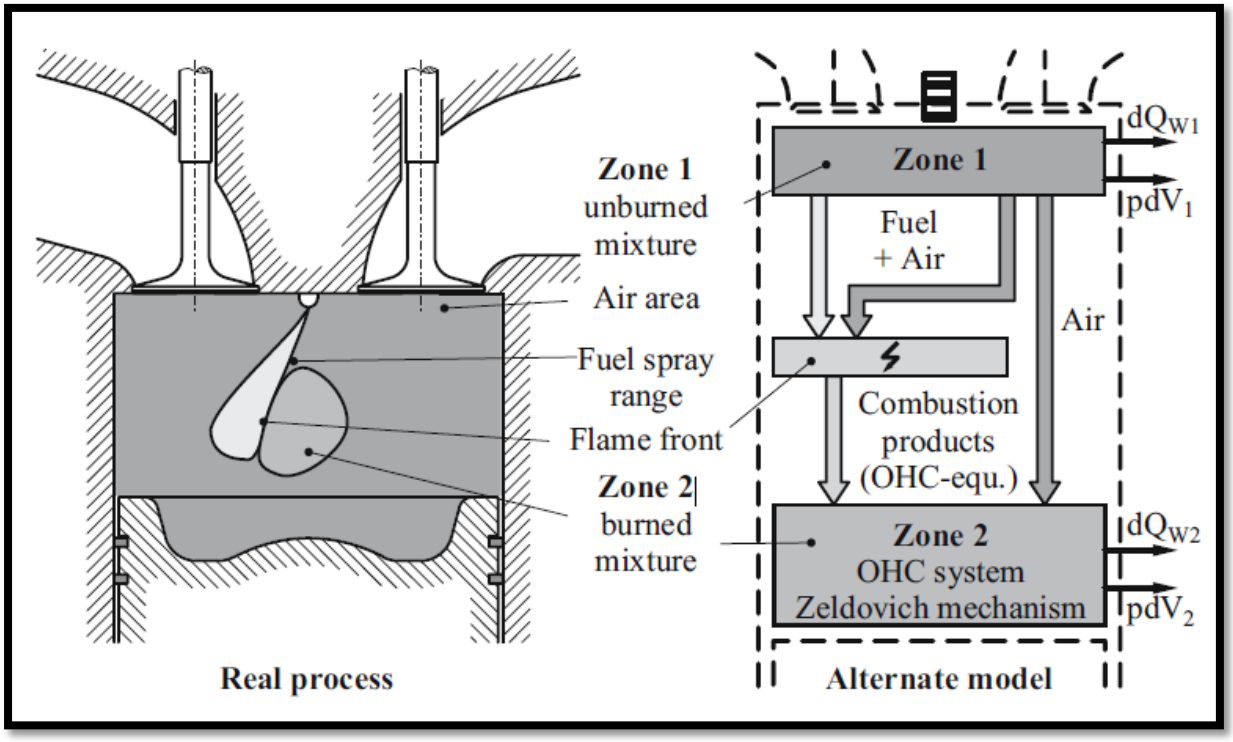

Figure 4.4 Two-zone cylinder model [Gunter P et al., 2006]

5. Model modification

5.1 Overall methodology

Methanol dual fuel engines have gained interest in recent years. Thus only limited information on the engines is available at the moment. To carry out the simulation on methanol engine, prime inputs need to be obtained ideally by an engine experiments. However, without the experiment, how to obtain necessary input was the major difficulty. In this thesis, a prime input which is in-cylinder pressure is acquired by the pressure diagram in a published reference [Lijiang Wei et al., 2015] as this reference provides detail information compared to other references. The pressure values are read by naked eyes. To increase accuracy of pressure-reading, interpolation is used to calculate intermediate values between crank angles. Interpolation is a good mathematical method to estimate intermediates values within the range of a discrete set of known data. Although there must be inevitable pressure-reading errors, the overall characteristics of pressure trends can be inputted.

The in-cylinder pressure read by naked eyes is used as the main input in the heat release model. With the in-cylinder pressure, the heat release model can calculate the combustion reaction rate (CRR) based on the first law of thermodynamics. Reaction coordinate (RCO) is obtained by integration of the combustion reaction rate. The purpose of reaction coordinate is to determine multiple vibe function parameters, which are used as the main input in the in-cylinder model. Lastly, the simulation results from two different models are compared and analyzed to find out the effects of methanol fuel on in-cylinder process.

5.2 Assumptions and Engine data

5.2.1 Assumptions

In order to carry out the simulation based on data from literature, some assumptions are made as below.

1. As initial conditions are not given, p1 is calculated based on the equation (5.1)

$$p_1 = \frac{p_2}{r_c^{n_{comp}}} \quad (5.1)$$

where p_2 and r_c are the pressure at start of iso-volumetric combustion and effective compression ratio, respectively.

$$r_c = \frac{V_1}{V_2} \quad (5.2)$$

2. Both air and stoichiometric gases are considered to be ideal but non-perfect gases, the internal energy and enthalpy of in-cylinder gases are functions of temperature.

3. In practice, methanol evaporation takes place at many places such as on the surface of inlet valve, on the wall of inlet manifold, on the cylinder walls and in the inlet manifold. Many parameters affect evaporation event, for example, the size of droplets, surrounding air velocity and temperature, injection pressure and in-cylinder wall temperatures. However, it is not possible to predict methanol evaporation event by the current Model C. For this reason, methanol fuel is assumed to completely evaporate in the port before inlet valve close. No further evaporation and heat absorption takes place after inlet valve close (IC). [Tuominen, 2016] [Tutak, 2015] [Kasseris, 2011]

4. Methanol exits as homogenous pre-mixtures gases in the cylinder at inlet valve close (IC)

5. According to single zone principle, there are no unburned gases in the cylinder. For this reason, regardless different fuel ratios, all the fuels which are injected into the cylinder are completely combusted.

6. Both fuels have the same combustion duration.

5.2.2 Engine Data and additional inputs.

Engine data and additional inputs can be found in below **Table 5.1** and **Table 5.2**.

Table 5.1 Specifications of the engine [Lijiang Wei et al., 2015]

Description	Specification
Engine type	6-cylinder DI engine
Bore × stroke (mm)	126 × 130
Connecting rod length (mm)	219
Crank radius (mm)	65
Displacement (L)	9.726
Compression ratio	17
Max. torque/speed (N m/rpm)	1500/1200–1500
Rated power/speed (kW/rpm)	247/1900
Fuel injection system	Common rail
Combustion chamber	ω bowl in piston
Intake valve open	−36 °CA ATDC
Intake valve close	246 °CA ATDC
Exhaust valve open	−258 °CA ATDC
Exhaust valve close	30 °CA ATDC

Table 5.2 Input data [Lijiang Wei et al., 2015]

	Diesel fuel (Kg/h)	Alcohol fuel (Kg/h)	Air/methanol ratio	Overall air/fuel ratio
RMD=0	46.62	0	0	29.45
RMD=0.55	37.29	20.46	67.32	23.85
RMD=1.54	27.98	43.01	31.86	19.3

Injection pressure (Diesel)	100 Mpa
Injection pressure (Methanol)	0.4 Mpa

$$\mathrm{RMD} = \frac{m_{methanl}}{m_{diesel}} \tag{5.3}$$

where RMD means mass ratio between methanol and diesel fuel. When RMD is 0, it represents only diesel combustion.

5.3 Addition of methanol fuel properties

In order to analyze the instantaneous state of the in-cylinder process during combustion, it is required to keep track of the composition, pressure and temperature variations of combustion gases at any time. These properties are varied based on time and highly dependent on the properties of fuel. In conventional diesel engine model, only one fuel is considered but in dual fuel engine model, additional fuel information needs to be inputted to achieve dual fuel combustion.

In the original diesel engine model, in-cylinder gases consist of air and stoichiometric gas generated by diesel fuel combustion. However in dual fuel engine model, stoichiometric gas produced by methanol combustion needs to be included in in-cylinder gases constituents. According to the assumption (5) in section 5.2.1**,** unburned fuel gases do not take into account in the in-cylinder gases constituents.

5.3.1 Specific heat of methanol

Specific heat (Cp) is necessary to calculate heat of combustion. Specific heat can be obtained by the power series expansion of the normalized temperature [Staperma, 2010d]

$$\mathrm{C_p} = \sum_{k=1}^{m} \mathrm{a_k} * \theta^{k-1} \tag{5.4}$$

where a_k is the coefficients for the polynomial to calculate the specific heat of methanol. Detail values are given in **Table 5.3.** θ is the Normalized temperature and it can be expressed as,

$$\theta = \frac{\mathrm{T} - \mathrm{T_{shift}}}{T_{norm}} \tag{5.5}$$

where

T_{shift}: The kelvin temperature can be shifted to a non-zero point. Normally, T_{shift}=0 K

T_{norm}: Normalized temperature, T_{norm}=1000 K

Table 5.3 The coefficients for the polynomial to calculate c_p [Yaws, 1996]

Formula	**Name**	a'_1	a'_2	a'_3	a'_4	a'_5
CH_3OH	Methanol	40.046	-3.8287E-02	2.4529E-04	-2.1679E-07	5.9909E-11
$Cp= a'_1+ a'_2*\theta + a'_3*\theta^2+ a'_4*\theta^3+ a'_5*\theta^4$ (J/mol/k)						

a_k' in the **Table 5.3** stands for the the coefficients for the polynomial in J/mol/K. Unit conversation from J/mol/k to J/Kg/K can be done by the equation (5.6)

$$a_k = \frac{1000 * a_k'}{m_M} \quad [\frac{J}{kmol} * \frac{Kmol}{Kg} * \frac{1}{k}] \tag{5.6}$$

where m_M means the respective molar mass of methanol.

Based on the relation between C_v and C_p (5.7), the specific heat of methanol at constant volume can be calculated.

$$C_v = C_p - R \tag{5.7}$$

$$R = \frac{R'}{m_M} \tag{5.8}$$

where R' means the universal gas constant in J/Kmol/K

5.3.2 Specific internal energy and specific enthalpy of methanol (u_{sgg}, h_{sgg})

After obtaining specific heat values, it is possible to calculate specific internal energy and specific enthalpy by existing Matlab codes in the model [Ding, 2011], [Georgescu, 2013]. Both specific internal energy and specific enthalpy can be calculated based on the equations below [Staperma, 2010d]

$$\mathrm{du} = \mathrm{C_v} * dT$$

$$\Delta\ \mathrm{u_j} = \mathrm{u_j} - \mathrm{u_{ref,j}} = \int_{T_{ref}}^{T} C_{v,j} * dT \tag{5.9}$$

$$\mathrm{dh} = \mathrm{C_p} * dT$$

$$\Delta\ \mathrm{h_j} = \mathrm{h_j} - \mathrm{h_{ref,j}} = \int_{T_{ref}}^{T} C_{p,j} * dT \tag{5.10}$$

$$\mathrm{dT} = \mathrm{T_{norm}} * d\theta \tag{5.11}$$

$u_{ref,j}$ and $h_{ref,j}$ indicate internal energy and enthalpy of each constituent at reference condition, respectively. As the methanol specific heat is given by the power series expansions, internal energy and enthalpy variation ($\triangle u_j$, $\triangle h_j$) of each constituent can be calculated by integration.

$$\Delta\ h = \mathrm{h_j} - h_{j,ref} = \sum_{k=1}^{m} \frac{a_{k,j}}{k} * T_{norm} * \theta^k - \sum_{k=1}^{m} \frac{a_{k,j}}{k} * T_{norm} * \theta_{ref}^k \tag{5.12}$$

$$\Delta\ u = \mathrm{u_j} - u_{j,ref} = \Delta\ h - T_{norm} * R_j * (\theta - \theta^{ref}) \tag{5.13}$$

The final specific internal energy (u_{sgg}) and specific enthalpy (h_{sgg}) for methanol stoichiometric gas can be found by the summation of all the constituents.

$$\mathrm{u_{sgg}} = \sum_j x_j^{sgg} * u_j^{sgg}$$
$$\mathrm{h_{Sgg}} = \sum_j x_j^{sgg} * h_j^{sgg} \tag{5.14}$$

5.3.3 Stoichiometric air/fuel Ratio of methanol

A stoichiometric ratio indicates the required air and fuel amount to achieve complete combustion. Under the stoichiometric combustion condition, all the fuel and air are consumed to produce combustion products. A stoichiometric mixture consists of the exact amount of both fuel and oxidizer and this mixture can achieve the maximum flame temperature because all the energy released by chemical reaction is used to heat up the combustion products.

Different from diesel fuel, methanol contains oxygen (O) in its chemical formula. (CH_3-OH) In case of oxygenated fuels, the general formula of combustion stoichiometry can be defined as below equation (5.15), [McAllister et al., 2011]

$$C_\alpha H_\beta O_\gamma + \left(\alpha + \frac{\beta}{4} - \frac{\gamma}{2}\right) * (O_2 + x * N_2) \rightarrow \alpha * CO_2 + \frac{\beta}{2} * H_2O + x * \left(\alpha + \frac{\beta}{4} - \frac{\gamma}{2}\right) * N_2 \qquad (5.15)$$

where x is the mole ratio of N_2 and O_2. From the equation above (5.15), the amount of stoichiometric air can be calculated.

In practice, however, combustion does not take place with stoichiometric condition. Generally, the amount of air required for fuel combustion is different from the amount of stoichiometric air. For this reason, there are several definitions which are frequently used to quantify the combustible mixture.

1) Air/Fuel Ratio (afr)

$$\text{afr} = \frac{m_a}{m_f} \qquad (5.16)$$

where m_a and m_f indicate the respective mass of air and fuel.

2) Stoichiometric Air/Fuel Ratio (σ)

$$\sigma = \frac{m_{a\_min}}{m_f} = \frac{\left(\alpha + \frac{\beta}{4} - \frac{\gamma}{2}\right) * (1 + x) * M_{air}}{M_f} \quad (5.17)$$

where sigma(σ) and $m_{a,min}$ are a stoichiometric ratio and stoichiometric air mass, respectively. In addition M_f and M_{air} represent the average masses per mole of fuel and air.

3) Air excess Ratio (λ)

$$\lambda = \frac{afr}{\sigma} \quad (5.18)$$

Lambda (λ) is the most common definition for internal combustion engines. It stands for the ratio between the actual air-fuel ratio and the stoichiometric air-fuel ratio.

4) Equivalence ratio (ø)

$$\emptyset = \frac{1}{\lambda} \quad (5.19)$$

It is the normalized ratio between the stoichiometric fuel-air ratio and the actual fuel-air ratio. If ø is larger than 1 (ø >1), it is considered to be rich mixture. On the other hand, if If ø is lesser than 1 (ø <1), it is called as lean mixture. When ø=1, it is a stoichiometric mixture.

5.3.4 Lower Heating Value of methanol

One of the significant characteristics of methanol fuel is its lower LHV compared to diesel fuel. Correct calculation of LHV for methanol fuel contributes to increase of simulation accuracy. Heating value is an effective tool to quantify the maximum heat energy which is produced by combustion at standard conditions. (101.3Kpa, 25℃) Based on the phase of H2O in the

combustion products, heating value can be classified into Higher Heating Value (HHV) and Lower Heating Value (LHV). When H2O exits as the gases in the combustion products, the value of heat release is called as Lower Heating Value (LHV). If H_2O is condensed to liquid, the value of heat release is considered to be Higher Heating Value (HHV) due to extraction of latent heat. The relation between LHV and HHV can be expressed in equation (5. 20)

$$\mathrm{LHV} = \mathrm{HHV} - \frac{N_{H2O} * M_{H2O} * h_{fg}}{N_{fuel} * M_{fuel}} \tag{5.20}$$

where N and M are the mole number and mass of substances, respectively. h_{fg} is latent heat of water. Detail calculation steps of methanol LHV can be found in **Appendix I**.

5.4 Heat loss model

During the combustion, temperature difference between combustion gases and the cylinder walls increases. As a result, the heat can transfer from combustion gases to the cylinder walls, which is defined as heat loss. The wall temperatures are not easy to measure and these values do not have significant effects on heat loss value. [Ding, 2011] Since wall temperatures are not given by the experiment data, the values from the original model are used. In practice, wall temperatures vary with time and location due to piston movement and the variation of in-cylinder temperature. However, the wall temperatures are considered to be mean values and treated as constant in the model. Heat loss can be described by below equation (5.21) [Staperma, 2010c]

$$\dot{Q}_{loss} = \sum_{i=1}^{3} \{\alpha_{g \to w} * (T - T_{wall}) * A_{wall_i}\} \tag{5.21}$$

With i=1, cylinder wall

i=2, cylinder head

i=3, piston crown

The wall areas (A_{wall}) can be calculated by the below equations,

$$A_{wall,1} = \pi * D_b * L_s \quad (5.22)$$

$$A_{wall,2} = A_{wall,3} = \frac{\pi}{4} * D_b^2 \quad (5.23)$$

The area of piston crown and the area of cylinder head are assumed to be the same.

Heat transfer coefficient (α) is calculated by Woschini formula.

$$\alpha = C_1 * \frac{1}{D_b^{0.214}} * \frac{p^{0.786}}{T^{0.525}} * \left(C_3 * c_m + C_4 * \frac{p-p_0}{p_1} * \frac{V_s}{V_1} * T_1\right)^{0.786} \quad (5.24)$$

Both stroke volume (V_s) and mean piston speed (C_m) can be calculated by the equation (5.25) and (5.26)

$$c_m = 2 * L_s * \frac{RPM}{60} \quad (5.25)$$

$$V_s = \frac{\pi}{4} * D_b^2 * L_s \quad (5.26)$$

The constant C_3 is related to the effect of swirl velocity. There are two options for C_3

Gas Exchange $C_3 = 6.18 + 0.417 * \frac{w_t}{c_m}$ (5.27)

Compression and expansion $C_3 = 2.28 + 0.308 * \frac{w_t}{c_m}$ (5.28)

In this thesis, the scope of simulation is confined to in-cylinder process. For this reason, "Compression and Expansion" value (5.28) is applied to this model.

The constant C_4 is determined based on the shape of combustion chamber. There are two options which were suggested by Woschini

Direct injection $C_4 = 0.00324$ (5.29)

Pre-chamber $C_4 = 0.00622$ (5.30)

In the methanol dual fuel engine, combustion takes place by direct injection of pilot fuel so "Direct injection" value is chosen for the simulation. Due to lack of measured data, the values of wall temperature and swirl velocity are adopted from the original model. Instead, C_1 is considered as a variable to estimate heat loss.

5.5 Modification in the in-cylinder model

5.5.1 Introduction of Vibe function

Heat release rate plays a key role in understanding the combustion process. With introduction of vibe functions into the model, it is possible to analyze heat release characteristics. The vibe function is based on the principle of chain reactions and it can predict the fuel burn rate during combustion process. In order to understand Vibe function, it is necessary to be aware of basic equations for chain reactions.

The fuel molecules are broken up into a number of active radials by oxygen attacks. The reaction rate for the formation of active radicals is proportional to the quantity of fuel molecules.

$$\frac{dm_f^+}{dt} = k * m_f \quad (5.31)$$

In addition, the increase of active radicals is proportional to the decrease of fuel quantity.

$$dm_f^+ = -\mu * dm_f \quad (5.32)$$

With the combination of equations (5.31) and (5.32) above, the reaction rate can be defined.

$$\xi = \frac{\mathrm{dm_f}}{dt} = -\frac{k}{\mu} * m_f \tag{5.33}$$

Depending on the determination of reaction constants k and μ, different types of vibe function can be defined. Linear vibe function assumes that both k and μ are the constant value. However, linear vibe function is not suitable for the simulation due to its limited freedom in shaping the heat release. Instead of linear vibe function, non-linear vibe function is adopted in the model. It assumes that reaction constant is dependent on time but it does not depend on instantaneous quantity of the fuel molecules or radicals.

$$\mathrm{k = f(t) = c_1 * (t - t_0)^m} \tag{5.34}$$

The benefit of non-linear vibe function is that reaction rate starts off at zero and it ends at zero or near zero due to depletion of fuel molecules at the end of combustion. Linear vibe function, however, shows the maximum reaction rate as soon as ignition commences, which is not the realistic phenomenon.

Vibe function can be descried by normalized combustion progress (X) and normalized rate of combustion (Z).

$$\mathrm{X} = \frac{mass\ of\ fuel\ burnt}{Total\ mass\ of\ fuel} = \frac{m_f}{m_{f,0}} \tag{5.35}$$

$$\mathrm{Z} = \frac{\mathrm{dX}}{\mathrm{d\tau}} = \xi * \frac{t_{comb}}{m_{f,0}} \tag{5.36}$$

$$\tau = \frac{time\ since\ begin\ of\ combustion}{total\ combustion\ duration} = \frac{t - t_0}{\Delta t_{comb}} \tag{5.37}$$

where τ is normalized combustion time.

X and Z can be expressed with vibe parameters "a" and "m",

$$X = 1 - e^{-a*\tau^{m+1}} \tag{5.38}$$

$$Z = a * (m + 1) * \tau^{m} * e^{-a*\tau^{m+1}} \tag{5.39}$$

where "m" is a shape parameter and the effects of shape parameter "m" can be found in **Figure 5.5.1**.

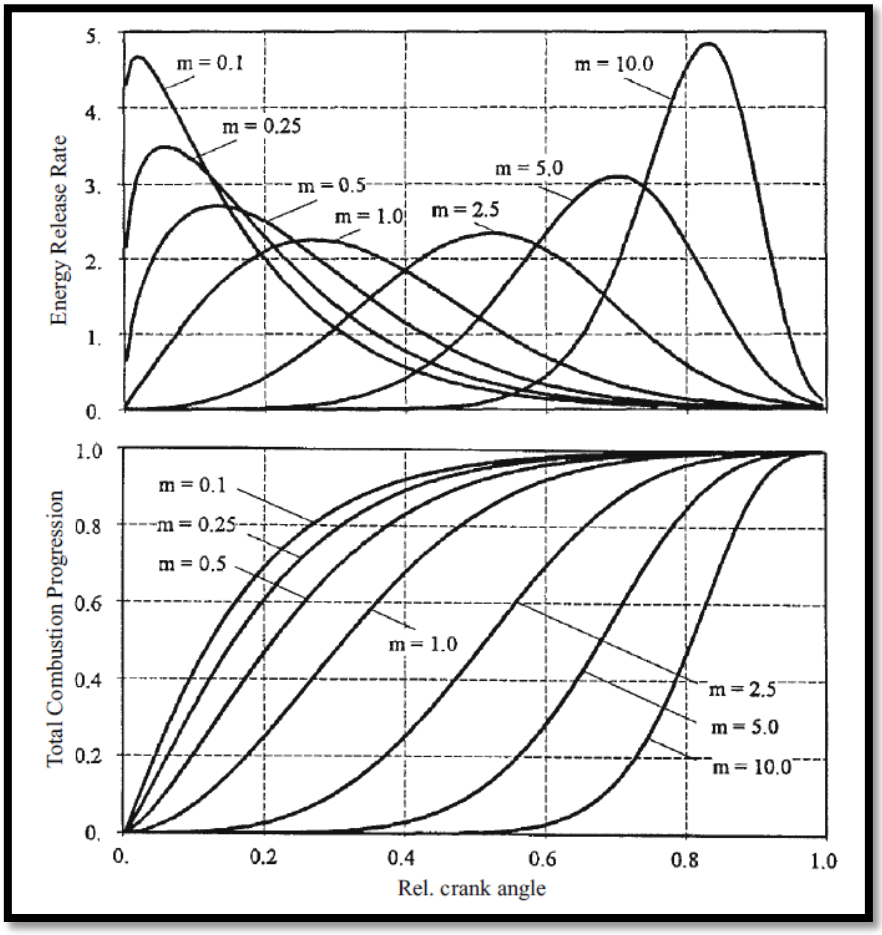

Figure 5.5.1 Effect of shape parameter 'm' [Gunter P et al., 2006]

Quick combustion reaction can be described by small value of m. The peak of heat release rate is shown in the beginning of the combustion. However, with increase of value 'm', peak of heat release rate becomes retarded.

In addition, the parameter "a" is related to combustion efficiency and the effects of the parameter "a" are illustrated in **Figure 5.5.2.**

$$\eta_{\text{comb}} = 1 - e^{-a} \tag{5.40}$$

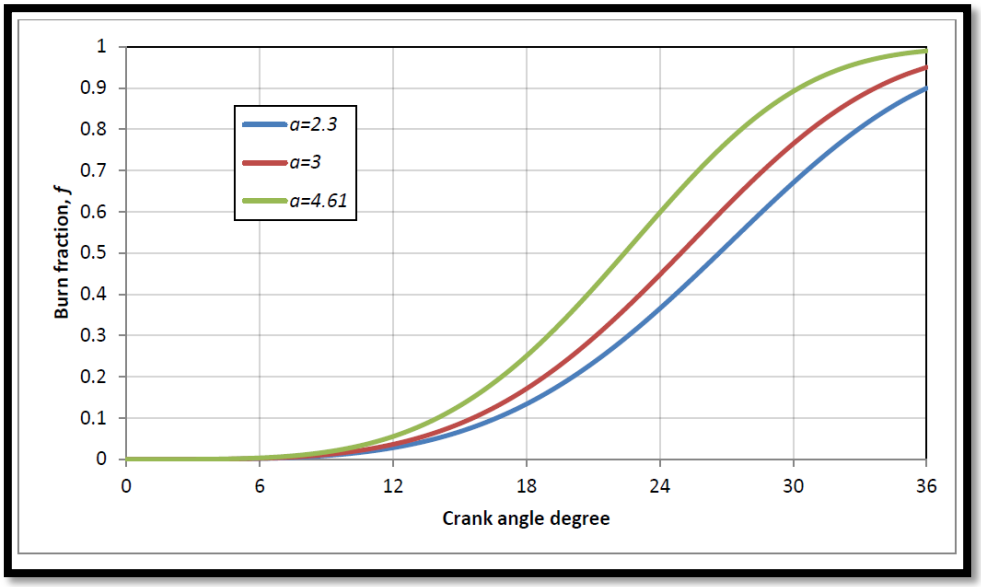

Figure 5.5.2 Variation of burn fraction with respect to "a" [Abbaszadehmosayebi, 2014]

If the value of parameter "a" becomes lower, combustion efficiency decreases and it leads to lower burn fraction.

It is assumed that the combustion efficiency (η_{comb}) is 99.9 % for the simulation regardless different fuel ratios, then finally the parameter "a" becomes,

$$\mathrm{a} = -\ln(1 - \eta_{\text{comb}}) = -\ln(0.001) = 6.908 \tag{5.41}$$

Vibe functions for diesel and methanol share the same value of parameter "a" in the simulation.

Instead of single vibe function, multiple vibe functions can describe more accurate and realistic combustion process.

$$X = \sum_{k=1}^{n} b_k * X_k = \sum_{k=1}^{n} b_k * \left(1 - e^{-a*\tau^{m_k+1}}\right) \quad (5.42)$$

With vibe function, it is possible to gain combustion reaction rate (CRR) if both combustion duration and total amount of fuel injection are known.

$$\xi = \mathrm{CRR} = Z * \frac{m_f^{comb}}{\Delta t_{comb}} \quad (5.43)$$

The combustion duration (Δt_{comb}) can be calculated, if the start of combustion (SOC) and the end of combustion (EOC) are given.

$$\Delta\, t_{comb} = (EOC - SOC) * \frac{60}{RPM*2\pi} \quad (5.44)$$

5.5.2 Split vibe functions

This section mainly discusses the method of the modification for dual fuel combustion. Unlike conventional diesel engines, the heat release of dual fuel engine is produced by two different fuels. In case of spark ignition engine (SI), the role of the spark is limited to induce ignition and it does not contribute to in-cylinder heat release. In dual fuel engine, however, the role of pilot fuel is more than the just spark and the pilot fuel keeps injecting onto ongoing combustion after start of ignition. As a result, the contribution of pilot fuel to the total release rate is substantial. For this reason, it is required to make clear division between diesel fuel combustion and methanol fuel combustion.

The purpose of introducing vibe function is to calculate in-cylinder heat release rate. In order to distinguish heat release from different fuels, two independent vibe functions are adopted in the model. Double vibe function is to represent diesel fuel combustion and single vibe function is for methanol fuel combustion.

Vibe function for diesel: $$X_{diesel} = b_1 * \left(1 - e^{-a*\tau_{Diesel}^{m_1+1}}\right) + b_2 * \left(1 - e^{-a*\tau_{Diesel}^{m_2+1}}\right) \quad (5.45)$$

Vibe function for methanol: $$X_{methanol} = b_3 * \left(1 - e^{-a*\tau_{Methanol}^{m_3+1}}\right) \quad (5.46)$$

where the parameters "b_1" and "b_2" indicate weighting factors for the diesel combustion. In detail, b_1 and b_2 stands for premixed combustion and diffusive combustion, respectively. "b_3" represents weighting factor for the methanol fuel combustion.

Diesel vibe functions consist of double vibe functions but methanol vibe function consists of single vibe function. When double vibe functions were applied to methanol combustion, the results did not show realistic phenomenon because there was a negative combustion reaction rate.

Figure 5.5.3 and **Figure 5.5.4** show the results of singe vibe function for methanol combustion. Both graphs show positive combustion reaction rate and combustion progress.

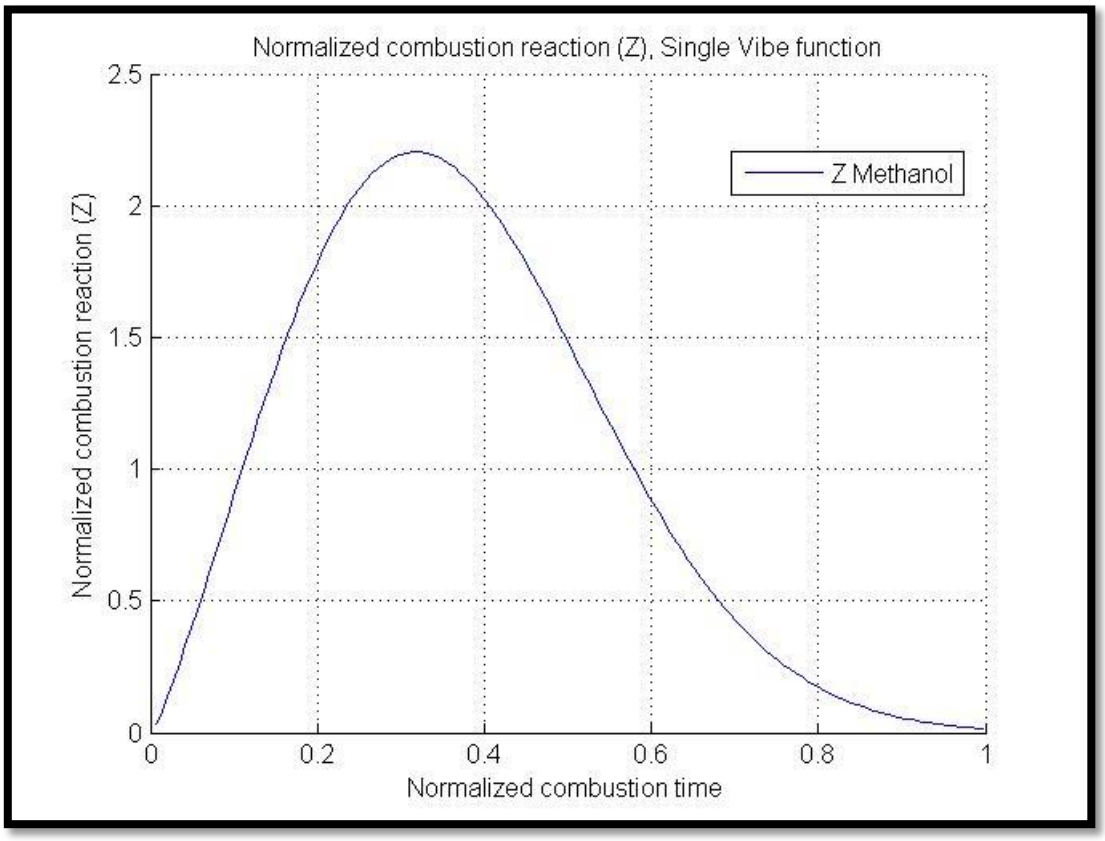

Figure 5.5.3 Normalized combustion rate (Z) with single vibe function (methanol)

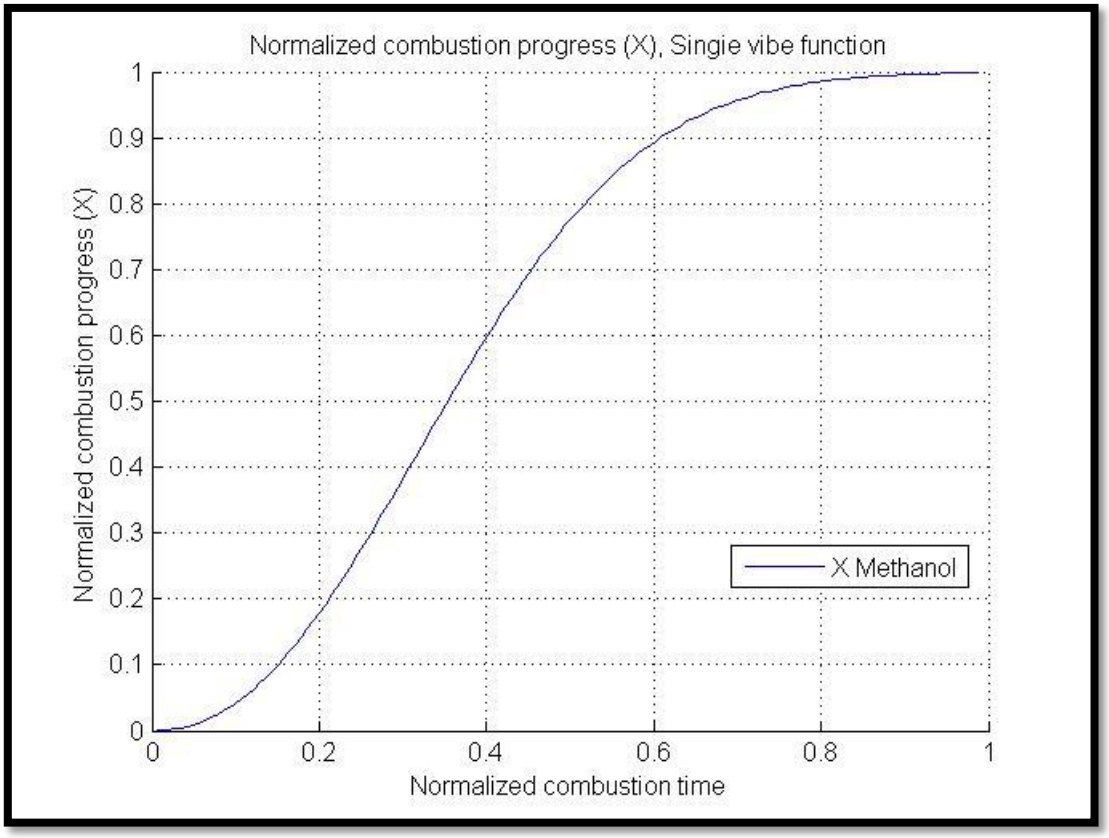

Figure 5.5.4 Normalized combustion progress (X) with Single vibe function (methanol)

Figure 5.5.5 and **Figure 5.5.6** show the results of double vibe function for methanol combustion.

As double vibe function is used to describe methanol combustion, X and Z consist of two terms. Z_1 and X_1 stand for the 1st terms in the double vibe function and Z_2 and X_2 are the 2nd terms. The figures show that Z_2 and X_2 have negative trends. However, once combustion starts, both combustion reaction and combustion progress need to be positive.

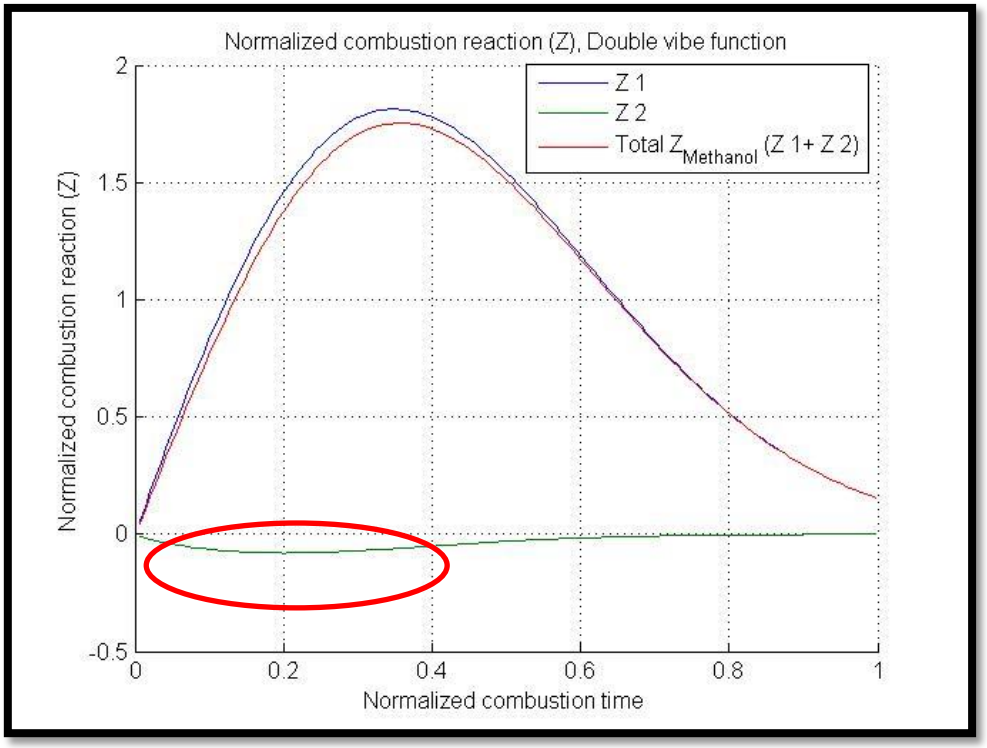

Figure 5.5.5 Normalized combustion rate (Z) with double vibe function (methanol)

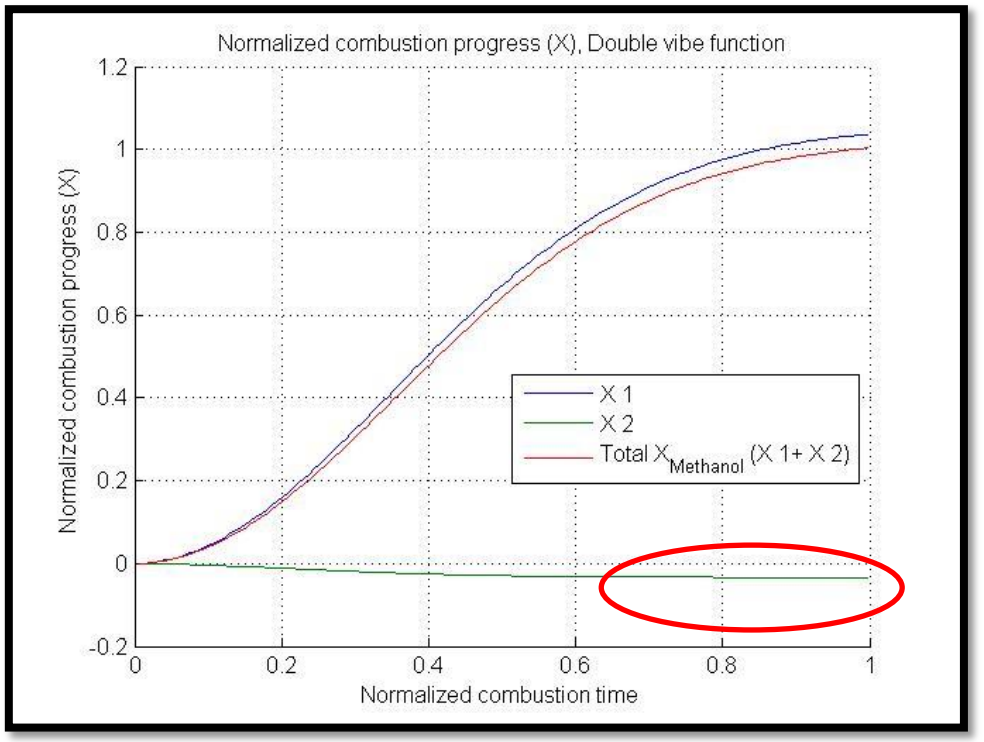

Figure 5.5.6 Normalized combustion progress (X) with double vibe function (methanol)

Due to the limit of the model, the combustion duration for both fuels is assumed to be the same regardless of different fuel injection ratios. Detail explanation of the limits regarding different combustion duration can be found in **Appendix IV**

$$\tau_D = \tau_M = \frac{Crank\ angle - SOC_D}{EOC_D - SOC_D} = \frac{Crank\ angle - SOC_M}{EOC_M - SOC_M} \tag{5.47}$$

The independent vibe functions for both fuels use "crank angle" as the common input and finally the combustion reaction rates for each fuel can be calculated by the separated reaction rate blocks as shown in **Figure 5.5.7**.

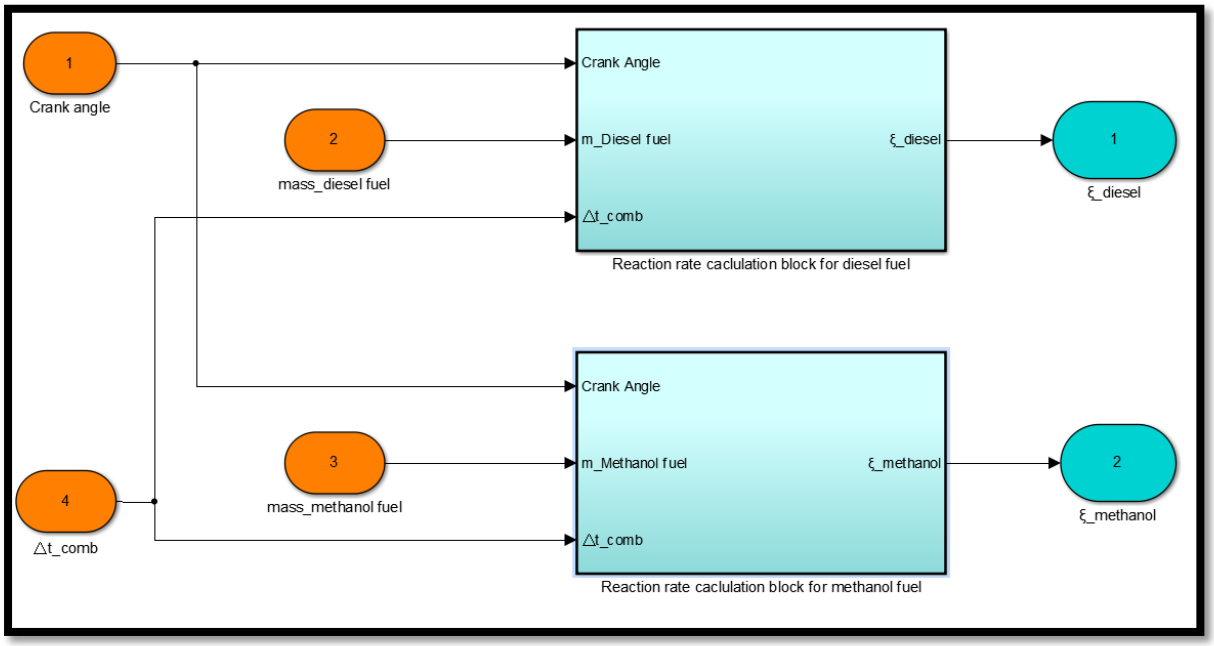

Figure 5.5.7 Reaction rate calculation blocks for both fuel

Based on separated reaction rates for each fuel, it is possible to split the heat release of dual fuel combustion into diesel heat release and methanol heat release.

$$\dot{Q}_{\text{Diesel}} = \xi_D * u_{comb\,Diesel} = \frac{dx_D}{d\tau} * \frac{m_{diesel}}{\Delta t_{comb}} * u_{comb\,Diesel} \tag{5.48}$$

$$\dot{Q}_{\text{Methanol}} = \xi_M * u_{comb\,Methanol} = \frac{dx_M}{d\tau} * \frac{m_{methanol}}{\Delta t_{comb}} * u_{comb\,Methanol} \tag{5.49}$$

where $u_{comb,fuel}$ is heat of combustion and it can be calculated by

$$\mathrm{u}_{\mathrm{comb}_{\mathrm{fuel}}} = u_{fuel} + \sigma * u_{air} - (1+\sigma) * u_{stoichiometric\ gas} \tag{5.50}$$

Total heat release rate in dual fuel combustion can be obtained by adding the heat release rate of diesel fuel combustion and methanol fuel combustion.

$$\dot{\mathrm{Q}}_{\mathrm{total}} = \dot{\mathrm{Q}}_{\mathrm{Diesel}} + \dot{\mathrm{Q}}_{\mathrm{Methanol}} = \frac{dx_D}{d\tau} * \frac{m_{diesel}}{\Delta t_{comb}} * u_{comb\,Diesel} + \frac{dx_M}{d\tau} * \frac{m_{methanol}}{\Delta t_{comb}} * u_{comb\,Methanol} \tag{5.51}$$

5.6 Modification in the heat release model

Heat release of both methanol and diesel fuels can be constructed by the separated vibe functions in the in-cylinder process model. To determine the vibe parameters for each vibe function, two separated reaction coordinates (RCO) need to be obtained in the heat release model. With in-cylinder pressure input, the heat release model calculates Gross Apparent Heat Release Rate (GAHRR). The heat energies from methanol fuel and diesel fuel contribute to determination of the GAHRR as the in-cylinder pressure is a result of methanol and diesel fuel combustion. To obtain separated RCO, GAHRR needs to be split into GAHRR $_{Diesel}$ and GAHRR $_{Methanol}$. Overall produces to obtain split RCO is illustrated in **Figure 5.6.1**.

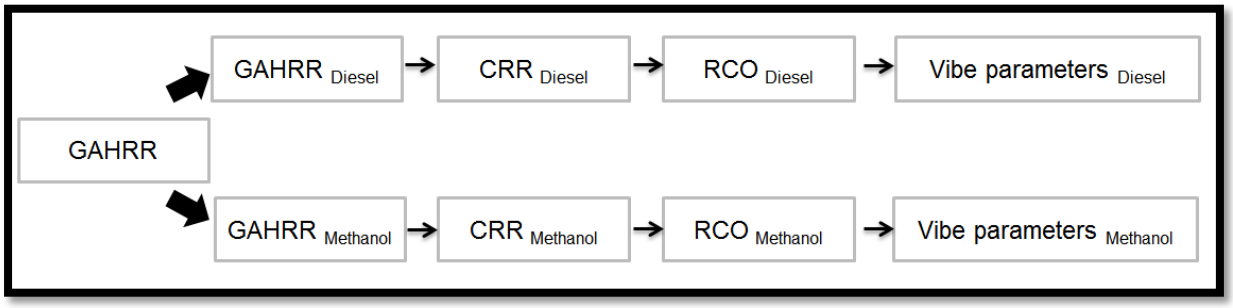

Figure 5.6.1 Procedure to obtain split RCO

However, it is difficult to distinguish heat release rates between diesel fuel and methanol fuel in the heat release model. Thus, a proper separation of GAHRR is very important to estimate heat release rates of both fuels.

In this thesis, energy fraction of each fuels are used to separate GAHRR.

$$\dot{Q}_{\text{Total}} = (1 - Xg) * \dot{Q}_{Diesel} + Xg * \dot{Q}_{Methanol} \tag{5.52}$$

where Xg is energy fraction of methanol fuel. Energy fraction of methanol fuel can be calculated by the equation below.

$$\text{Methanol Energy fraction (Xg)} = \frac{m_{methanol} * LHV_{methanol}}{m_{diesel} * LHV_{diesel} + m_{methanol} * LHV_{methanol}} \tag{5.53}$$

Energy fraction of diesel fuel can be obtained by,

$$\text{Diesel Energy fraction} = (1 - \text{Xg}) \tag{5.54}$$

For example, in case of RMD=1.54, the total heat release rate $Q_{RMD=1.54}$ consists of 40% of $Q_{Methanol}$ and 60% of Q_{Diesel}.

$$\dot{Q}_{\text{RMD=1.54}}(100\%) = \dot{Q}_{methanol}\ (40\%) + \dot{Q}_{Diesel}(60\%) \tag{5.55}$$

Once Q_{Diesel} is defined, it is possible to calculate $Q_{methanol}$ because $Q_{RMD=1.54}$ can be obtained by the in-cylinder pressure input. In RMD=0 combustion, heat release rate consists of only diesel fuel since no methanol fuel is injected. Then it can be considered as 100% of Q_{Diesel}. Q_{diesel} (60%) can be calculated if energy fraction of diesel fuel is multiplied.

$$\dot{Q}_{Diesel}(60\%) = \dot{Q}_{RMD=0}\ (100\%) * (0.6) \tag{5.56}$$

Finally, $GAHRR_{Diesel}$ and $GAHRR_{Methanol}$ can be obtained.

$$\dot{\mathrm{Q}}_{\mathrm{RMD=1.54}}(100\%) - \dot{Q}_{Diesel}(60\%) = \dot{Q}_{methanol}\ (40\%) \tag{5.57}$$

Determination of vibe parameters

With separated GAHRR, combustion reaction rates (CRR) for both fuels can be calculated

$$\mathrm{CRR}_{\mathrm{Diesel}} = \frac{GAHRR_{Diesel}}{u_{comb_{Diesel}} + e_f}\ [Kg/s] \tag{5.58}$$

$$\mathrm{CRR}_{\mathrm{Methanol}} = \frac{GAHRR_{Methanol}}{u_{comb_{Methanol}}}\ [\mathrm{Kg/s}] \tag{5.59}$$

In case of diesel fuel, there is "e_f" term in denominator as it is injected as liquid phase. However, according to the assumption, methanol fuel is in the gas phase after inlet value close (IC). Therefore "e_f" term is not taken into account.

After obtaining CRR, it is possible to determine vibe parameters by using curve fitting. Before carrying out curve fitting function, a monotonous increase function needs to be obtained. It can be done by integrating CRR. **Figure 5.6.2** shows CRR of methanol when RMD=1.54 was applied. After integration of CRR, it becomes RCO and it has a monotonous increasing trend as shown in **Figure 5.6.3**.

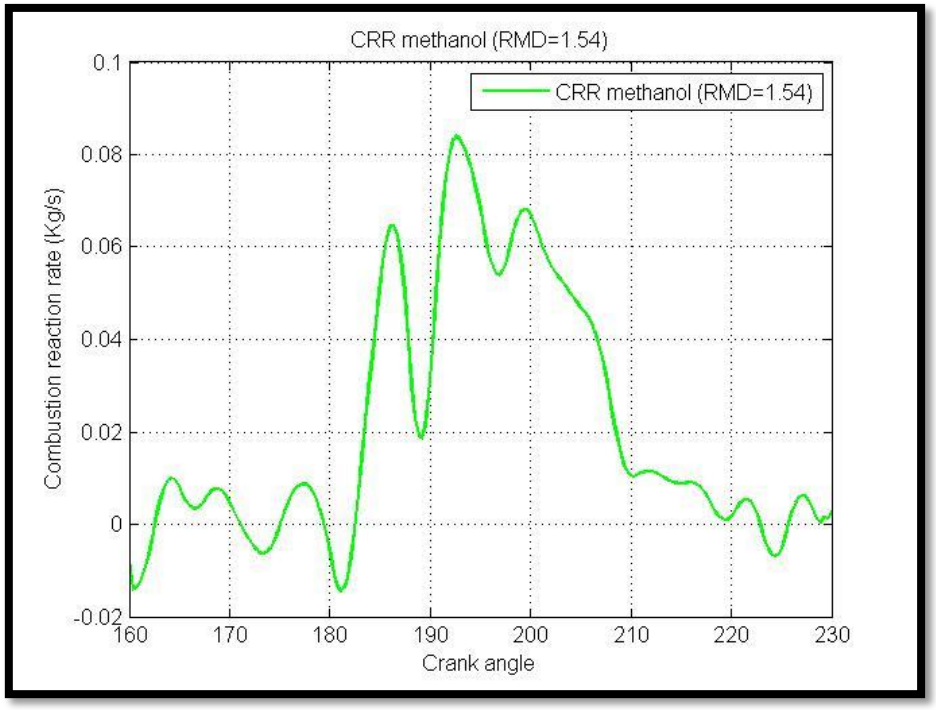

Figure 5.6.2 Combustion reaction rate of methanol fuel (RMD=1.54)

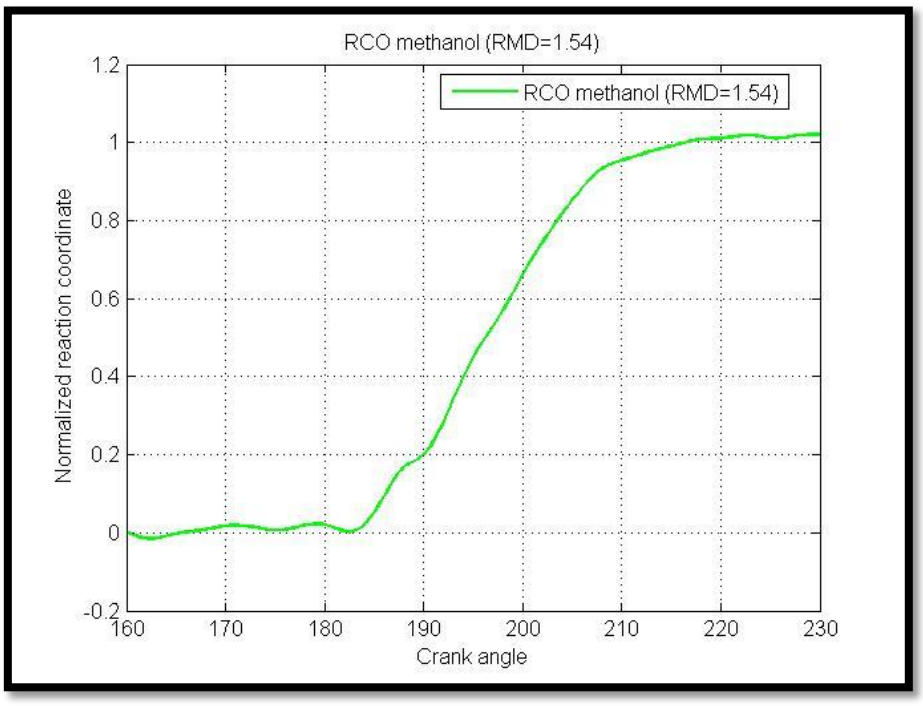

Figure 5.6.3 RCO methanol (RMD=1.54)

Based on RCO, curve fitting can be carried out. The result of curve fitting can be found in **Figure 5.6.4**. The black line on the figure is the RCO of methanol fuel and it is used as a benchmark. Blue line is the curve fitting result and it is constructed by vibe parameters.

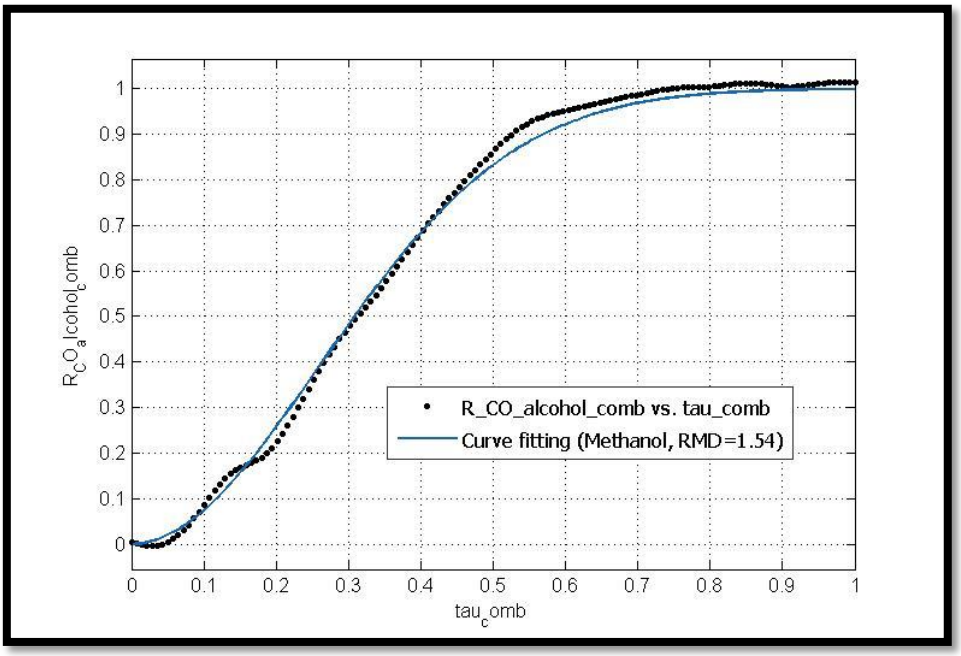

Figure 5.6.4 RCO VS Curve fitting (Methanol fuel)

Curve fitting results of all RMD and vibe parameters can be found in **Appendix II**.

6. Simulation results and analysis

6.1 Introduction

This chapter will present the results of the simulation with different methanol/diesel injection ratios. The relevant energy fractions for each RMD can be found in **Table 6.1.** Since pressure of RMD=0 is given only for -5.5 diesel injection timing (DIT) case, simulation is conducted based on DIT=-5.5. Different injection timings are not tested because it is not possible to separate GAHRR without RMD=0 data in this thesis.

Table 6.1 Fuel Ratio between Methanol and Diesel fuel

Fuel mass Ratio	Diesel fuel (Kg/h)	Alcohol fuel (Kg/h)	Energy fraction of methanol
RMD=0	46.62	0	0 %
RMD=0.55	37.29	20.46	20 %
RMD=1.54	27.98	43.01	40 %

As the model C consists of heat release model and in-cylinder process model, both results will be shown and will be compared. The reference data which is used for this simulation only provides the information between -20 (B)TDC and +50 (A)TDC. For this reason, heat release model which uses the pressure values from the reference data as main input can only carry out the simulation within the mentioned range above. However, as in-cylinder model uses the output of heat release model as main input, it can carry out the simulation within the range between inlet valve close (IC) to exhaust valve open (EO). Based on the simulation results, the effect of methanol fuel on in-cylinder process in dual fuel premixed engine will be analyzed and discussed.

6.2 Heat release rate

6.2.1 Heat release rate results

In the in-cylinder process model, end of combustion for all the cases were assumed at 230 CA as the experimental data provided the information within the range between 160 CA (-20 BTDC) and 230 CA (50 ATDC). In addition, all the vibe parameters in in-cylinder process model are calculated based on the given range. Nevertheless, the simulation results still depict the characteristics of methanol effects on combustion.

The **Figure 6.1** below illustrates the comparisons between the reference heat release rate and simulations results. Overall trends are similar with the reference heat release for both models and the results in the in-cylinder model show adequate accuracy. The peak heat release rate values can be found in **Table 6.2**.

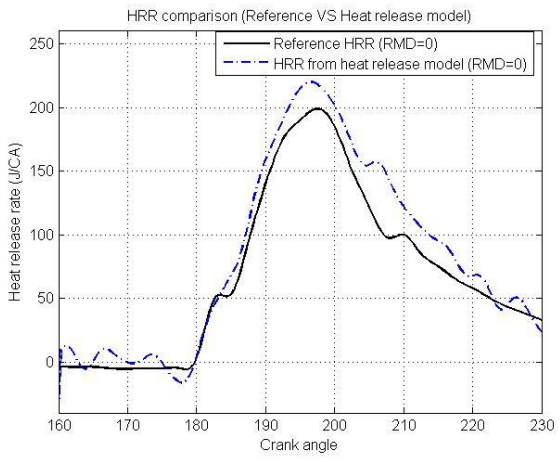

Reference data VS Heat release model (RMD=0)

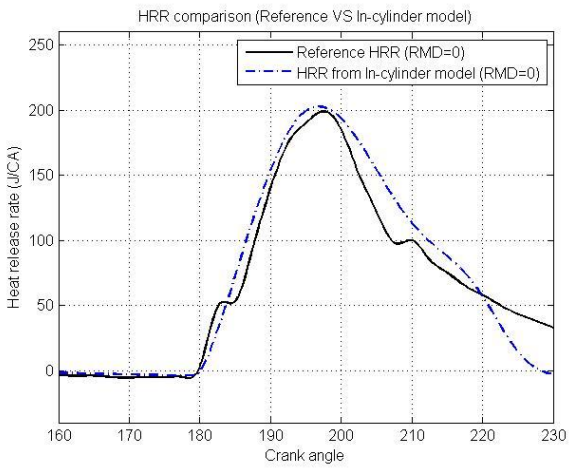

Reference data VS In-cylinder model (RMD=0)

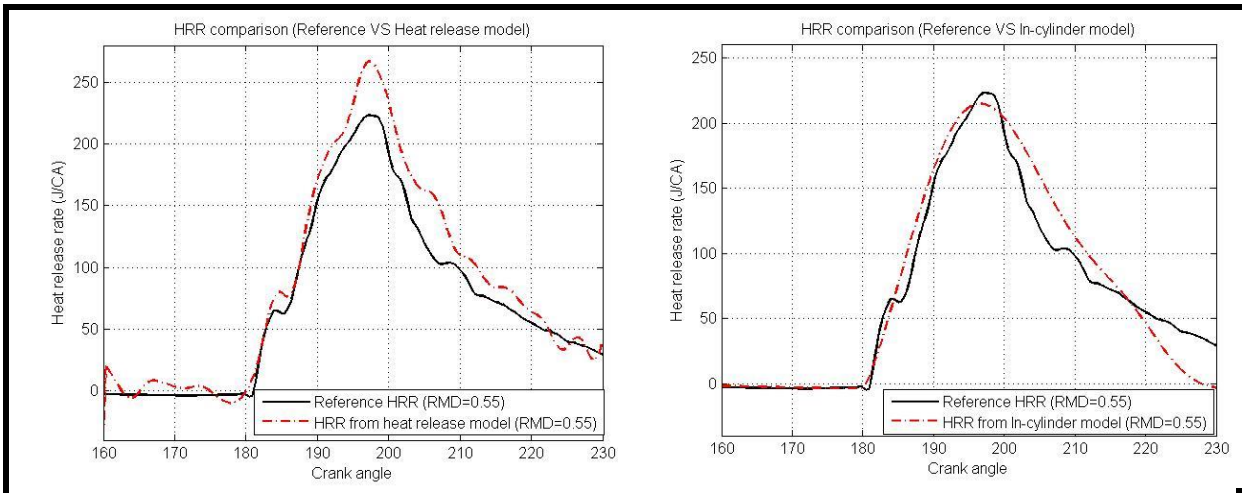

Reference data VS Heat release model (RMD=0.55)	Reference data VS In-cylinder model (RMD=0.55)

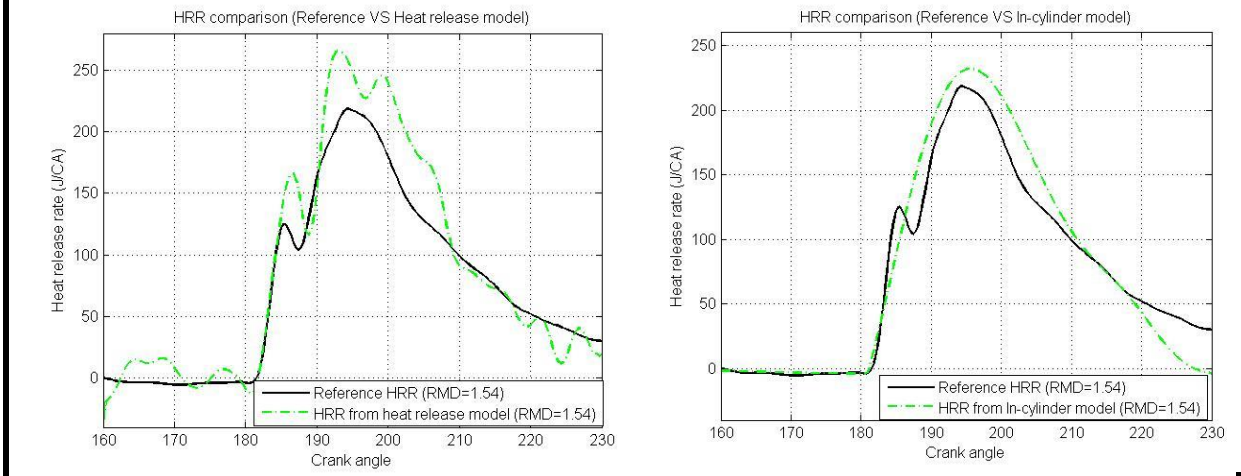

Reference data VS Heat release model (RMD=1.54)	Reference data VS In-cylinder model (RMD=1.54)

Figure 6.1 Heat release rate comparisons (Reference data VS simulation results)

Table 6.2 Peak heat release rate comparison (Reference VS In-cylinder model)

	RMD=0	RMD=0.55	RMD=1.54
Reference (J/CA)	199	223	219
In-cylinder model (J/CA)	202.8	215	232
Error (%)	1.9	-3.6	5.9

On the left side of **Figure 6.1**, the separated peaks can be seen in the heat release model. The first peak represents the combustion of diesel fuel and the second peak is associated with the combustion of methanol fuel. The reason for separated peaks is that both fuels have different combustion duration. However, in the in-cylinder process model, it is not able to depict the separated peaks due to the limit of the model. The model cannot determine the exact start of combustion timing between diesel and methanol fuel. For this reason, the common combustion duration is used to calculate vibe parameters for both fuels in the in-cylinder model.

6.2.2 Analysis of heat release rate

Start of combustion (Ignition delay)

Figure 6.2 and **Figure 6.3** show that start of combustion varies with different fuel ratios. With increase of methanol injection, retarded start of combustion takes place due to longer ignition delay.

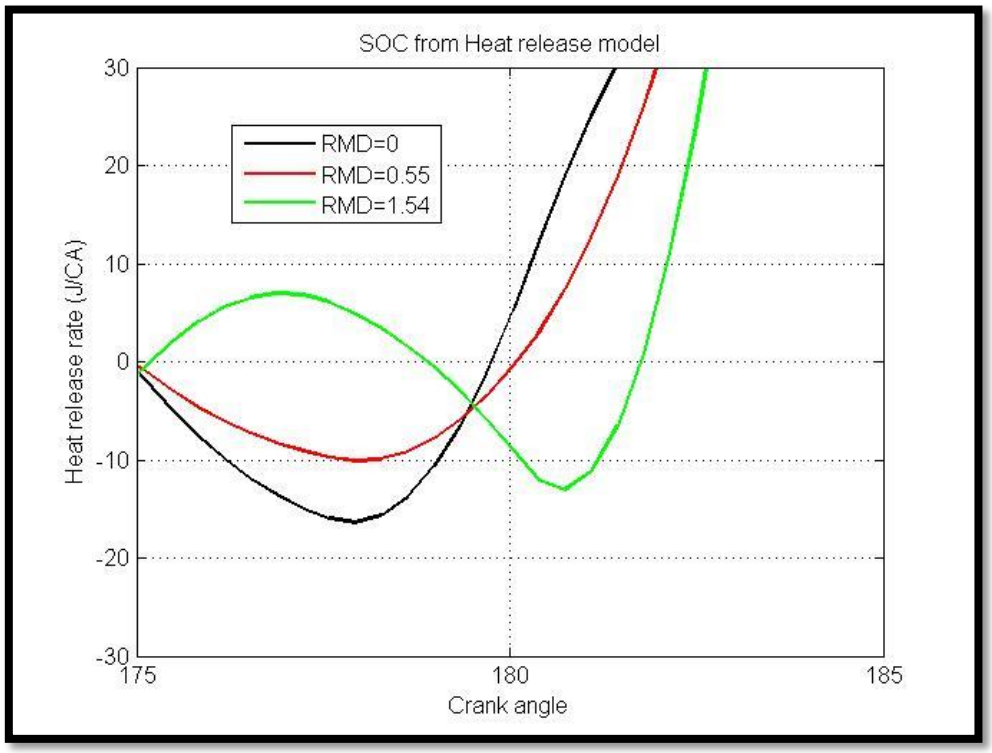

Figure 6.2 Start of combustion in Heat release rate model

Table 6.3 Start of ignition crank angle in heat release rate model

	SOC in HRR model (CA)
RMD=0	179.7
RMD=0.55	180
RMD=1.54	181.8

In case of RMD=1.54 in heat release model, the positive heat release can be seen before ignition occurs. However it does not mean any physical phenomenon. It is caused by heat release fluctuation. Heat release rate is very sensitive to input pressure value and detail explanation can be found in **Appendix III**. Since pressure values are read by naked eyes to input in the heat release model, there are pressure-reading errors and it causes the fluctuations.

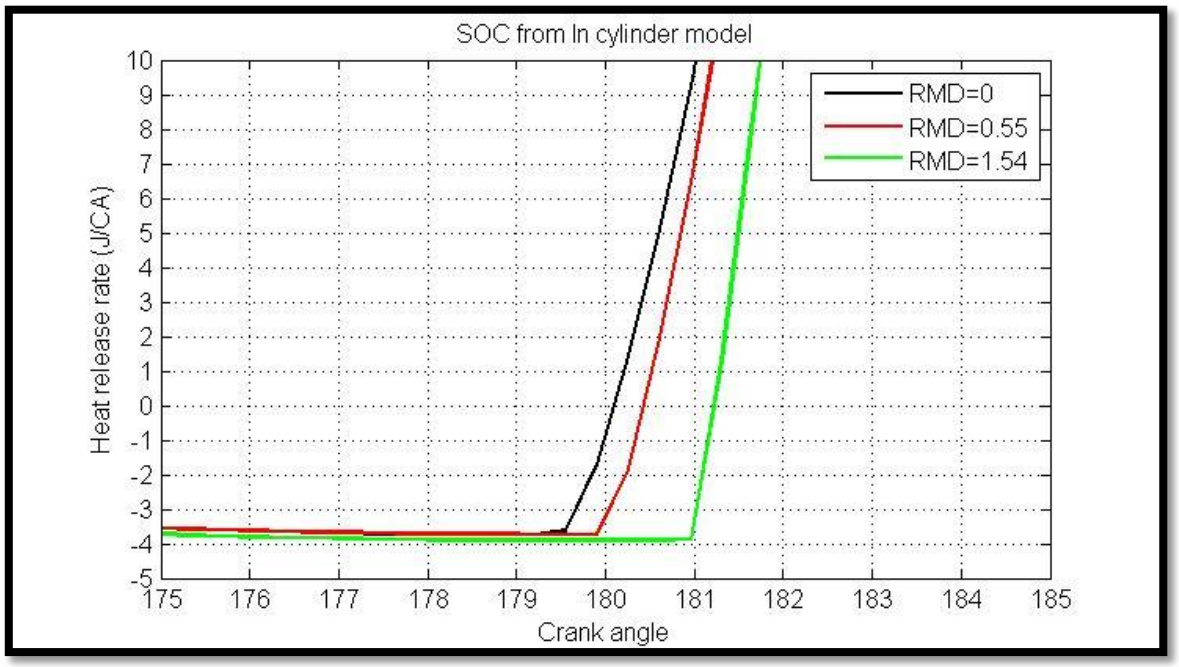

Figure 6.3 Start of combustion in in-cylinder process model

Table 6.4 Start of ignition crank angle in in-cylinder process model

	SOC in In-cyl' model (CA)
RMD=0	179.5
RMD=0.55	180
RMD=1.54	181

In the in-cylinder model, starts of combustions (SOC) are determined based on the Reaction coordinate in the heat release model. Small variations of SOC values (Δ1 CA) have been made to find the best results.

The effect of high heat of evaporation prolongs the ignition delay. Due to higher heat absorption with increase of methanol injection, in-cylinder temperature decreases accordingly and temperature plays a key role in determining ignition delay. [Heywood, 1988]

$$\tau_{\mathrm{id}} = A * p^{-n} * \exp\left(\frac{E_A}{RT}\right) \tag{6.1}$$

where A and n are constants dependent on fuels. EA is the apparent activation energy for auto ignition process.

As shown in **Figure 6.4**, ignition delay becomes longer as the temperature decreases.

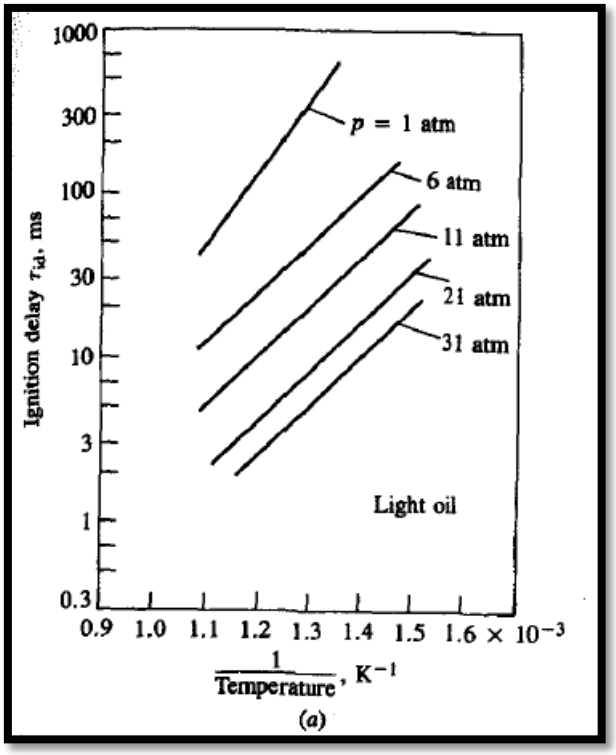

Figure 6.4 Effect of temperature on ignition delay [Heywood, 1988]

The chemical kinetics of methanol-diesel combustion is highly affected by temperature. [Yin, 2016] When methanol and diesel fuel are mixed, the procedure of dehydrogenation of diesel and methanol fuels takes place. The first step of chemical reaction is,

$$\mathrm{CH_3}OH \rightarrow CH_3 + OH \tag{6.2}$$

This OH is an important radical in the chemical reaction. Methanol fuel reacts with OH radicals,

$$\mathrm{CH_3}OH + OH = CH_3O + H_2O$$

$$\mathrm{CH_3}OH + OH = CH_2OH + H_2 \tag{6.3}$$

In case of diesel fuel, chemical reaction with OH can be describe as below,

$$\mathrm{C_x}H_y + OH \rightarrow C_xH_{y-1} + H_2O \tag{6.4}$$

With oxygen addition, HO_2 and CH_2O can be produced by below chain reactions

$$\mathrm{CH_3}O + O_2 = CH_2O + HO_2$$

$$\mathrm{CH_2}OH + O_2 = CH_2O + HO_2 \tag{6.5}$$

Then HO_2 is converted into inactive radical, which is H_2O_2

$$\mathrm{HO_2} + HO_2 = H_2O_2 + O_2 \tag{6.6}$$

Especially, at lower temperature, converting active OH radical into inactive H2O2 radical is predominant. With increase of inactive radical, start of ignition is delayed. However, with increase of temperature, H_2O_2 radicals rapidly decompose into OH and it shortens ignition delay. [Yin, 2016]

Other factor which influences on ignition delay is cetane number.

$$\mathrm{E_A} = \frac{618{,}840}{Cetane+25} \tag{6.7}$$

The effect of cetane number on ignition delay is illustrated in **Figure 6.5**

Cetane number of methanol fuel is much lower than that of diesel fuel and it causes longer ignition delay.

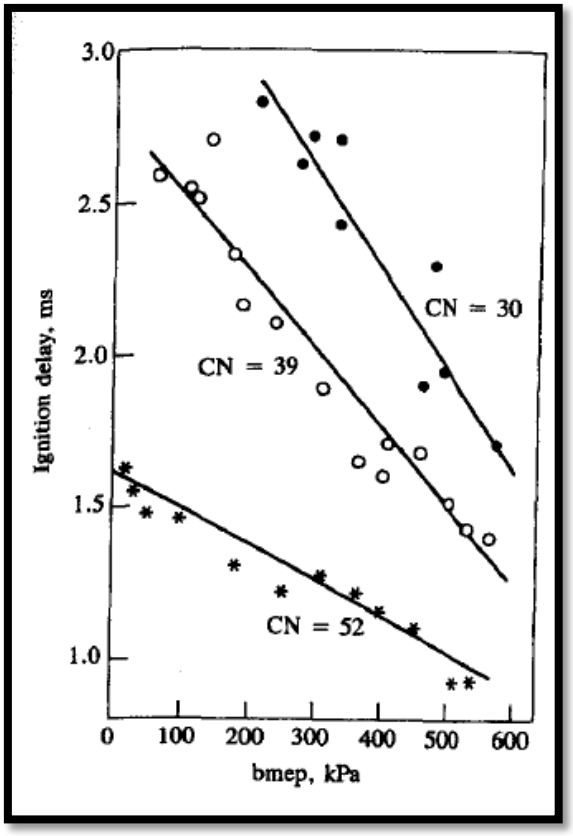

Diesel (Cetane)	Methanol (Cetane)
38~58	<5

Figure 6.5 Effect of cetane number on ignition delay [Heywood, 1988]

When diesel fuel mixes with methanol fuel, overall cetane number of the diesel-methanol mixtures deceases. Consequently, activation energy for auto ignition increases and it takes longer time to initiate start of combustion.

Combustion duration

With increase of methanol injection, decrease of combustion duration can be observed in **Figure 6.6**. Overall combustion duration of RMD=1.54 is shorter than other 2 cases despite of lower

chemical kinetic and longer ignition delay. With increase of ignition delay due to the cooling effect, more time is allowed for diesel fuel to premix with methanol-fuel mixtures in the cylinder. As a result, the quantity of premixed diesel fuel increases as well as the mixing quality of diesel and the mixtures improves. Consequently, the fraction of diesel fuel premixed combustion increase and more fuel can be burned during premixed combustion process. It can be seen from **Figure 6.7.** With increase of methanol injection, peak rise of premixed combustion can be observed. Although separated peaks have not appeared in in-cylinder model due to the limitation of model, the most rapid gradient of RMD=1.54 tells that premixed combustion becomes stronger with increase of methanol injection as shown in **Figure 6.8.**

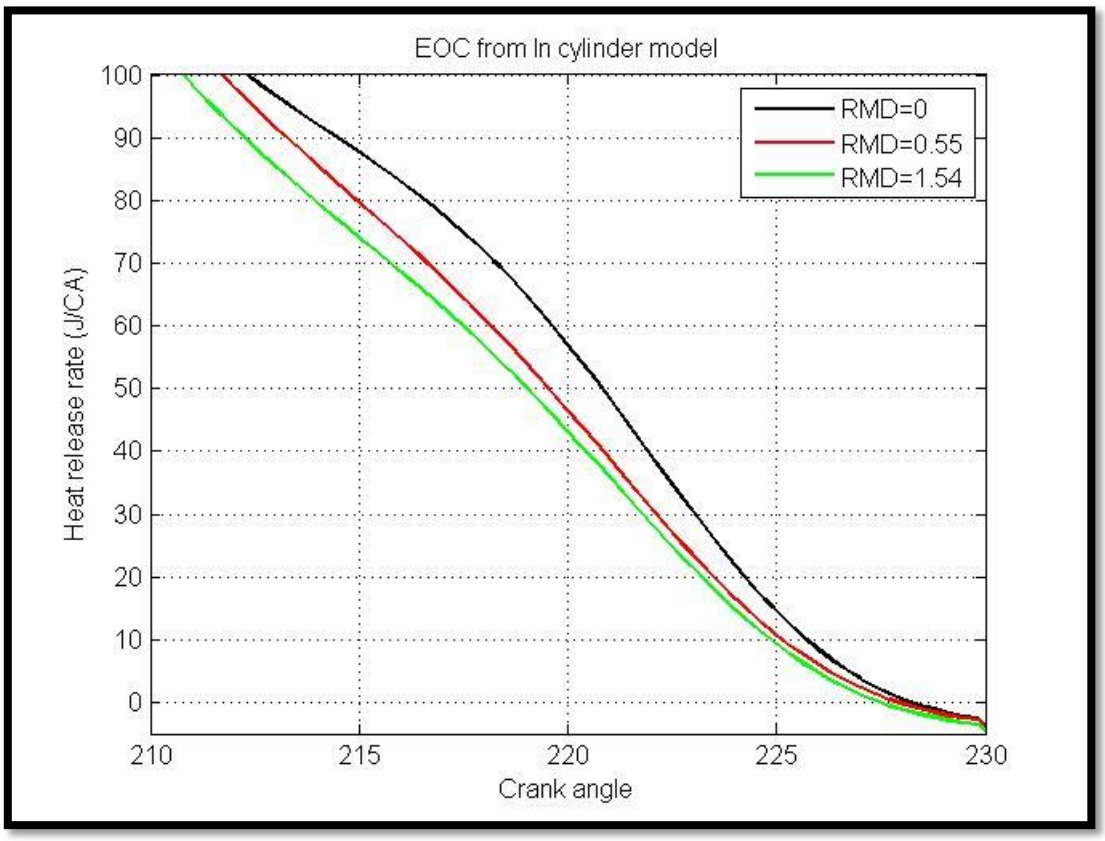

Figure 6.6 End of combustion comparison (In-cylinder model)

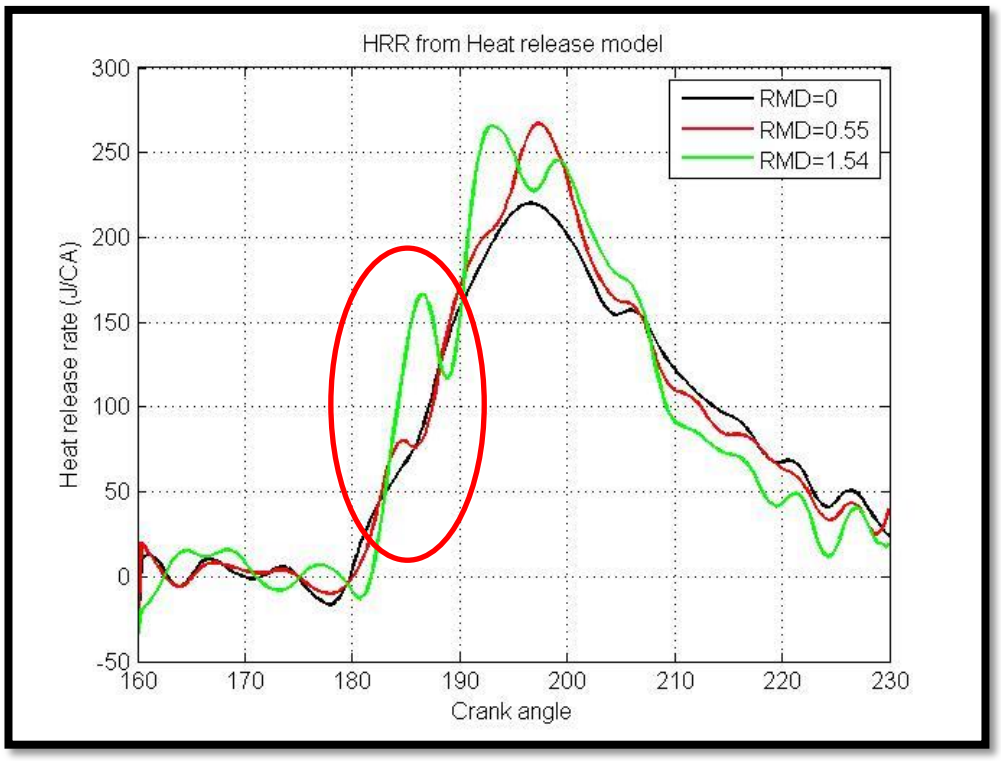

Figure 6.7 Heat release rate in heat release model

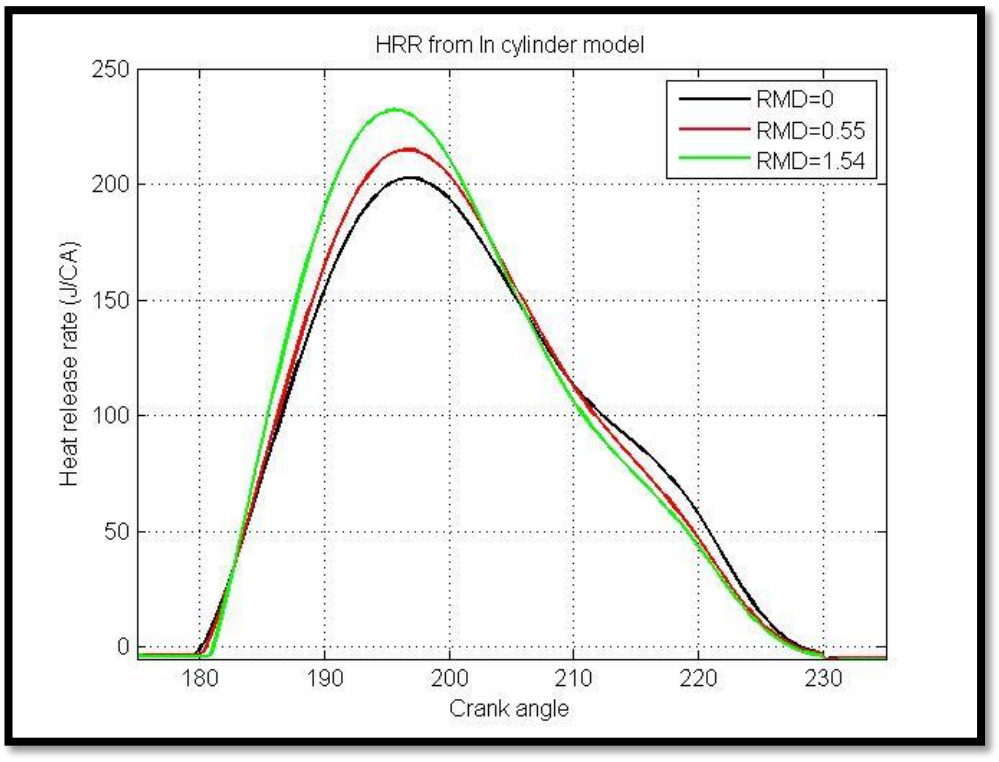

Figure 6.8 Heat release rate in in-cylinder model

The maximum heat release rate

In dual fuel operation mode, overall heat release rate is higher than that with only diesel operation. It can be explained by the cooling effect caused by heat of evaporation. With methanol injection, the temperature of in-cylinder charge decreases and it leads to longer ignition delay. The longer ignition delay contributes to higher heat release rate because it allows more time for diesel fuel premixing. In only diesel mode, premixed combustion takes place by diesel-air pre-mixtures. However, in dual fuel mode, methanol fuel also takes part in premixed combustion process. In conclusion, as methanol fuel contributes to heat release in premixed combustion and more diesel fuel is premixed in dual fuel operation, heat release rates of dual fuel become higher than only diesel operation.

Other characteristic of heat release rate is that peak value of heat release rate decreases with increase of methanol injection. The peak heat release of RMD=0.55 is slightly higher than that of RMD=1.54.

Table 6.5 Peak value of heat release rate in Heat release model

Peak value of HRR	RMD=0.55	RMD=1.54	Difference
Reference (J/CA)	**223**	**219**	**4**
Heat release model (J/CA)	**267**	**265**	**2**

In case of RMD=1.54, longer ignition delay occurs due to the cooling effect. Consequently, initial ignition takes place after TDC, where the piston starts moving downwards. During the expansion process, in-cylinder pressure and temperature decrease due to increase of in-cylinder volume. Lower temperature reduces chemical kinetics and it has negative impacts on combustion efficiency. In addition, available time for combustion also reduces. There might be some amount of fuel which is not able to burn within this limited time of the combustion. Other reason for lower combustion is due to the flame quenching. With increase of methanol injection, the temperature of in-cylinder charges decrease. This increases flame quenching. Due to the mentioned causes,

combustion efficiency decreases and it leads to lower heat release rate.

However, in-cylinder process model is not able to describe this phenomenon. **Figure 6.8** and **Table 6.2** show that RMD=1.54 has the highest peak value among all other test cases in the in-cylinder process model, which is different from the reference [Lijiang Wei et al., 2015]. This error comes from the assumption. Regardless of the amount of methanol injection, it is assumed that all the fuels are completely combusted. The value of vibe parameter "a" is 6.908 (η_{comb}=99.9%) for all the test cases because in-cylinder process simulation is conducted based on this assumption. For this reason, RMD=1.54 has higher peak value than RMD=0.55 in the in-cylinder process model. However, when lower combustion efficiency (η_{comb}=99.2%) is applied to RMD=1.54, both peak value of heat release rate and maximum temperature decrease. Test results can be found in **Figure 6.9, 6.10** and **Table 6.6**. In **Figure 6.9**, η_{comb}=99.2% was applied to only RMD=1.54.

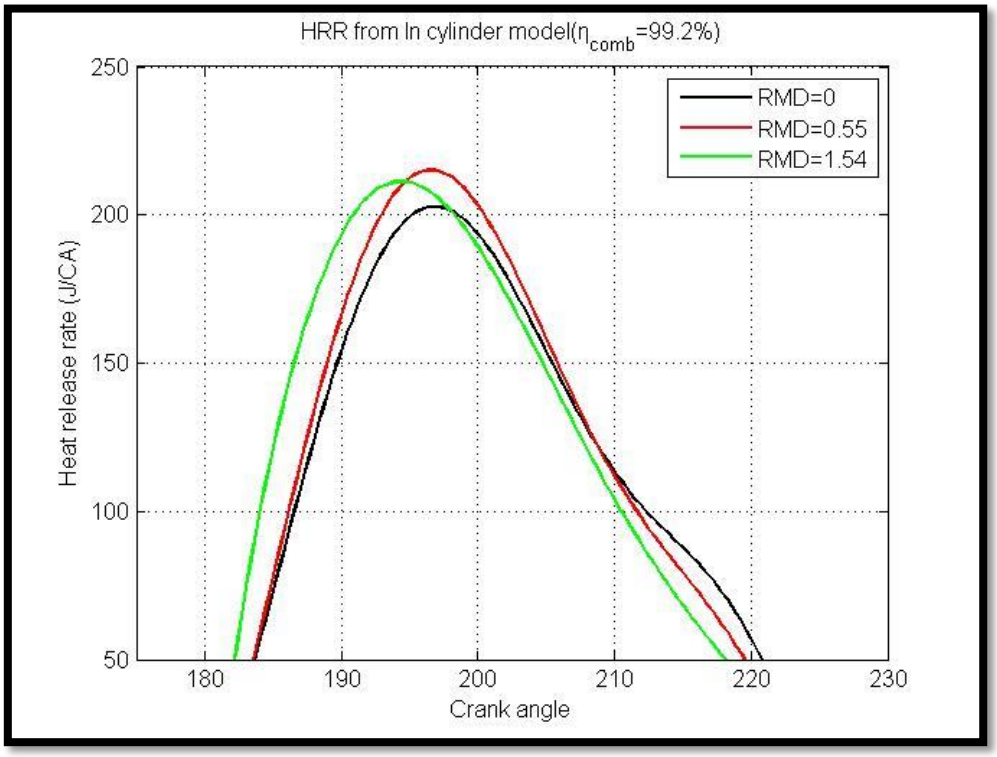

Figure 6.9 Heat release rate of RMD=1.54 (η_{comb}=99.2%)

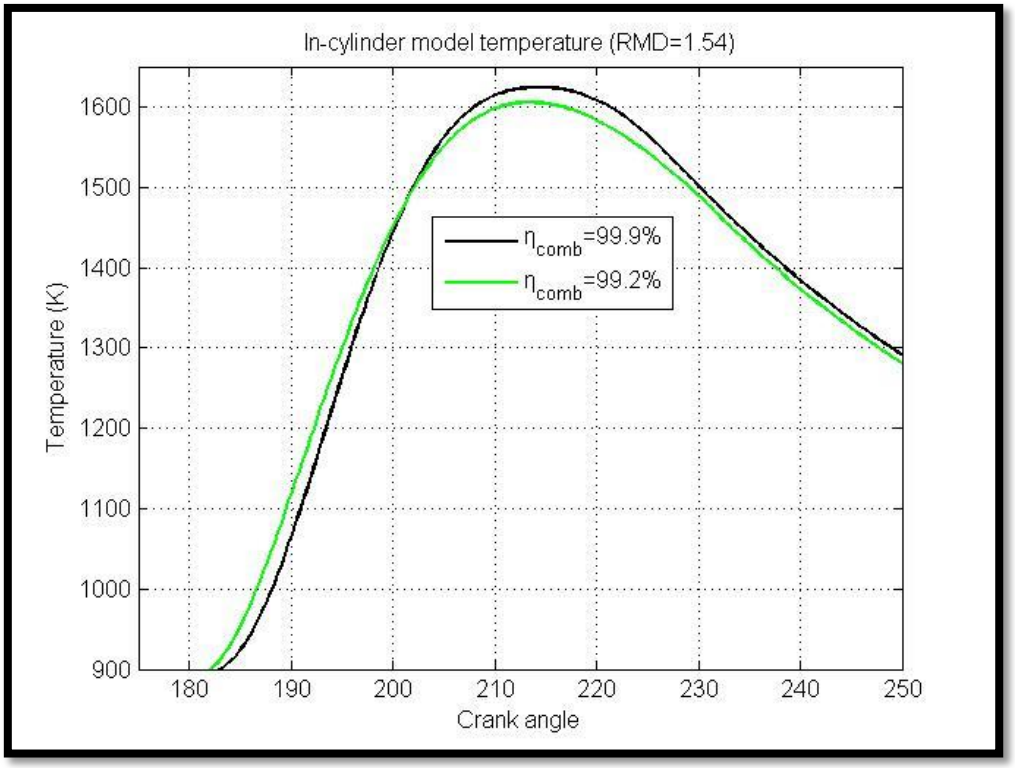

Figure 6.10 Temperature of RMD=1.54 (η_{comb}=99.2%)

Table6.6 Temperature and heat release comparison (η_{comb}=99.9% VS η_{comb}=99.2%)

	T_max (K)	Peak HRR(J/CA)
η_{comb}=99.9%	**1618**	**219**
η_{comb}=99.2%	**1605**	**211**

6.3 Pressure

6.3.1 Pressure results

The pressures in the heat release model are shown in **Figure 6.11**. These pressures are considered as the reference pressure and main input of this simulation. The plateau areas of the pressures show different features based on the various fuel ratios because the cooling effect and

ignition delay vary with fuel ratios.

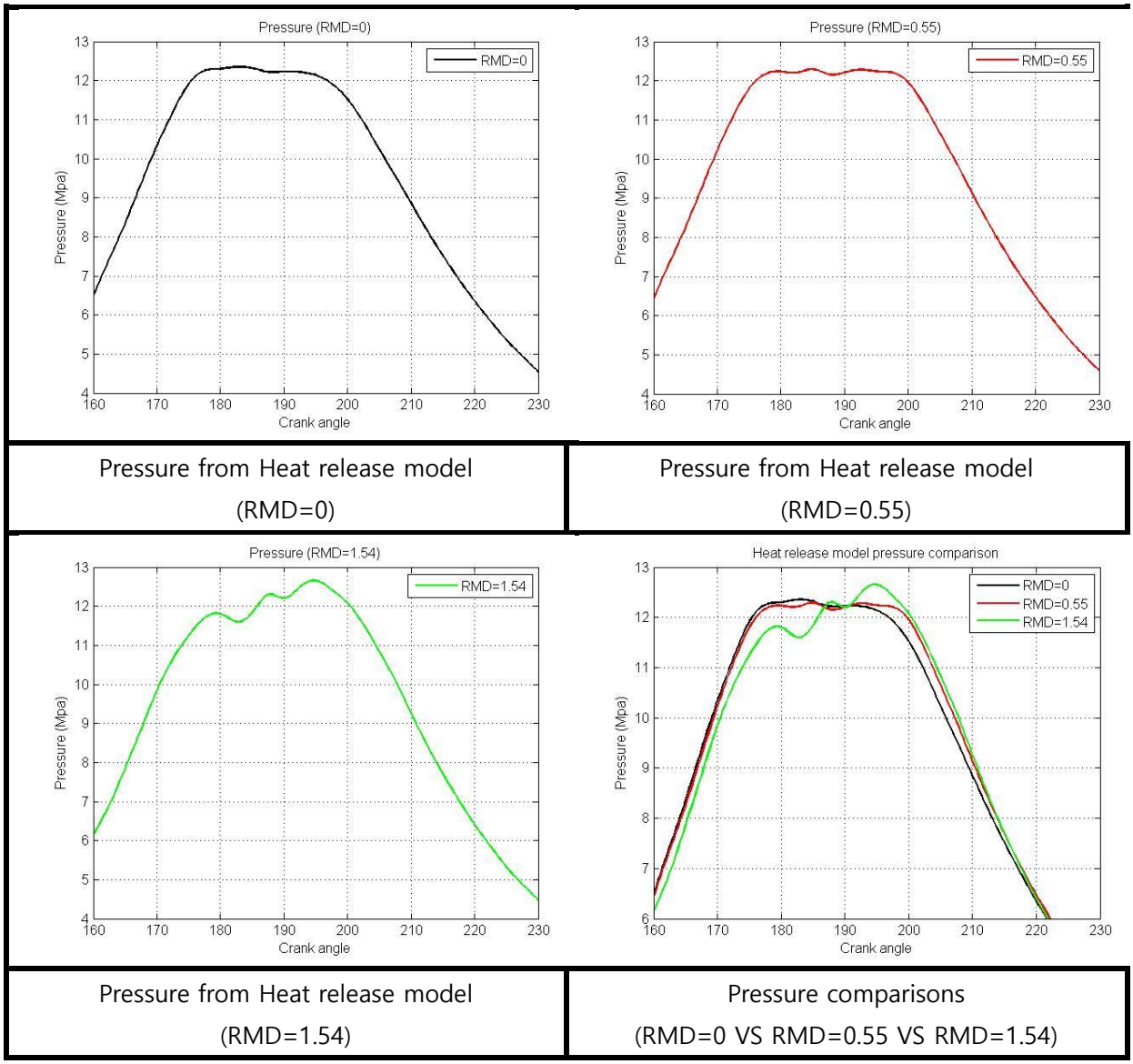

Figure 6.11 Input pressures (Heat release model)

Figure 6.12 illustrates the pressure comparisons between heat release model and in-cylinder process model. The pressures in the heat release model were obtained from the reference paper [Lijiang Wei et al., 2015]. The in-cylinder process model predicted in-cylinder pressures quite accurately. Therefore, overall pressure trends between two models were well matched in all the cases

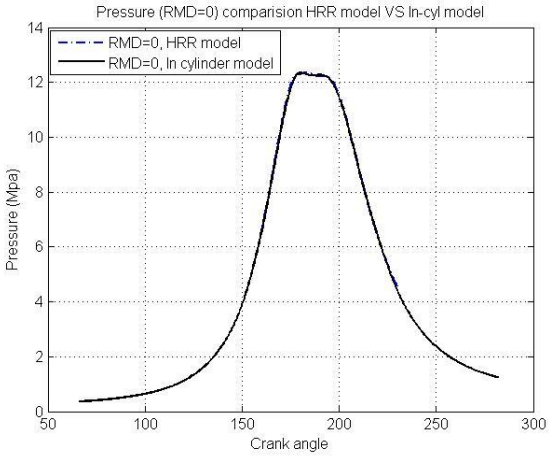

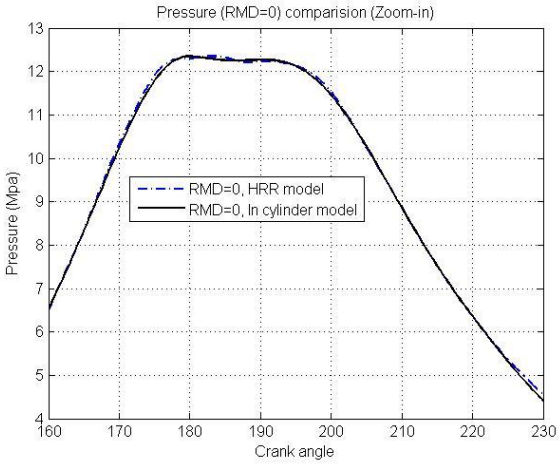

Pressure (RMD=0) HRR model VS In-cyl' model	Zoom-In (RMD=0)

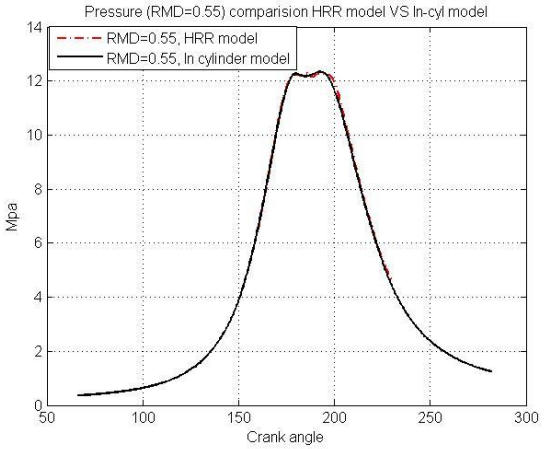

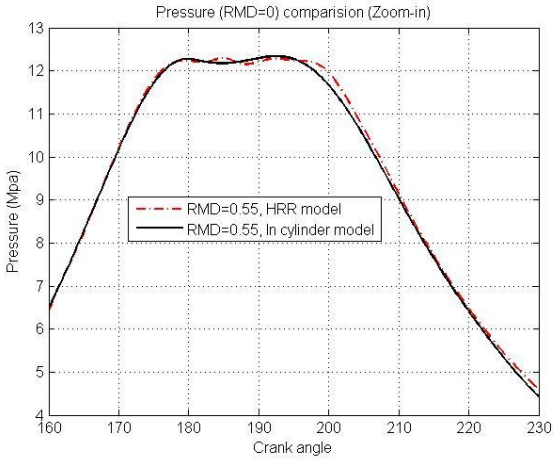

Pressure (RMD=0.55) HRR model VS In-cyl' model	Zoom-In (RMD=0.55)

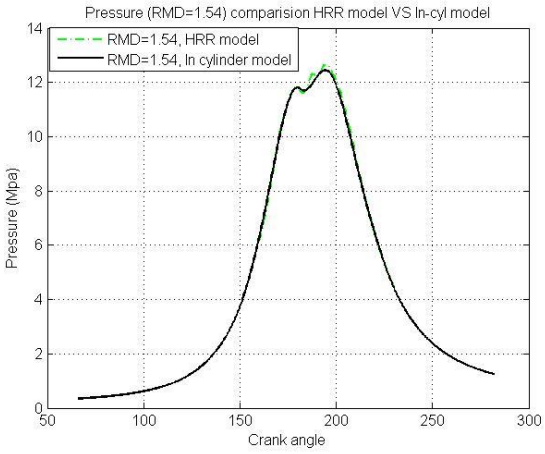

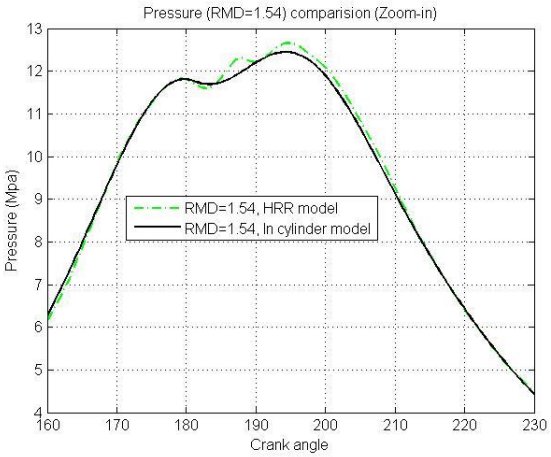

Pressure (RMD=1.54) HRR model VS In-cyl' model	Zoom-In (RMD=1.54)

Figure 6.12 Pressure comparisons between Heat release model and In-cylinder model

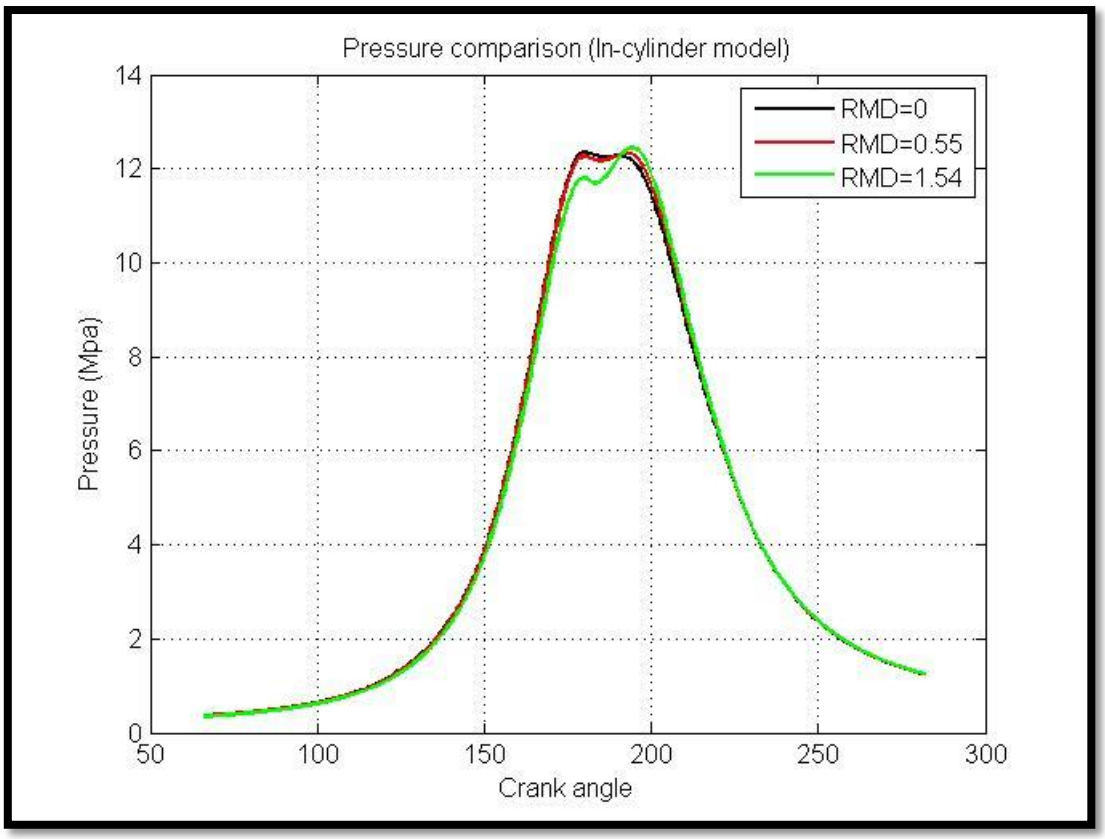

Figure 6.13 Pressure results in In-cylinder model

Figure 6.13 displays the comparisons of in-cylinder pressures with respect to different RMD in the in-cylinder model. These pressures can describe the characteristics and effects of methanol dual fuel combustion and detail explanation can be found in section **6.3.2**

6.3.2 Pressure analysis

Two major characteristics can be found in both heat release model and in-cylinder model. Figure

6.13 shows that at the end of compression (180 CA), RMD=0 has the highest pressure among all the other cases, on the other hand RMD=1.54 has the lowest pressure value.

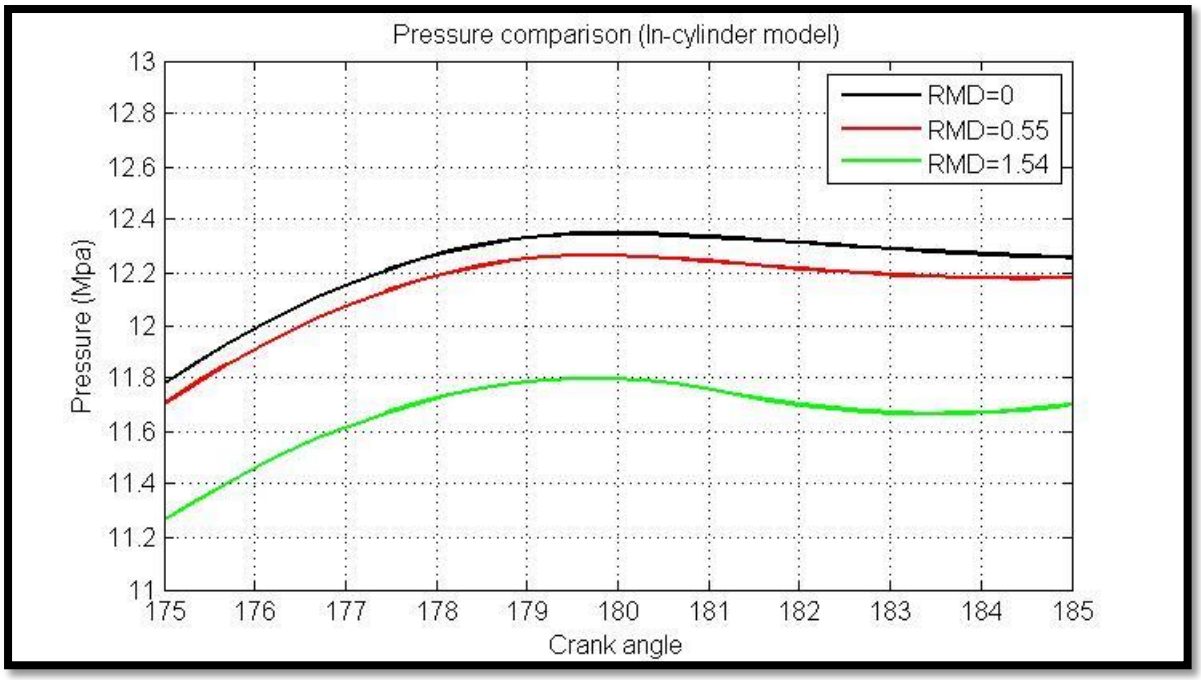

Figure 6.14 Pressure comparisons at TDC (In-cylinder model)

The characteristics of both the cooling effect and the premixed dual fuel concept give rise to this phenomenon. Unlike direct injection with high pressure concept, methanol fuel already exists in the cylinder before diesel fuel injection takes place. Methanol fuel is injected in the port where supply air goes through. Initially, methanol fuel is injected in liquid phase and as soon as methanol fuel injection takes place, it starts to absorb the heat energy from the surroundings. During heat absorption, methanol fuel starts evaporating and mixes with supply air. The more methanol fuel is injected, the lower temperature of methanol-air mixture can be generated due to the effect of heat of evaporation. The pressure gap between RMD=0.55 and RMD=1.54 is larger than the pressure gap between RMD=0 and RMD=0.55. It proves that higher dose of methanol leads to larger pressure drop due to higher cooling effect of methanol.

Table 6.7 Pressure values at TDC

	Pressure at 180 CA (Mpa)	Difference (Mpa)
RMD=0	12.35	0
RMD=0.55	12.27	-0.08
RMD=1.54	11.8	-0.55

On the contrary, the pressure results display opposite trends in the expansion process. **Figure 6.15** shows that methanol dual fuel modes have higher pressure value than only diesel mode in the expansion process. For example, the pressure values at 195 CA can be found in **Table 6.8** As methanol injection increases, the methanol-air mixtures in the cylinder become richer. As a result, the size of the immediate vicinity of pilot fuel combustion increases **Region II** in **Figure 2.5.8** and it leads to great heat release. For this reason, dual fuel modes have higher pressure than only diesel mode.

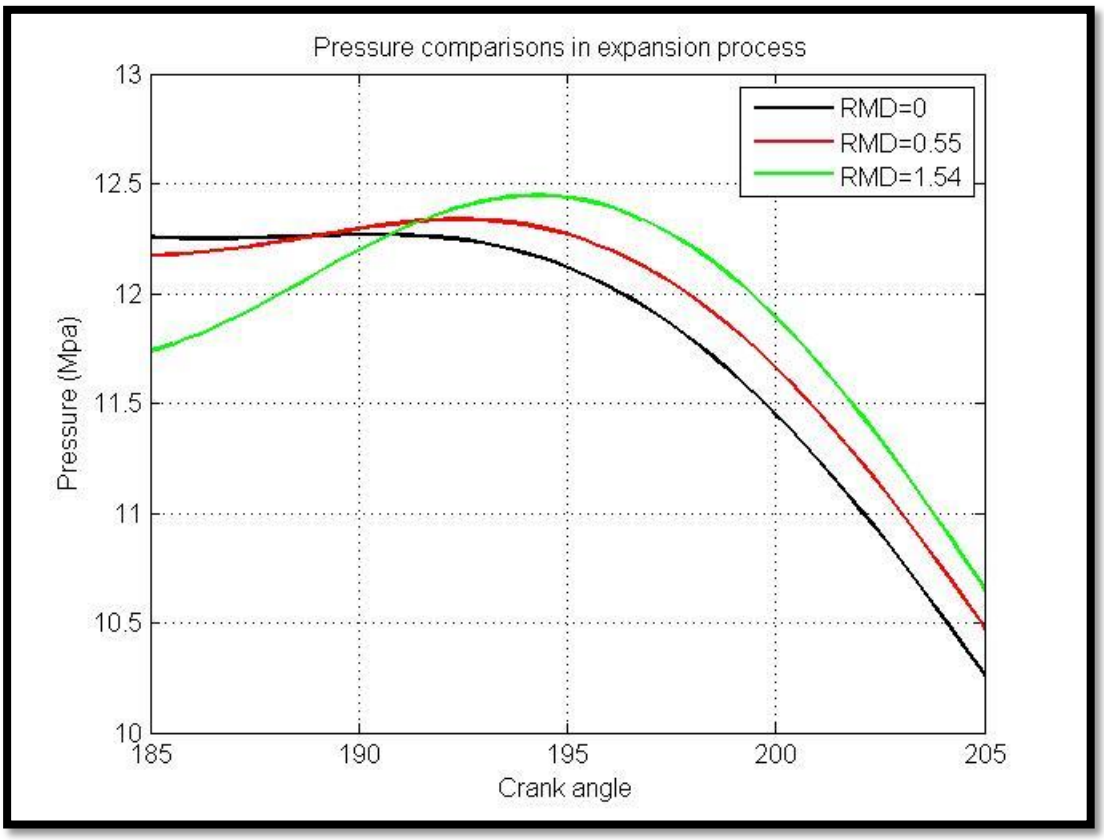

Figure 6.15 Pressure comparisons in expansion process (In-cylinder model)

Table 6.8 Pressure values at 195 CA (Expansion stroke)

	Pressure at 195 CA (Mpa)	Difference (Mpa)
RMD=0	12.12	0
RMD=0.55	12.27	0.15
RMD=1.54	12.44	0.32

6.4 Temperature

6.4.1 Temperature results

The temperatures in **Figure 6.16 and Table 6.9** are the simulation results of different methanol injection ratios in the heat release model. The maximum temperatures and the locations (Crank angle) for peak temperature vary with different methanol injection ratios. Higher methanol injection leads to higher maximum temperature and the crank angle for maximum temperature is advanced. On the other hand, no methanol injection case shows the lowest in-cylinder temperature with the most retarded crank angle for maximum temperature. Detail explanation of this phenomenon can be found in section **6.4.2**

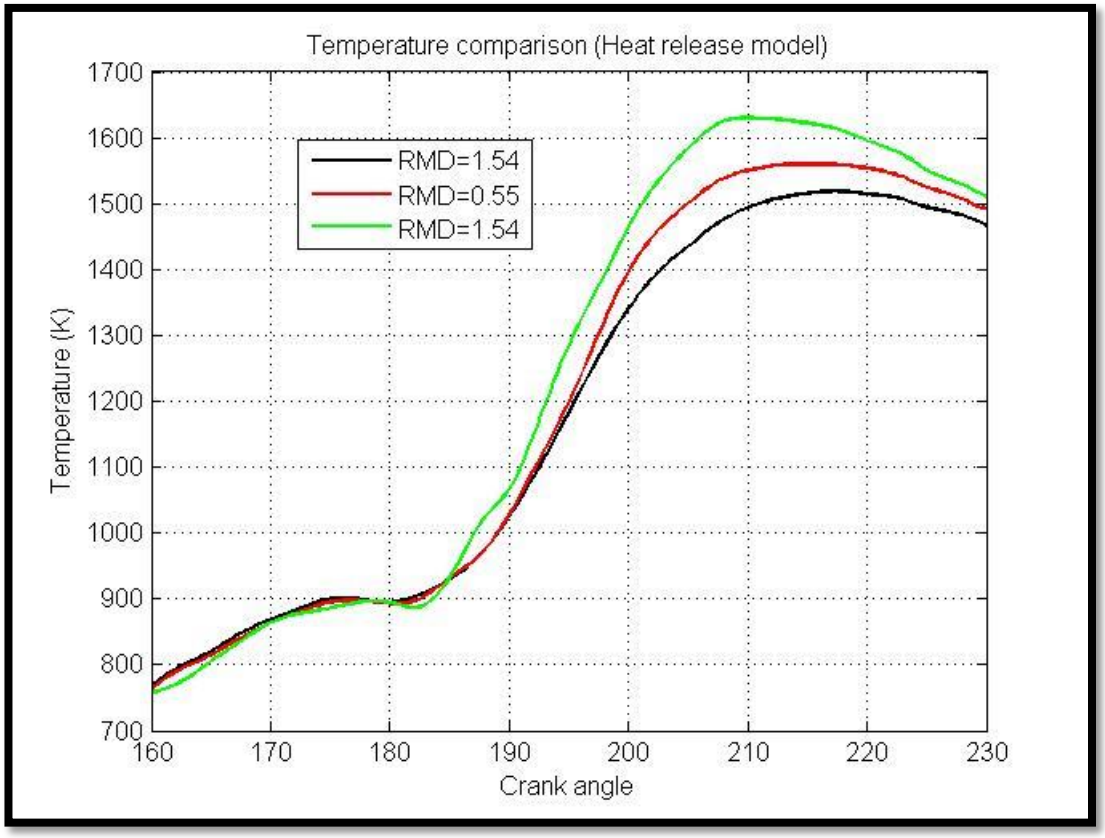

Figure 6.16 Temperature results in Heat release model

Table 6.9 T_max in Heat release model

Temperature results in Heat release rate model		
	T_max (K)	Crank angle (CA)
RMD=0	1520	217
RMD=0.55	1560	213
RMD=1.54	1630	210

The temperatures in **Figure 6.17** illustrate the comparison of the simulation results between heat release rate model and in-cylinder process model. Both results are quite well matched. The differences between two models can be found in **Table 6.10 & 6.11.**

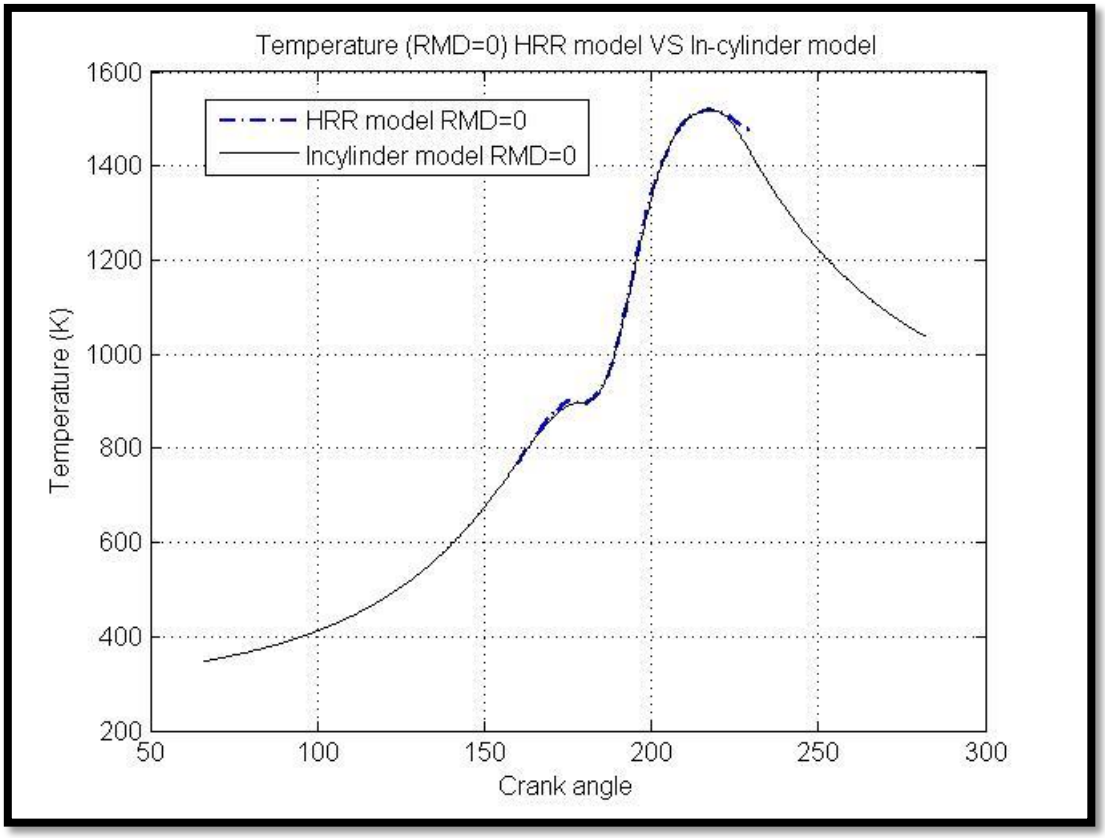
Temperature (RMD=0) HRR model VS In-cylinder model
HRR model RMD=0
Incylinder model RMD=0
Temperature (K)
Crank angle
1600
1400
1200
1000
800
600
400
200
50
100
150
200
250
300

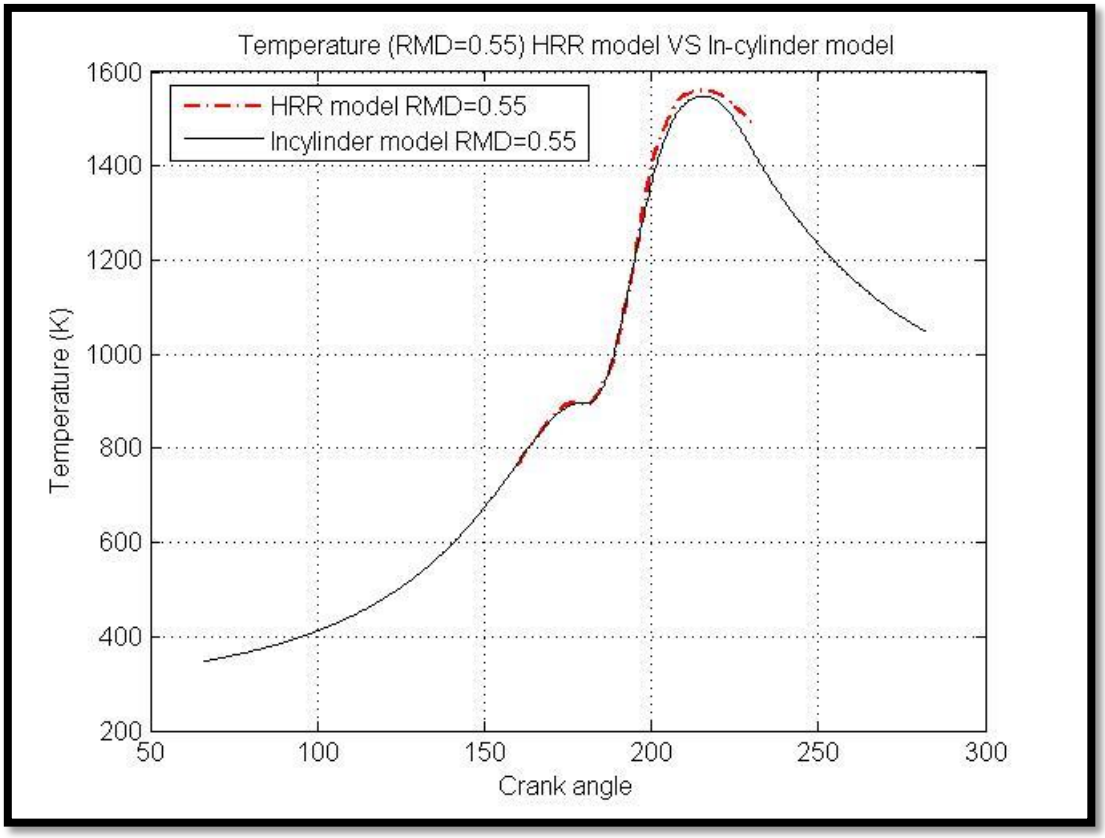
Temperature (RMD=0.55) HRR model VS In-cylinder model
HRR model RMD=0.55
Incylinder model RMD=0.55
Temperature (K)
Crank angle
1600
1400
1200
1000
800
600
400
200
50
100
150
200
250
300

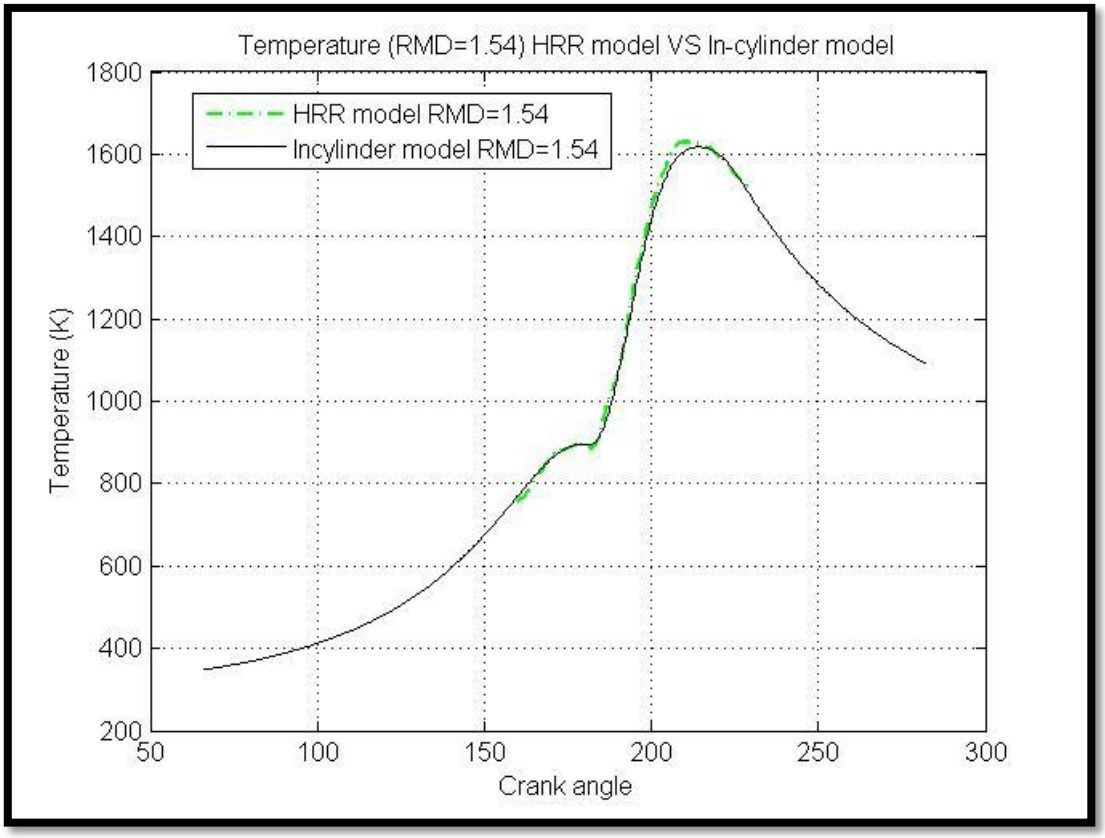

Figure 6.17 Temperature comparisons between Heat release model and In-cylinder model

Table 6.10 T_max in the In-cylinder model

Temperature result in the In-cylinder model		
	T_max (K)	Crank angle (Deg)
RMD=0	1519	217
RMD=0.55	1523	215
RMD=1.54	1618	214

Table 6.11 Difference between HRR model and in-cylinder model

Difference between HRR model & In-cylinder model			
	T_max different (K)	**Crank angle (Deg)**	**Temperature Errors (%)**
RMD=0	1	0	0.07%
RMD=0.55	37	2	2.4%
RMD=1.54	16	4	0.9%

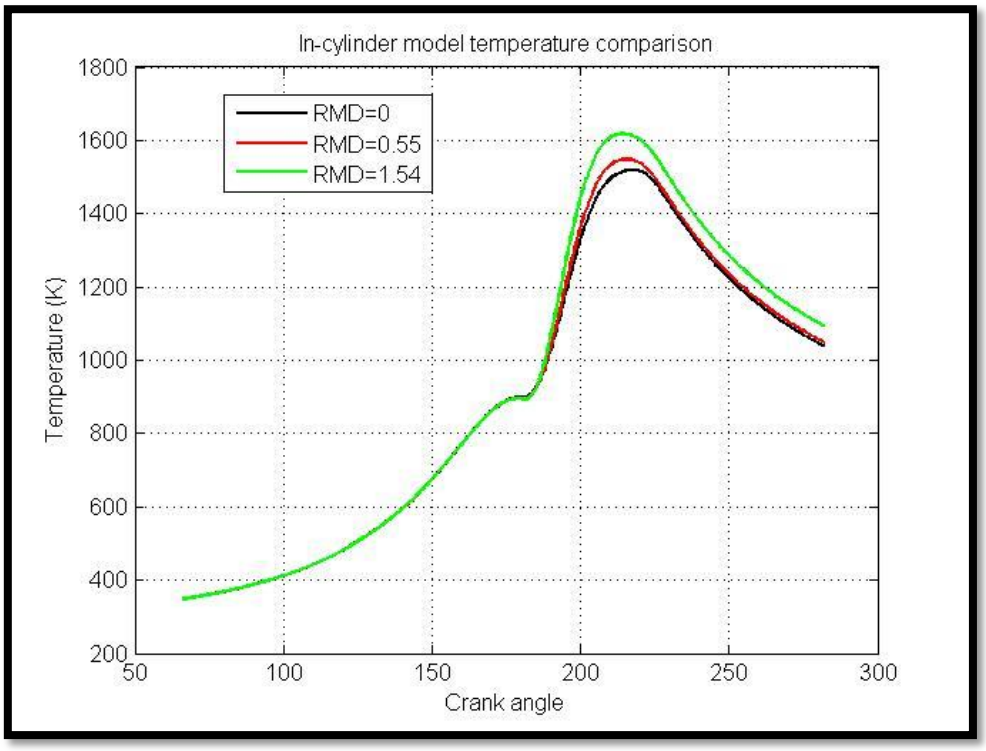

Figure 6.18 Temperature comparisons (In-cylinder model)

According to the experiment data [Lijiang Wei et al., 2015], maximum temperature for all the cases should be above 1800 K but the simulation results show roughly 250~350K lower values as shown in **Table 6.12**. The main cause of the error is due to lack of the initial condition data. Especially, initial pressure (p1) has a large influence on maximum temperature. As shown in **Table 6.13** and **Figure 6.19**, minor difference of p1 significantly changed the maximum temperature.

According to the assumption (1), p_1 is calculated based on p_2. However, p_2 was read by the naked eyes so there might be minor pressure-reading error and this can affect p_1 value.

Table 6.12 Maximum temperature difference (RMD=1.54)

Experimental data	Simulation result (Heat release model)	Difference	Error
T_max ≅ 1870 K	T_max = 1630 K	240 K	12.8 %

Table 6.13 Variation of maximum temperatures with different p1 (RMD=1.54)

p1 (Bar)	T_Max (K)	Error (%)
3.4	1630	12.8
3.3	1703	8.9
3.2	1755	6.1
3.1	1810	3.2
3	1868	0.1

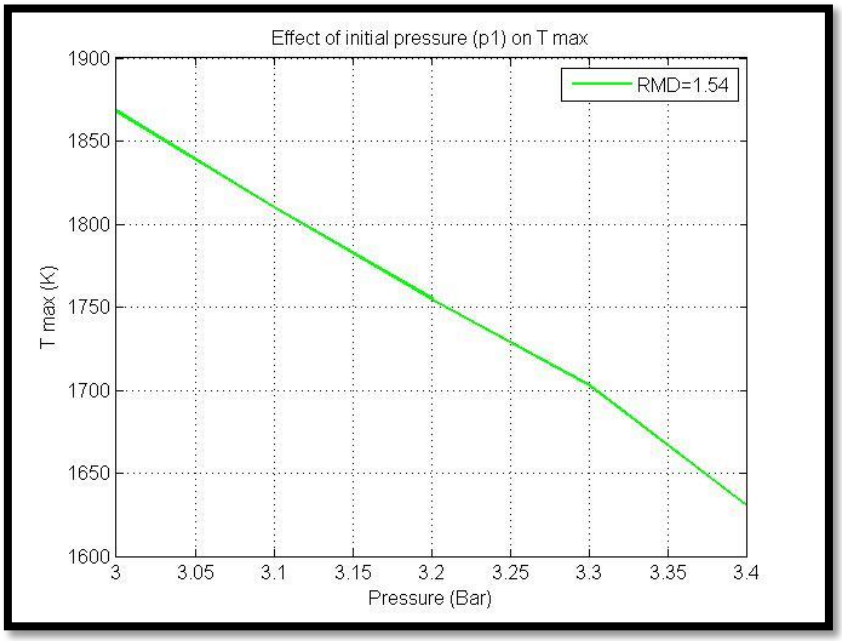

Figure 6.19 Effect of initial pressure on T max (RMD=1.54)

6.4.2 Temperature analysis

Figure 6.20 shows in-cylinder temperature around TDC. With increase of methanol injection, temperature of in-cylinder charge decreases due to the heat of evaporation. As a result, before TDC, RMD=1.54 has the lowest temperature value, on the other hand, RMD=0 has the highest temperature values. Both methanol injection cases (RMD=0.55 and RMD=1.54) show relatively larger temperature decreases than only diesel case right after TDC. Due to the cooling effect, ignition delay prolongs with increase of methanol injection. During ignition delay, in-cylinder volume increases as piston moves downward after TDC and in-cylinder temperature decreases accordingly. After ignition takes place, however, RMD=1.54 shows the most rapid temperature gradient. It can be explained by the strong premixed combustion with longer ignition delay.

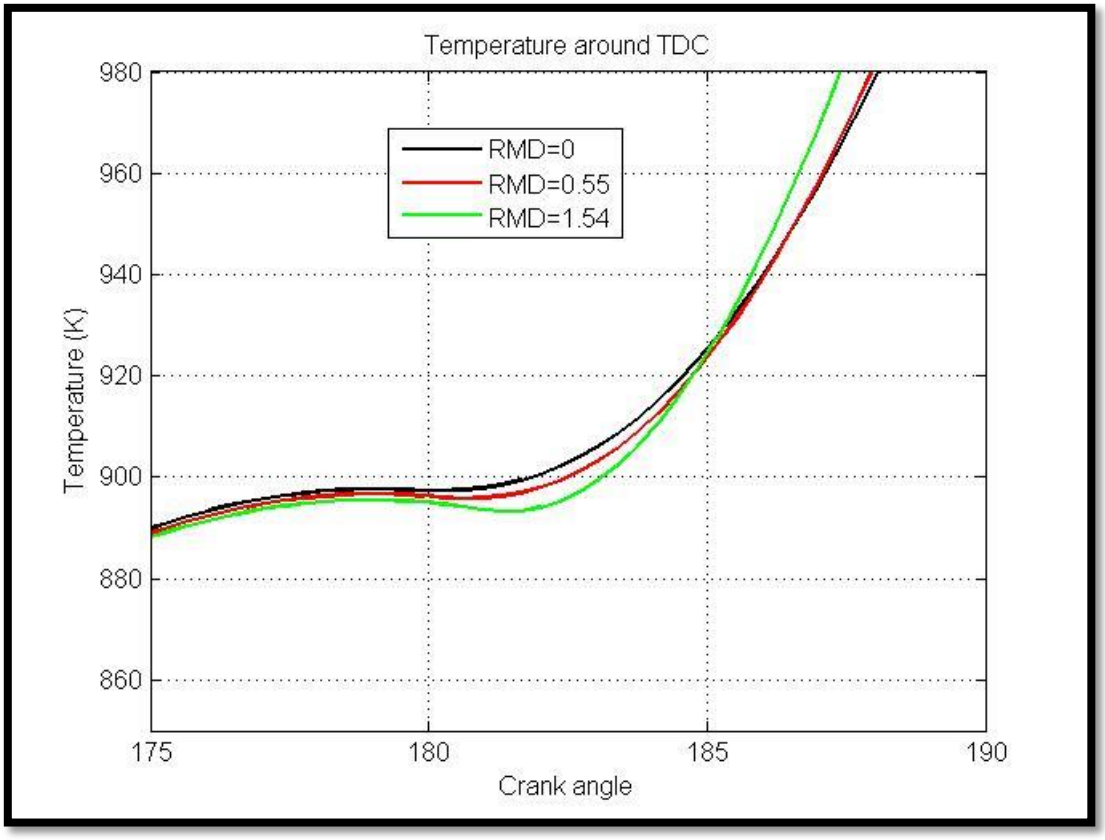

Figure 6.20 Temperatures around TDC

In case of maximum in-cylinder temperature, the results are opposite to the hypothesis. **Figure 6.21** showed that RMD=1.54 had the highest maximum temperature despite of the highest cooling effect. The intensity of premixed combustion is a key factor to understand this phenomenon. Increase of methanol injection decreases in-cylinder charge temperature as well as delays the start of ignition. In the meantime the methanol fuel-air mixtures in the cylinder become richer as methanol injection increases. In addition, the time for premixing process of pilot fuel will extend due to delayed start of ignition. As a result, premixed combustion becomes stronger with higher methanol injection. The stronger premixed combustion rapidly boosts in-cylinder temperature due to a large amount of heat release.

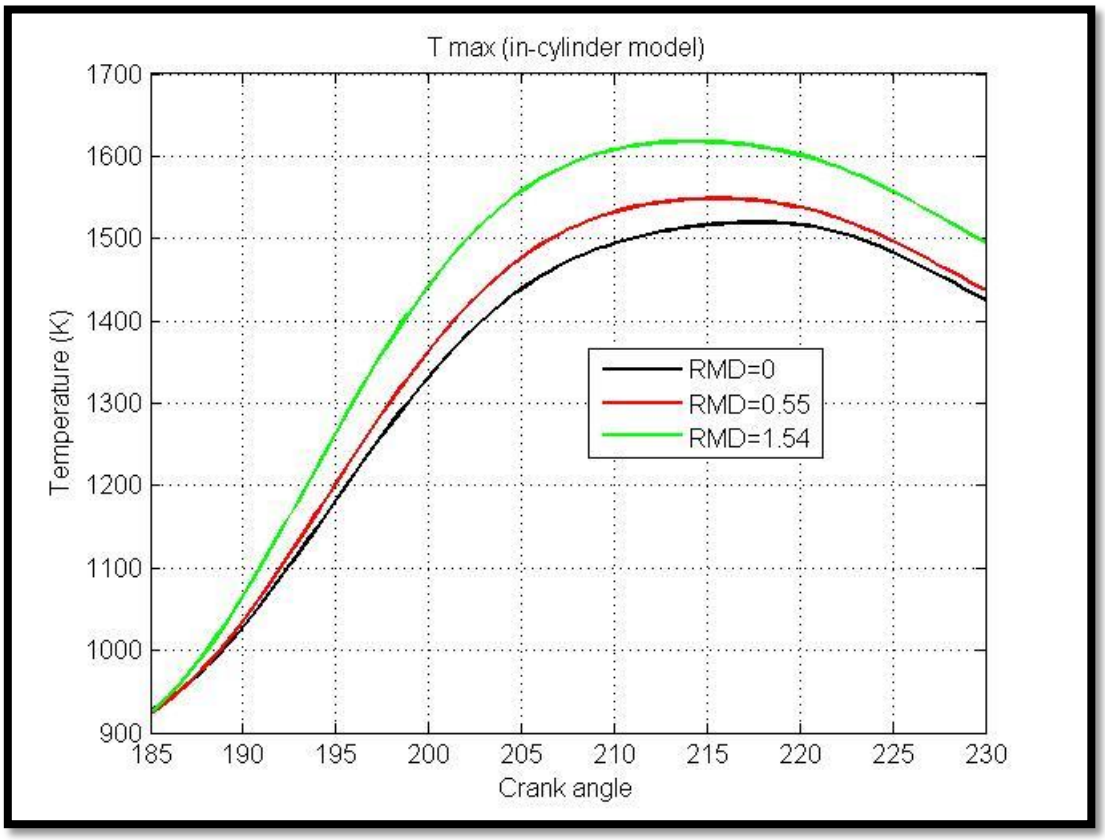

Figure 6.21 T_max comparisons (In-cylinder model)

However, the opposite result can be obtained if diesel injection timing is delayed because the injection timing of pilot fuel is also a major factor to affect maximum in-cylinder temperature. According to the experimental data [Lijiang Wei et al., 2015] as shown in **Figure 6.22**, when pilot fuel was injected at 0 TDC instead of -5.5 TDC, RMD=0 showed the highest maximum temperature. On the other hand, RMD=1.54 had the lowest maximum temperature. In advanced diesel injection timing, the maximum temperature rises with increase of methanol injection. However, in retarded diesel injection timing, the maximum temperature decreases with increase of methanol injection.

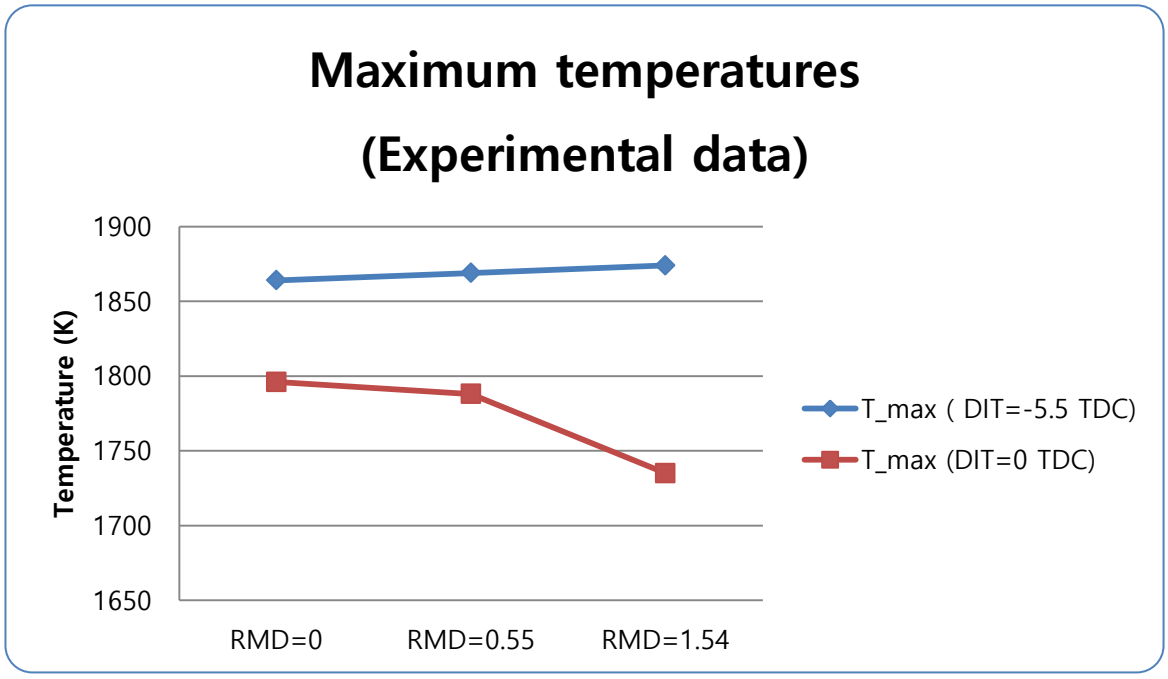

Figure 6.22 T max based on different pilot injection timing (-5.5 TDC VS 0 TDC) [Lijiang Wei et al., 2015]

In addition, ignition delay becomes more sensitive to pilot fuel injection timing with increase of methanol injection [Lijiang Wei et al., 2015]. Even if the same quantity of methanol fuel is injected, ignition delay becomes longer with retarded pilot fuel injection timing due to additional temperature decrease during expansion stroke. Detail values can be found in **Table 6.14**.

Table 6.14 Variation of ignition delay with respect to injection timing and RMD ratio [Lijiang Wei et al., 2015]

Ignition delay (Deg)			
	Injection timing at -5.5 TDC	**Injection timing at 0 TDC**	**△ Ignition delay**
RMD=0	5.4	5.6	0.2
RMD=1.54	7.3	8.7	1.4

On the other hand, the time for premixing process increases with longer ignition delay. In the competition of all these factors, the effects of heat of evaporation and expansion process are more dominant than effect of premixed combustion. With the retarded pilot fuel injection, starting point of ignition is gradually far away from the TDC. Accordingly, effect of premixed combustion becomes weak as the piston goes down due to expansion stroke and it reduces in-cylinder temperature. Therefore, in dual fuel premixed combustion engine, both diesel injection timing and fuel ratio have a huge influence on determination of maximum in-cylinder temperature. Investigation of the effects of diesel injection timing is recommended in order to better understand methanol combustion.

6.5 BSFC

Brake specific fuel consumption (BSFC) is the ratio between mass fuel consumption to the engine power. As engine power is produced by diesel and methanol fuels, both fuel masses as well as Lower Heating Values are included in the equation. [Chaichan, 2014]

$$\mathrm{BSFC} = \frac{\dot{m}_D + \left(\frac{LHV_M}{LHV_D}\right) * \dot{m}_M}{Brake\ power} \quad [g/Kwh] \tag{6.8}$$

Under the same engine output and operating load condition, the value of BSFC is higher when methanol fuel is injected, compared to only diesel operation. In addition, more methanol fuel injection leads to increase of BSFC value and it is described in **Figure 6.23**. This is mainly due to

lower LHV of methanol. To maintain the same engine power, the larger quantity of methanol fuel needs to be injected in dual fuel mode.

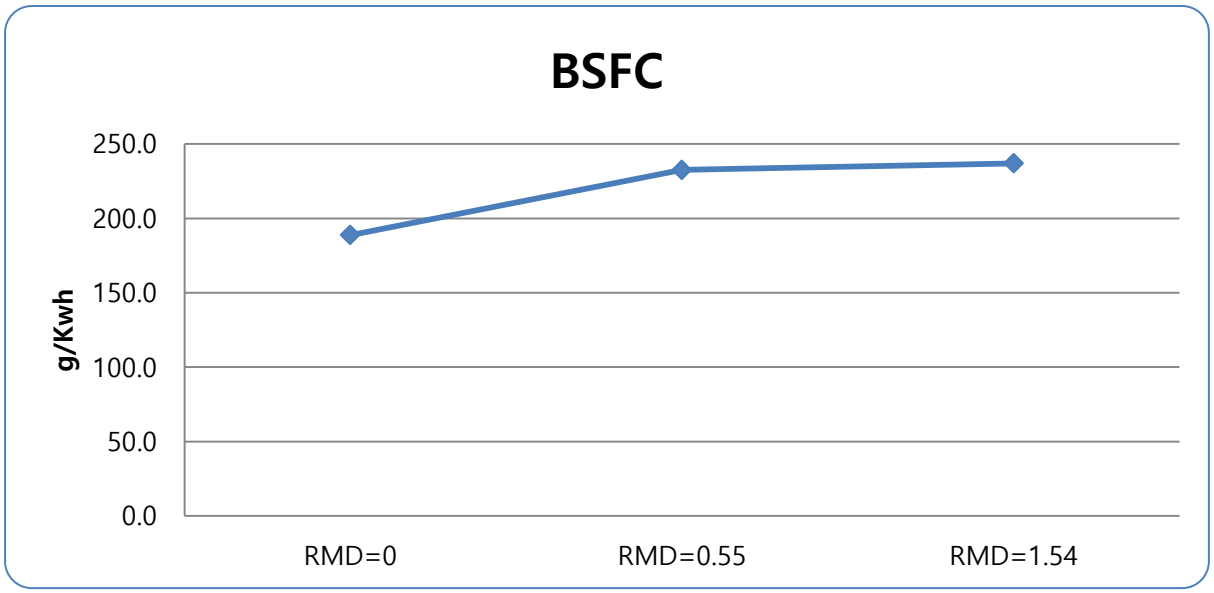

Figure 6.23 Brake specific fuel consumption comparisons

Table 6.15 BSFC comparison table

	RMD=0	RMD=0.55	RMD=1.54	Unit
BSFC	188.7	232.6	237.0	g/Kwh
Difference	0	23.2	25.5	%

6.6 Brake thermal efficiency

Brake thermal efficiency is an indicator to assess how efficiently fuel energy can be converted into mechanical power. It can be calculated by equation (6.9), [Chaichan, 2014]

$$\eta_{\text{thermal}} = \frac{Brake\ power}{(\dot{m}_D * LHV_D) + (\dot{m}_M * LHV_M)} * 100\% \quad (6.9)$$

With increase of methanol injection, brake thermal efficiency decreases because methanol fuel causes longer ignition delay. With late start of ignition, the combustion process proceeds when the piston moves downwards. As a result, less fuel energy can be converted into mechanical power consequently, brake thermal efficiency decreases. Besides, with increase of methanol injection, more methanol-air mixtures are trapped in crevices and flame quenching become strong due to the cooling effect. Therefore, less fuel can contribute to power production and it reduces thermal efficiency.

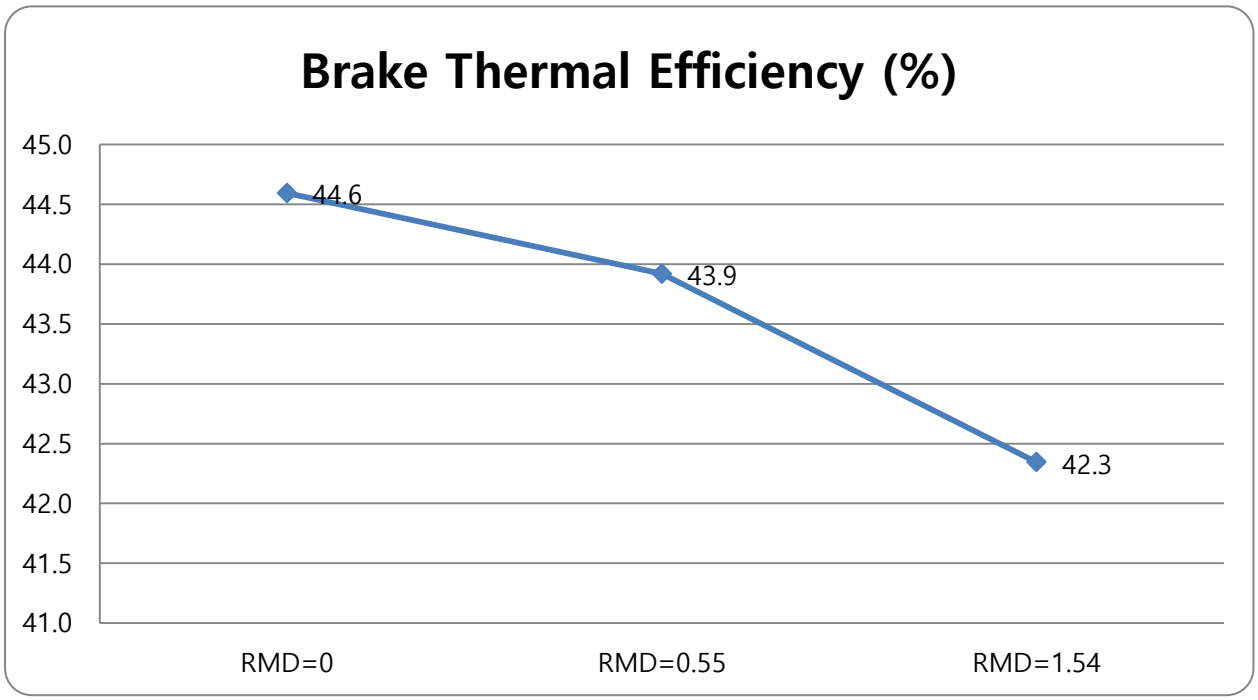

Figure 6.24 Brake Thermal efficiency comparisons

7. Conclusions and recommendations

7.1 Conclusion

The main objective of the thesis is to find out the effects of methanol fuel on in-cylinder process in internal combustion engine. Additionally, modifying the current engine models is also a part of the thesis work to understand the capabilities and limitations of the models.

Methanol fuel has distinctive physical properties compared to conventional fossil fuels. Especially 4 time higher heat of evaporation and half of LHV can affect combustion process. To maintain the same output, more methanol fuel need to be injected due to its lower LHV and this amplifies the effect of heat of evaporation. The **Table 7.1** below illustrates initial hypothesis and the simulation results.

Table 7.1 Comparison table between hypothesis and simulation results

	Hypothesis	**Simulation results**
Heat release	Increase	Increase
Ignition delay	Longer	Longer
T max	Decrease	Increase
BSFC	Increase	Increase
BTE	Decrease	Decrease

It was found out that the cooling effect caused by heat of evaporation affected in-cylinder process. With increase of methanol fuel, the cooling effect also increased. Due to the cooling effect, ignition delay prolonged and it led to stronger premixed combustion. Large amount of heat released during premixed combustion and it increased the overall heat release rate. That was the reason why methanol dual combustion had higher heat release rate than only diesel combustion.

However, in dual fuel mode, maximum heat release rate decreased with increase of methanol injection. It was due to lower combustion efficiency caused by the longer ignition delay and flame quenching. With increase of methanol injection, start of ignition retarded and initial ignition took place after TDC. The effect of expansion process and shorter available time for combustion reduce

the combustion efficiency. Moreover, the temperature of methanol-air mixtures decreased with increase of methanol injection. Lower temperature increased flame quenching. These led to decrease of peak heat release rate.

In case of maximum temperature, the simulation showed the opposite results to the hypothesis. With increase of methanol injection, maximum in-cylinder temperature increased. Not only the cooling effect but also diesel injection timing had a major influence on in-cylinder maximum temperature. With advanced diesel injection timing, maximum temperature increased with increase of methanol injection because of stronger premixed effect at advanced diesel injection timing. On the other hand, with retarded diesel injection timing, maximum temperature decreased with increase of methanol injection. In this case, the effect of the expansion process and lower in-cylinder charges were more dominant than the effect of premixed combustion.

In dual fuel combustion, overall BSFC were higher than only diesel combustion. Due to its lower LHV, more methanol fuel needs to be injected to maintain the same engine power.

Brake thermal efficiency was decreased in dual fuel mode. As methanol fuel caused longer ignition delay, combustion took place during the expansion stroke. In addition, strong flame quenching took place with higher methanol injection. As a result, less fuel energy was converted into mechanical work.

From the point of modeling view, the current engine models can describe overall characteristics of methanol dual fuel combustion. Diesel fuel combustion and methanol fuel combustion were constructed by two independent vibe functions. The vibe parameters for two different vibe functions were calculated by separated reaction coordinates in the heat release model. However, the models were not able to differentiate the combustion durations between diesel fuel and methanol fuel. With different combustion duration, the accuracy of simulation will be increased.

In conclusion, combustion was affected by the physical properties of methanol fuel. Type of engine and operating condition also had significant influences on in-cylinder process. There were several factors which affected engine combustion and the dominance of factors varied with operating condition. In addition, the model can predict overall characteristics of methanol combustion. However, further development of model is required to increase simulation accuracy.

7.2 Recommendations

The main objective of this thesis is to investigate the effects of methanol fuel on combustion in premixed dual fuel engine. It is found out that operating conditions of engine also played a key role in combustion process. For better understanding of methanol combustion, further researches are necessary.

■The effects of various pilot fuel injection timing need to be investigated as pilot fuel injection timing is one of important factors to determine ignition timing and overall combustion shape.

■It is important to find out operating limit of methanol dual fuel engines. Various air-fuel ratios need to be investigated to study the operation limits because it has large influence on misfire/knocking phenomena.

■Woschni's model from original model C was used in this thesis to evaluate the heat transfer coefficient. However, further study is recommended to find out that whether the woschni's model is suitable for methanol port injection engine or not.

■In this thesis, combustion efficiency was assumed to be 99.9%. However, actual combustion efficiency needs to be found out to investigate the influence of combustion efficiency on emissions of methanol combustion.

■Last but not least, it is important to incorporate methanol fuel evaporation model to improve the accuracy of port injection methanol engine. In addition further modification of model is necessary to differentiate combustion durations for different fuels.

Appendix I- LHV of methanol

In general, LHV is called as the Heat of combustion (Q_c) and it can be defined by

$$Q_c = H_R - H_p \quad \text{(A1.1)}$$

where H_R and H_P stand for the enthalpy of reactants and products, respectively.

Combustion equation of methanol fuel is,

$$CH_3OH + 1.5 * O_2 \rightarrow CO_2 + 2H_2O + Q_c \quad \text{(A1.2)}$$

During combustion process, reactants are converted into products and heat energy is released by the rearrangement of chemical bonds in the reactants. The standard enthalpy of formation (h_f^o) is used to quantify the chemical bond energy at standard condition (25℃, 1 atm). Since O_2 and N_2 are the most stable form, they have zero enthalpy of formation. The necessary enthalpy of formation values for methanol combustion can be found in **Table A1**.

Table A1 Enthalpy of formation of methanol combustion

Species	**Enthalpy of formation ($\bar{h}_f^o$) (KJ/Kmol)**
H_2O (g)	-241,830
CO_2 (g)	-393,520
CH_3OH (l)	-238,430

The heat of combustion per kmol of CH_3OH at standard condition is,

$$Q_c = \left(\bar{h}_f^o\right)_{CH_3OH(l)} - 1 * \left(\bar{h}_f^o\right)_{co2} - 2 * \left(\bar{h}_f^o\right)_{H2O} \quad \text{(A1.3)}$$

$$Q_c = \left(-238{,}430\,\frac{KJ}{Kmol\ CH_3OH}\right) - \left(\frac{1\ Kmol\ CO_2}{Kmol\ CH_3OH}\right) * \left(-393{,}520\,\frac{KJ}{Kmol\ CO_2}\right) - \left(\frac{2Kmol\ H_2O}{Kmol\ CH_3OH}\right) * \left(-241{,}820\,\frac{KJ}{Kmol\ H_2O}\right) = 638{,}730\ KJ/Kmol$$

LHV of methanol in MJ/KG is calculated by dividing molecular weight of methanol,

$$LHV = \frac{638{,}730\frac{KJ}{Kmol\ CH_3OH}}{32\frac{Kg\ CH_3OH}{Kmol\ CH_3OH}} = 19{,}960\,\frac{\mathrm{KJ}}{\mathrm{Kg}} = 19.960\,\frac{\mathrm{MJ}}{\mathrm{KG}} \quad \text{(A1.4)}$$

Appendix II - Curve fitting results and Vibe parameters

With vibe parameters, non-dimensional combustion reaction (Z) and non-dimensional combustion progress (X) can be illustrated. **Figure A2.1** is only diesel mode and **Figure A2.2** and **Figure A2.3** are dual fuel mode. As increase of RMD, the size of Z_{Diesel} and X_{Diesel} decreased but the size of $Z_{Methanol}$ and $X_{Methanol}$ increased.

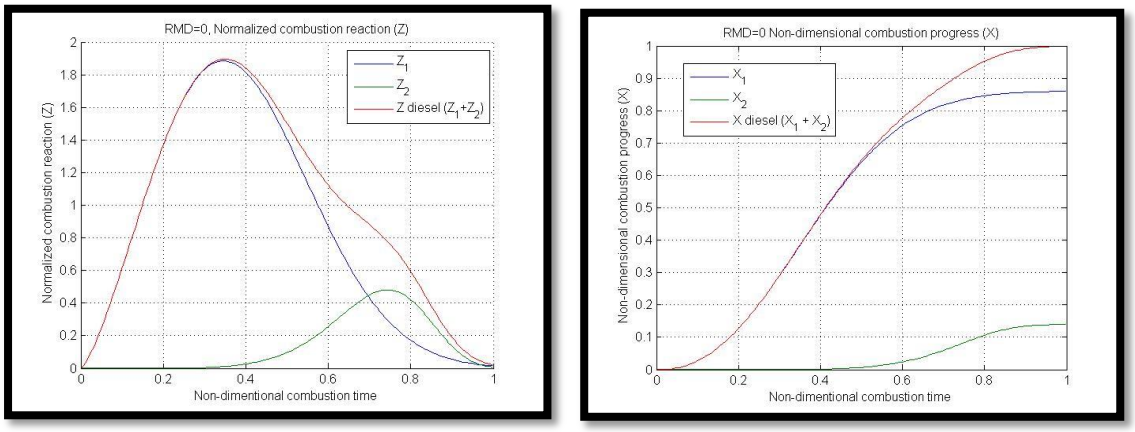

Figure A2.1 Non-dimensional combustion reaction (Z) and progress (X) of RMD=0

Table A2.1 Vibe parameters of RMD=0

	Diesel combustion				**Methanol combustion**		η_{comb}
RMD=0	b1	m1	b2	m2	b3	m3	a
	0.8605	1.341	0.1395	6.057	0	0	6.908

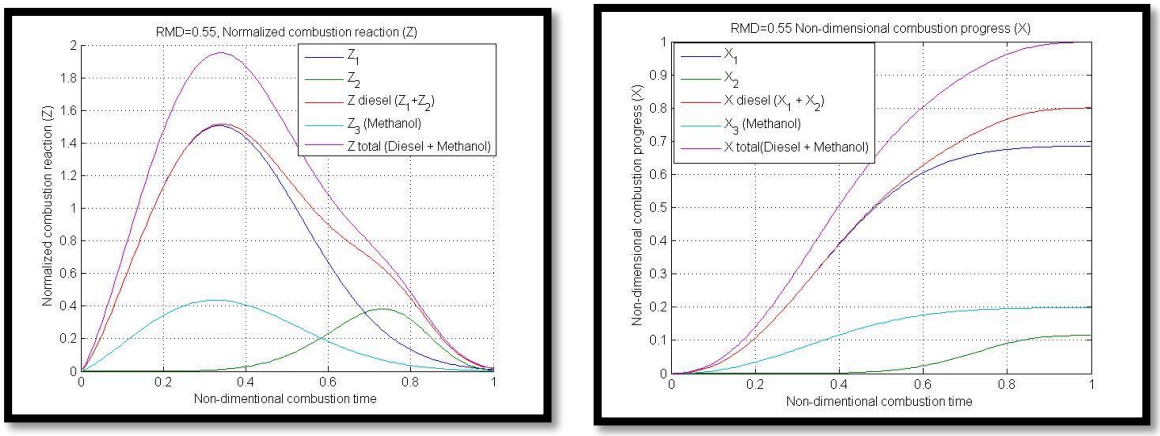

Figure A2.2 Non-dimensional combustion reaction (Z) and progress (X) of RMD=0.55

Table A2.2 Vibe parameters of RMD=0.55

	Diesel combustion				**Methanol combustion**		η_{comb}
RMD=0.55	b1	m1	b2	m2	b3	m3	a
	0.8564	1.303	0.1436	5.696	1	1.252	6.908

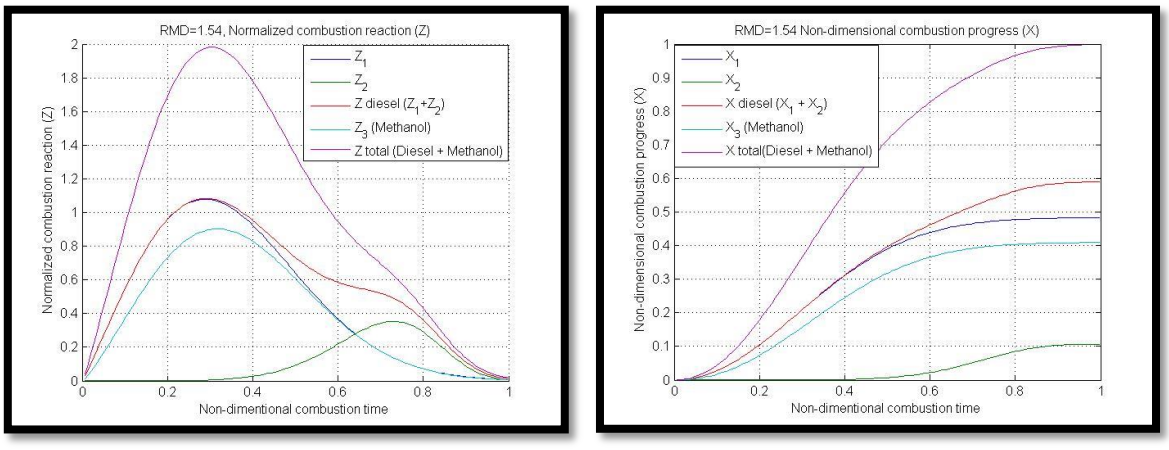

Figure A2.3 Non-dimensional combustion reaction (Z) and progress (X) of RMD=1.54

Table A2.3 Vibe parameters of RMD=1.54

	Diesel combustion				Methanol combustion		η_{comb}
RMD=1.54	b1	m1	b2	m2	b3	m3	a
	0.8191	1.079	0.1809	5.642	1	1.211	6.908

The curve fitting results can be evaluated by the goodness of fit, which is R-square. The range of R-square is between 0 and 1. If R-square is 1, it means the fitting result perfectly reproduces the original line. **Table A2.4** shows the fitting results of all RMD cases. Overall fit results are good because R-square values are above 0.99.

Table A2.4 Curve fitting results (Accuracy)

R-square		
	Diesel	Methanol
RMD=0	0.9933	N/A
RMD=0.55	0.9932	0.9909
RMD=1.54	0.9998	0.9984

The contribution of vibe parameters to normalized combustion reaction (Z) and progress (X) can be investigated by changing the values of vibe parameters. For example, **Figure A2.4** shows the effects of parameter "m" on methanol combustion of RMD=0.55.

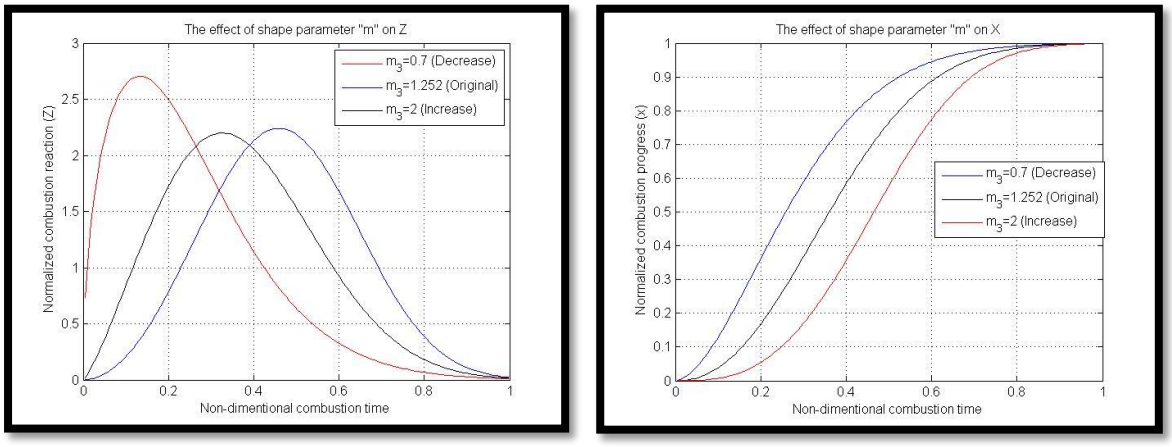

Figure A2.4 The effect of parameter "m" on Z and X (Methanol combustion of RMD=0.55)

m3=1.252 was the original value. When m3 decreased (m3=0.7), peak point of Z is advanced and has rapid gradient. It means that the fast reaction rate can be described by decrease of m3. With decrease of m3, combustion duration became shorter. On the right figure in **Figure A2.4**, m3=0.7 reached to X=1 faster than m3=2.

Figure A2.5 illustrates the effects of parameter "a" on Z and X. The parameter "a" represents combustion efficiency. Decrease of the value "a" stands for decrease of combustion efficiency. Due to the lower combustion efficiency, a=4 has the lowest combustion reaction (Z) and does not reach to X=1.

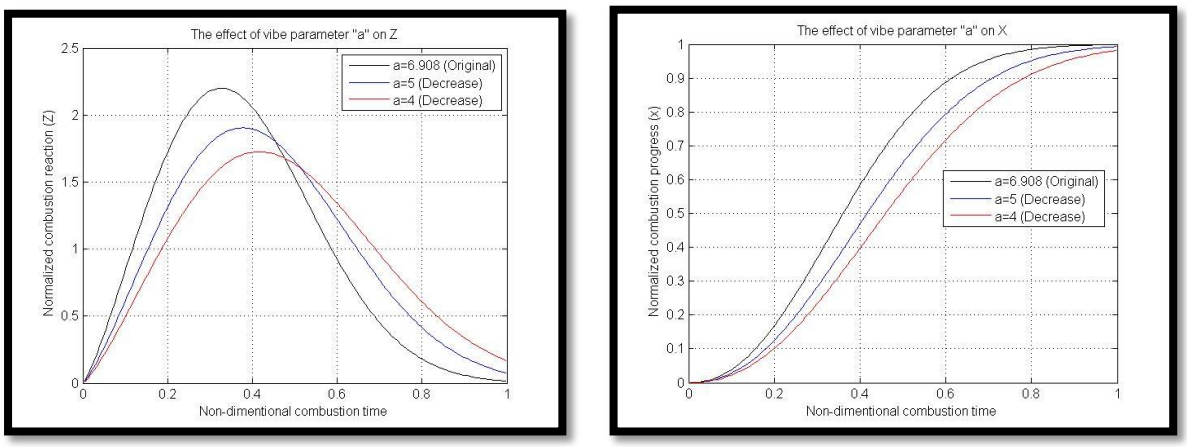

Figure A2.5 The effect of parameter "a" on Z and X (Methanol combustion of RMD=0.55)

Appendix III- Pressure sensitivity in the model

In this thesis, in-cylinder pressures were read by naked eyes as it was not possible to obtain the in-cylinder pressures by experiment at the moment. Therefore, there must be some pressure-reading errors. These errors had large influence on heat release rates. Although there was minor pressure reading-error, heat release rates were significantly changed.

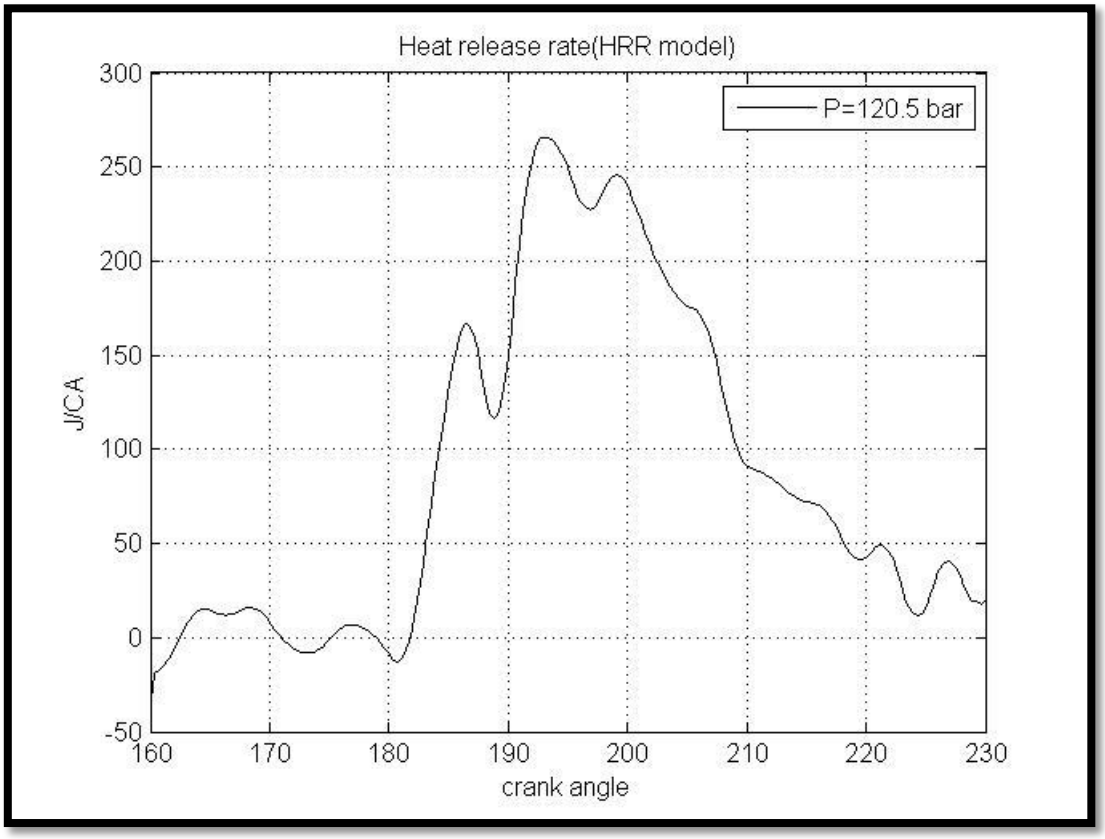

Figure A3.1 Heat release rate (P=120.5 bar at 200 CA)

In **Figure A3.1**, pressure was 120.5 bar at 200 CA. To see the sensitivity of heat release rate to pressure values, 119.5 bar and 121.5 bar were applied at 200 CA. As intermediates values were determined by interpolation, pressure change at 200 CA had influences on determination of neighboring values. The largest difference of heat release rate can be found at 199 CA.

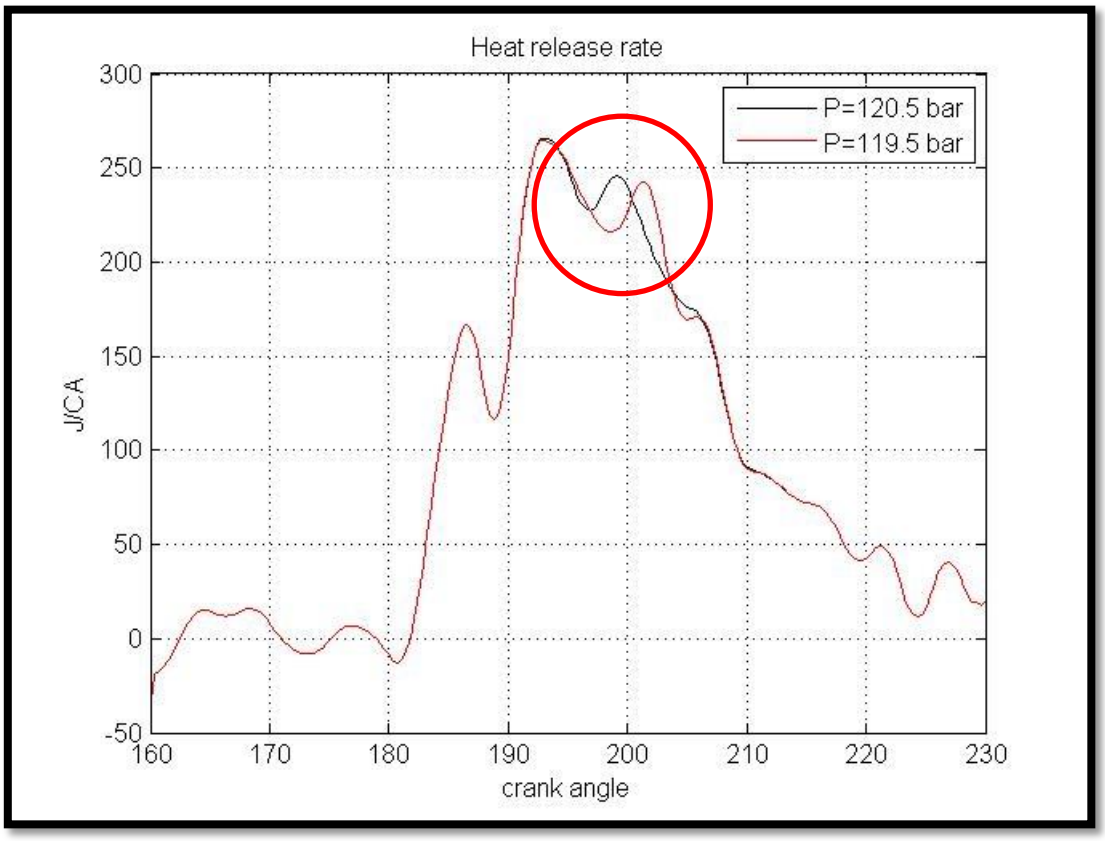

Figure A3.2 Heat release rate (P=119.5 bar at 200 CA)

Table A3.1 Heat release rate comparison between P=119.5 and P=120.5

1 bar decrease		
Pressure (Bar)	**120.5**	**119.5**
Q at 199 (J/CA)	**245.6**	**216.8**
△Q (J/CA)	**-28.8**	
Error (%)	**-11.7**	

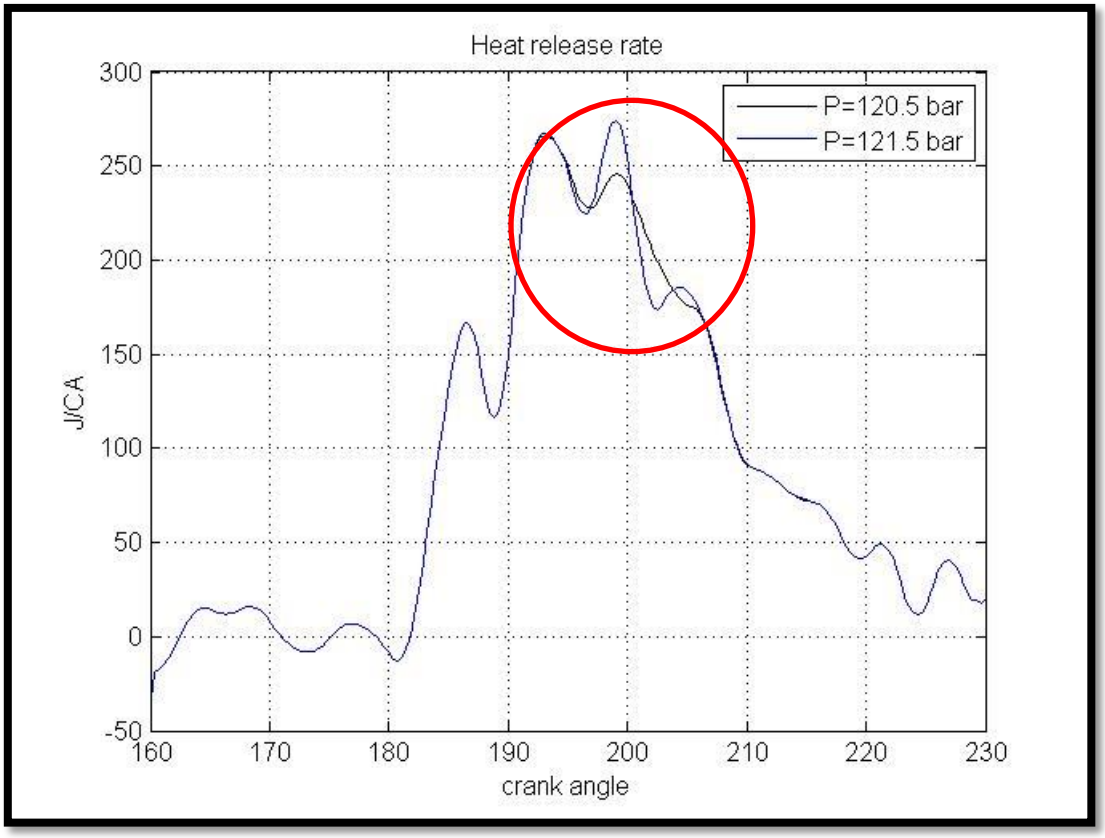

Figure A3.3 Heat release rate (P=121.5 bar at 200 CA)

Table A3.2 Heat release rate comparison between P=120.5 and P=121.5

1 bar increase		
Pressure (Bar)	**120.5**	**121.5**
Q at 199 (J/CA)	**245.6**	**274.4**
△Q (J/CA)	**28.8**	
Error (%)	**11.7**	

As shown in **Figure A3.2** and **Figure A3.3**, it can be seen that 1 bar differences have huge impact on heat release rates and it leads to significant changes in heat release rate.

Appendix IV- Limit of models

To increase simulation accuracy, it is necessary to differentiate between diesel combustion duration and methanol combustion duration. There was an attempt to apply different combustion durations. For example, longer ignition delay was applied to methanol combustion. Consequently, overall combustion duration of methanol fuel was shorter than that of diesel fuel. However, shorter combustion duration of methanol fuel led to a temperature difference between heat release model and in-cylinder model as shown in **Figure A4.1**. This is because methanol fuel consumption decreased with shorter combustion duration in the in-cylinder model. **Figure A4.2** shows the difference fuel consumption between heat release model and in-cylinder model. The blue line on the graph is the benchmark fuel consumption.

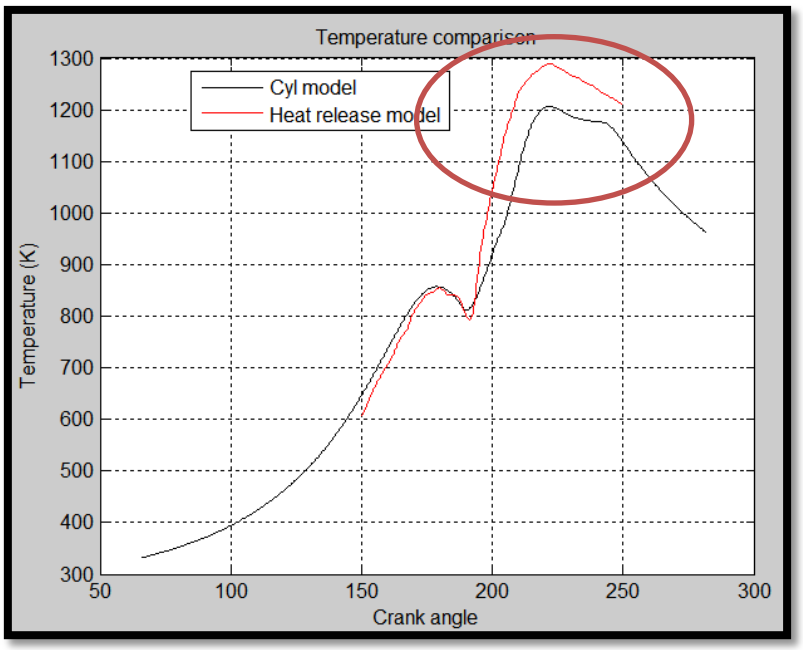

Figure A4.1 Temperature difference between heat release model and in-cylinder model

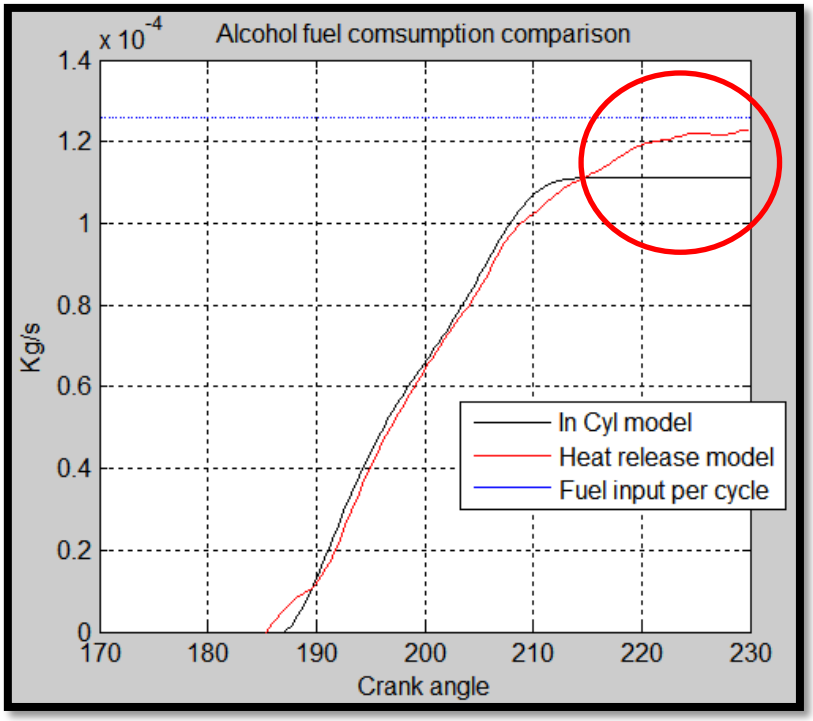

Figure A4.2 Alcohol fuel consumption comparisons between HRR model and in-cylinder model

Combustion duration (τ) is a key factor to determine vibe parameters and these vibe parameters are calculated based on reaction coordinate (RCO). However, combustion duration is an input of the in-cylinder model therefore it does not affect RCO because RCO is calculated in the heat release model. When shorter combustion duration was applied, it did not cover entire RCO range when curve fitting was carried out.

References

[IMO, 2016] International: IMO Marine Engine Regulations, 2016 https://www.dieselnet.com/standards/inter/imo.php ; Sep 10th 2016

[Stenhede, 2014] Thomas Stenhede, 2014
Methanol-Fuel for existing ship
Wärtsilä, GASDAGARNA, 2014

[Mitsui Chemicals, 2008] Mitsui Chemicals, 2008
Mitsui Chemicals to Establish a Pilot Facility to Study a Methanol Synthesis Process from CO_2 ,
http://www.mitsuichem.com/release/2008/080825e.htm Sep 20th 2016

[Maurya et al., 2011] R.K. Maurya, A.K. Agarwal. 2011
Experimental study of combustion and emission characteristics of ethanol fuelled port injected homogeneous charge compression ignition (HCCI) combustion engine
Applied Energy 88 (4) 1169–1180.]

[H. Xie et al., 2006] H. Xie, Z. Wei, B He, H. Zhao, 2006
Comparison of HCCI Combustion Respectively Fueled with Gasoline, Ethanol and Methanol through the Trapped Residual Gas Strategy,
(SAE paper 2006-01-0635).

[Fagerlund et al., 2014] Per Fagerlund, Bengt Ramne, 2014
Production of Methanol Sustainably and Related Engine Technology
Final report of PROMSUS Workshop groups summary

[Mphoswa, 2015] Roseman Mphoswa 2015
Production of Methanol from Biomass - PLANT DESIGN
Civil and Chemical engineering of the University of South Africa

[Karsen et al., 2009] Ulrik Karsen, Troels Johansen, Jesper Schramm. 2009
Ethanol as a fuel for Road Transportation
Technical university of Denmark

[Danielsson, 2008] Hans-Åke Danielsson. 2008.
"World premiere for Scania's first ethanol-powered trucks—rapid transition to sustainable urban transport,"
http://www.scania.com/group/en/world-premiere-for-scanias-first-ethanol-powered-trucks-%E2%88%92-rapid-transition-to-sustainable-urban-transport/; Sep 11th 2016

[Lijiang Wei et al., 2015] Lijiang Wei, Chunde Yao*, Guopeng Han, Wang Pan, 2015
Effects of methanol to diesel ratio and diesel injection timing on combustion, performance and emissions of a methanol port premixed diesel engine
Tianjin University, Tianjin 300072, China, Energy 95 (2016) 223e232

[Doornbosch et al., 2007] Doornbosch, R., and Steenblik, R.. 2007
Biofuels: Is the Cure Worse than the Disease?
Organisation for Economic Co-operation and Development

[Turkcan et al., 2013] Ali Turkcan, Ahmet Necati Ozsezen, Mustafa Canakci, 2013
Effects of second injection timing on combustion characteristics of a two stage direct injection gasoline–alcohol HCCI engine
Kocaeil University, Turkey

[Breda Kegl et al,. 2013] Breda Kegl, Marko Kegl, Stanislav Pehan. 2013
Green diesel engines
ISBN: 978-1-4471-5324-5 (Print) 978-1-4471-5325-2

[MAN Diesel & Turbo, 2014] MAN Diesel & Turbo, 2014
MAN_using Methanol fuel in the MAN B&W ME_LGI Series
MAN Diesel & Turbo. *5510-0172-00ppr*

[Ujjwal K saha, 2016] Ujjwal K saha, 2016
Internal combustion engines, Lecture 18
Indian institute of Technology Guwahati

http://www.iitg.ernet.in/scifac/qip/public_html/cd_cell/chapters/uk_saha_internal_combustion_engine/qip-ice-18-combustion%20in%20ci%20engines.pdf; Aug 18th 2016

[Anjeel, 2016] Anjeel's Automotive, 2016
Understanding of hydrogen properties (Flammability and Flammability range)
http://www.anjeel.com/auto/understanding_hydrogen_properties.html; Oct 15th 2016

[Heywood, 1988] Heywood JB, 1988
Internal combustion engine fundamentals
New York: McGraw-Hill

[Pulkrabek, 2004] Pulkrabek WW. 2004
Engineering fundamentals of the internal combustion engine
2nd ed. Upper Saddle River, NJ: Pearson Prentice Hall

[Königsson, 2012] Fredrik Königsson, 2012
Advancing the limits of Dual Fuel Combustion
Department of Machine Design, Royal Institute of Technology Stockholm ISBN 978-91-7501-427-2

[Warnatz, J et al., 1999] Warnatz, J., Maas, U. & Dibble, R. W. 1999
Combustion: Physical and Chemical Fundamentals, Modeling and Simulation, Experiments, Pollutant Formation.
2nd Springer-Verlag Berlin Heidelberg, 378 pp. ISBN 978-3-540-45363-5

[Groene, 2015] Ole Groene, 2015
Application of Methanol as fuel for ship
MAN Diesel & Turbo, JICEF Meeting in Kobe, Japan

[Flagan et al., 1988] Flagan, Richard C. and Seinfeld, John H. 1988
Fundamentals of air pollution engineering
Prentice-Hall, Inc., Englewood Cliffs, New Jersey. ISBN 0-13-332537-7

[Haraldson, 2015] Lennart Haraldson, 2015
Methanol as marine fuel
Wärtsilä, CIMAC NORWAY

[Stojcevski et al., 2016] Toni Stojcevski, Dave Jay, Luca Vicenzi, 2016
Operation experience of world's first methanol engine in a ferry installation
Wärtsilä Corporation, CIMAC Congress 2016, Helsinki

[Dou. 2012] Danan Dou. 2012
Application of Diesel Oxidation Catalyst and Diesel Particulate Filter for Diesel Engine Powered Non-Road Machines
Platinum Metals Rev., 2012, 56, (3), 144–154•

[Kang, 2002] B.M Kang, J.Y. Kim, S.B Lee, T.W. Lee, J.Y. Ha, 2002
A study on the reduction of Harmful Exhaust gas with Diesel-Methanol Stratified Injection System in a Diesel engine
The Korean Society of Automotive Engineers, Transaction of the Korean Society of Automotive Engineers 10(4), 43~50 (8pages)

[Kumar, 2010] Ashok Kumar, 2010
Air Quality
Sciyo, ISBN 978-953-307-131-2

[KARIM, 2015] GHAZI A.KARIM, 2015
Dual-Fuel Diesel Engines
CRC Press, ISBN 9781498703086 - CAT# K24645

[Mayer et al., 2016] Stefan Mayer, T.Murakami, K.Shimada, Niels Kjemtrup, 2016
Performance and Emission results from the MAN B & W low-Speed engine operating on Methanol
MAN Diesel & Turbo, CIMAN CONGRESS, Helsinki

[Lia et al., 2015] Xiaolu Lia, Xinqi Qiaoa, Liang Zhanga, Junhua Fanga, 2015
Combustion and emission characteristics of a two-stroke diesel engine operating on alcohol

[Ding, 2011] Y. Ding, 2011
Characteristic Combustion in Diesel Engines – using parameterized finite stage cylinder process models
PhD Thesis, Delft University of Technology

[Georgescu, 2013] Ioana Georgescu 2013
Characterizing the Transient Behavior of Dual-Fuel Engines
Master thesis, Delft University of Technology

[LIBEWHIZ, 2016] LIBEWHIZ, 2016
Effect of viscosity
http://www.lubewhiz.in/disel_fuel.html; Oct 12th 2016

[Gunter P et al., 2006] Gunter P. Merker · Christian Schwarz · Gunnar Stiesch · Frank Otto, 2006
Simulation of combustion and pollutant formation for engine-development
Springer-Verlag Berlin Heidelberg-ISBN 10 3-540-25161-8

[Yaws, 1996] Carl L. Yaws , 1996
Handbook of Thermodynamic Diagrams, Volume 1
Gulf Publishing Company, Houston. ISBN 0-88415-857-8

[Abbaszadehmosayebi, 2014] G.Abbaszadehmosayebi, 2014
Diesel engine heat release analysis by using newly defined dimensionless parameters
Ph.d thesis, Brunel university, Unite kingdom

[Yin, 2016] Zenghui Yin, Chunde Yao, Peilin Geng, Jiangtao Hu 2016
Visualization of combustion characteristic of diesel in premixed methanol–air mixture atmosphere of different ambient temperature in a constant volume chamber
Tianjin University, Tianjin 300072, China, Fuel 174 (2016) 242–250

[Staperma, 2010a] D. Staperma, 2010
Diesel Engines, Volume 1: Performance analysis

Royal Netherlands Naval College, The Netherlands

[Staperma, 2010b] D. Staperma, 2010
Diesel Engines, Volume 3: Combustion
Royal Netherlands Naval College, The Netherlands

[Staperma, 2010c] D. Staperma, 2010
Diesel Engines, Volume 4: Emissions and Heat transfer
Royal Netherlands Naval College, The Netherlands

[McAllister et al., 2011] McAllister,S. Fernandez-Pello, Chen,J-Y, 2011
Fundamentals of combustion process
Springer, ISBN: 978-1-4419-7942-1

[Staperma, 2010d] D. Staperma, 2010
Diesel Engines, Volume 6: Thermodynamic principles II
Royal Netherlands Naval College, The Netherlands

[Chaichan, 2014] Miqdam Tariq Chaichan, 2014
Combustion of Dual Fuel Type Natural Gas/Liquid Diesel Fuel in Compression Ignition Engine
IOSR Journal of Mechanical and Civil Engineering (IOSR-JMCE), e-ISSN: 2278-1684,p-ISSN: 2320-334X, Volume 11, Issue 6 Ver. IV (Nov- Dec. 2014), PP 48-58

[Pan et al., 2015] Wang Pan, Chunde Yao, Guopeng Han, Hongyuan Wei, Quangang Wang, 2015
The impact of intake air temperature on performance and exhaust emissions of a diesel methanol dual fuel engine
Tianjin University, Tianjin 300072, China Fuel 162 (2015) 101–110

[Andersson, 2015] Karin Andersson, Carlos Marquez Salazar, 2015
Methanol as a marine fuel report
FC Business Intelligence Ltd.

[Tuominen, 2016] Tino Tuominen, 2016
Potential of Methanol in Dual Fuel Combustion

Master's Thesis, Aalto University

[Methanol institute, 2016] Methanol institute, 2016
http://www.methanol.org/environmental-impact/; Nov 25th 2016

[Kasseris, 2011] Emmanuel P. Kasseris, 2011
Knock Limits in Spark Ignited Direct Injected Engines Using Gasoline/Ethanol Blends
Department of Mechanical Engineering, Massachusetts Institute of Technology

[Wojciech Tutak et al., 2015] Wojciech Tutak, Kristóf Lukács, Stanisław Szwaja, Ákos Bereczky, 2015
Alcohol–diesel fuel combustion in the compression ignition engine
Department of Energy Engineering, Budapest University of Technology and Economics, Fuel 154 (2015) 196–206

[Park, 2014] Su Han Park, Chang Sik Lee, 2014
Applicability of dimethyl ether (DME) in a compression ignition engine as an alternative fuel
Department of Mechanical Engineering, Hanyang University, Energy Conversion and Management 86 (2014) 848–863

[Wang et al., 2013] Ying Wang, Yuwei Zhao, Fan Xiao, Dongchang Li, 2013
Combustion and emission characteristics of a diesel engine with DME as port premixing fuel under different injection timing
School of Energy and Power Engineering, Xi'an Jiaotong University, Energy Conversion and Management 77 (2014) 52–60

[Hovda, 2011] Knut Erik Hovda, 2011
Methanol poisoning outbreaks – Rapid diagnosis and management
The Norwegian Center for NBC Medicine Department of Acute

Medicine Oslo University Hospital, Ullevaal Oslo, Norway

[Mestemaker et al., 2016] B. Mestemaker, Lars M Nerheim, D. Stapersma, I. Georgescu, 2016
Characterisation of Large Gas and Dual-fuel Engines
MTZ industrial, Vol. 6, Issue 3, ISSN: 2194-8682 (Print) 2194-8690 (Online)

[Broeren et al., 2013] M. Broeren, R. Kempener, G. Simbolotti, G. Tosato, 2013
Production of Bio-methanol
IEA-ETSAP and IRENA© Technology Brief I08

[IRENA Technology, 2013] IEA-ETSAP and IRENA Technology
Production of Bio-methanol
http://mnre.gov.in/file-manager/akshay-urja/july-august-2013/EN/40-43.pdf; 1st Dec, 2016

[G.D Nicola et al., 2011] G. D. Nicola, E. Santecchia, G. Santori, F. Polonara 2011
Advances in the Development of Bioethanol
ISBN 978-953-307-480-1, Published: August 1, 2011 under CC BY-NC-SA 3.0 license

[T.G Osberg, 2015] Torill Grimstad Osberg, 2015
The IGF code for GAS FUELLED SHIPS Development, content, supporting class rules
DNV GL, www.dnvgl.com

List of Figures

List of Tables